REVIEW ARTICLE

Check for updates

A review of proton exchange membranes modified with inorganic nanomaterials for fuel cells†

Muhammad Rehman Asghar, [ID] *[a] Weiqi Zhang,[a] Huaneng Su, [ID] [a] Junliang Zhang, [ID] [cd] Huiyuan Liu, [ID] [a] Lei Xing,[b] Xiaohui Yan[c] and Qian Xu [ID] *[a]

This review gives an overview of the application of inorganic nanoparticles in the proton exchange membrane (PEM) of direct methanol fuel cells (DMFCs). The effects of the polymer membrane's physical and chemical characteristics after adding nanoparticles are covered. The article also covers how composite membranes can replace expensive, high-methanol-permeable, low chemically stable, and poor-conductive Nafion membranes at high temperatures. The different types of nanomaterials including solid, hollow, one-dimensional-(1D), two-dimensional-(2D) and three-dimensional-(3D) nanomaterials including clay-based composite membranes are discussed. Along with different types of nanoparticle composite membranes, different methods of making membranes such as dip coating, composite membranes and non-woven mats are also included in the article. The research shows that direct inclusion of the nanoparticles in the polymer as well as solution gel techniques require a precise ratio of the polymer and particles, blending time and a controlled drying temperature. The strong interactions of inorganic nanoparticles with polymers not only tune the pore structure of the proton exchange membrane for promoting Grotthuss and vehicular mechanisms but also create a link to hydrophilic functional groups that promote the further refining of these nanoparticles. The tortuous and non-swelled paths created with the inclusion of nanoparticles in the membrane minimize the methanol permeability while maintaining high proton conductivity. This paper also discusses the advancements in inorganic nanoparticle-modified membranes, their application and future improvements for their better application in the membrane of DMFCs.

[a] *Institute for Energy Research, Jiangsu University, Zhenjiang 212013, China. E-mail: engr.rehman1240@sjtu.edu.cn, xuqian@ujs.edu.cn*

[b] *Department of Chemical and Process Engineering, University of Surrey, Guildford GU2 7XH, UK*

[c] *Institute of Fuel Cells, School of Mechanical Engineering, Shanghai Jiao Tong University, Shanghai, China*

[d] *MOE Key Laboratory of Power & Machinery Engineering, Shanghai Jiao Tong University, Shanghai, China*

† Electronic supplementary information (ESI) available. See DOI: https://doi.org/10.1039/d4ya00446a

Muhammad Rehman Asghar is a postdoc student at the Institute for Energy Research, Jiangsu University. He earned his PhD degree in power engineering and engineering thermophysics from Shanghai Jiao Tong University in 2020. His research work focuses on polymer and nanoparticle materials for the membranes of fuel cells and batteries. He has published more than 12 SCI journal articles. Moreover, he has professional experience in the design of battery modules in the field of power generation for industrial and household scales.

Muhammad Rehman Asghar

Xiaohui Yan is an associate professor in the Department of Mechanical Engineering, Shanghai Jiao Tong University. He earned his Bachelor's degree in Energy and Power Engineering from Xi'an Jiaotong University in 2012 and PhD degree in Mechanical Engineering from Hong Kong University of Science and Technology in 2016. His research interests focus on the transport phenomena in PEM fuel cells and PEM water electrolysis cells. He has published over 100 peer-reviewed papers in fuel cells and water electrolysis. He won the first prize of Shanghai Technology Invention Award and Outstanding Teaching Award of SJTU.

Xiaohui Yan

1. Introduction

As an alternative for replacement of non-environmentally friendly fossil fuels for power production, scientists around the globe are concentrating on smart energy systems with portable design, light-weight and less cost that convert chemical energy into electrical energy without producing harmful effects on the environment.[1–3] These days, lithium-ion batteries and fuel cells are becoming one of the first choices for power production due to their portable design.[4–11] Among the different types of fuel cells which are being used now in industry and for research, the DMFC is one of the most versatile power-producing devices because it uses methanol as an input source to produce electricity.[12] Due to its high power density and quick refueling capacity it is used as a charging source for batteries and the running of transportation. These prominent features make DMFCs a better candidate for fulfilling the emerging demand of the latest market for portable devices.[13,14]

As shown in Fig. 1, in a DMFC, methanol (CH_3OH) solution is oxidized at the anode catalyst layer, with the release of electrons (e^-) and protons (H^+) along with carbon dioxide (CO_2). The electrons pass by the external electrical circuit and reach the cathode while the proton flows inside the polymer membrane and reaches the cathode. At the cathode catalyst layer, the oxygen from the air or in some cases moist air reacts with both electrons and protons and converts into water.[15]

The overall reaction processes that occur in a DMFC are given in Table 1.

The DMFC single cell consists of different components of which the PEM is an integral or essential part on which the
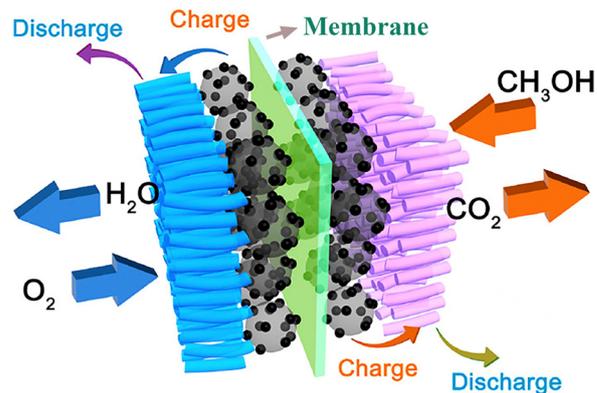

Fig. 1 Schematic diagram of the DMFC mechanism.[16] With copyright permission, 2018, American Chemical Society.

Table 1 Chemical reactions that occur on the electrodes of a DMFC

Input	Output
At the anode	
$CH_3OH + H_2O$	$CO_2 + 6H^+ + 6e^-$
At the cathode	
$3/2O_2 + 6H^+ + 6e^-$	$3H_2O$
Overall	
$CH_3OH + 3/2O_2$	$CO_2 + 2H_2O$

Prof. Qian Xu obtained his PhD degree in Mechanical Engineering from Hong Kong University of Science and Technology in 2013, and worked as a postdoctoral researcher at the same university until August 2014. From 2017 to 2018, he worked at the University of Waterloo, Canada, as a visiting scholar. Currently he is a Full Professor at Institute for Energy Research, Jiangsu University, China. His research programs focus on multi-scale multiphase heat and mass transport with electrochemical reactions in fuel cells and redox flow batteries. He has published over 170 peer-reviewed journal papers, 3 academic books and 6 chapters with more than 6700 citations (H-Index = 40), and applied 29 patents with 12 issued. He serves as the Editorial Board Member of Processes (MDPI), Carbon Footprints, as well as the reviewer for more than 50 international academic journals. He received the "Six Talent Peaks" award of Jiangsu Province, China, in 2016, and Outstanding Researcher Prize of Jiangsu Engineering Thermophysics Association in 2020. He was consecutively included in the "World's Top 2% Scientists" List released by Stanford University from 2021 to 2023.

Qian Xu

important parameters depend such as proton conductivity and methanol crossover protection. These parameters decide the overall performance of the DMFC.[16–22] The most common commercial proton exchange membrane is Nafion produced by Dupont, which is made from perfluorosulfonate resin [Fig. 1].

According to research, the maximum specific energy can be achieved using a 9 M (molar) or high methanol concentration solution in a DMFC, which fulfills the requirement to get high efficiency in the fuel cell.[23] The Nafion membrane is not suitable for application in DMFCs that use high concentration methanol due to its high methanol permeability, low proton conductivity, limited water uptake, high swelling, low chemical stability, etc. at room temperature as well as elevated temperature. Moreover, the high cost of Nafion membranes minimizes their application for fuel cells.[24,25] Different polymer based proton exchange membranes have been developed in order to cater to these deficiencies such as those based on cellulose and its derivatives,[26–30] poly-benzimidazole (PBI),[31–34] poly(ether ether ketones) (PEEK),[35–38] polystyrene sulfonate (PSS),[39,40] PVDF and its copolymers,[41–44] polysulfone (PSU),[45–48] polybenzimidazole (PBI),[49–52] etc. Composite membranes are among them that contain nontoxic, highly hydrophilic organic and inorganic nanoparticles, which sustain a uniform structure with the help of polymers to boost proton conductivity and provide coverage to minimize the methanol crossover. Different types of nanomaterials including Al_2O_3, SiO_2, TiO_2, GO, etc. have been found to be the most promising candidates for application in composite membranes. The ceramic and non-swelling nature of the nanoparticles creates a strong path for the proton to transfer from the anode to cathode while their interaction with polymers promotes the resistance of the methanol crossover[53] [Fig. 2]. The functional groups of the

nanoparticles create a strong physical interaction with the available functional groups of the polymers that ceases the movement of the polymer chain and ultimately increases mechanical strength and durability.[54,55] However, up to a specific limit, the addition of nanomaterials to the membrane increases the mechanical strength and when the nanoparticle amount increases, the agglomeration of particles in the membrane increases and the mechanical strength starts decreasing. Moreover, the high glass transition temperature of nanoparticles protects the membrane from degradation during the working of the fuel cell and increases the thermal stability of the prepared membrane. Moreover, the strong interaction with the nanoparticles increases the resistance against increased expansion of the porous structure, which contributes to the better stability of the fuel cell efficiency.[56] In the past few years, many research review articles have been published on the composite membrane related to DMFCs.[57–61] However, no one categorizes the nanoparticles in detail and mentions the publications on the different nanoparticles applied according to membrane manufacturing methods. This review article presents the recent inorganic nanoparticle-based composite membranes for application in DMFCs, methods of making different kinds of composite membranes, and their merits and demerits. Moreover, this article also provides data on the nanoparticle-based membrane based on the manufacturing methods.

2. Mechanisms of proton conduction in the PEM

There are generally two types of mechanisms responsible for the conduction of protons through the PEM, *i.e.* Grotthuss and vehicular mechanisms. As shown in Fig. 2(a), the Grotthuss mechanism involves movement of protons through formation and breakage of hydrogen bonds [O–H] between oxygen atoms of SO^{3-} groups (ionized) and hydronium ions [H_3O^+, $H_5O_2^+$, $H_9O_4^+$, *etc.*] from water.[63,64] Hydronium ions are produced when the protons [H^+] that originate during the methanol reduction reaction (MOR) or detach from the sulfonic groups [SO_3H (non-ionized)] attach to water molecules [H_2O]. On the
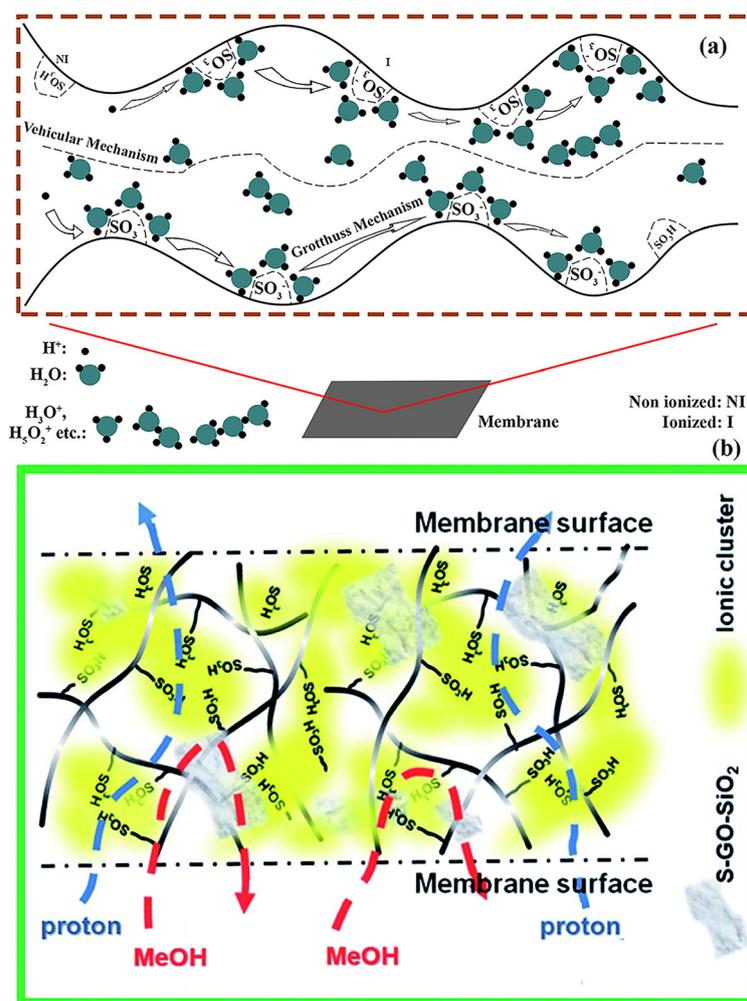

Fig. 2 (a) Explanation diagram of proton conduction mechanisms [Grotthuss and vehicular]. (b) Schematic diagram of the protons as well methanol passage through the nanoparticle modified membrane. With copyright permission, 2021.[62]

other hand, the vehicular mechanism involves protons moving through diffusion with the help of free water absorbed by the membrane.[65] Generally, the vehicular mechanism works under hydrated conditions, and when the relative humidity is low, the Grotthuss mechanism dominates. The Nafion membrane mainly consists of hydrophilic sulfonic groups [SO$_3$H] that are attached to the hydrophobic PTFE backbone. The hydrophilic sulfonic groups attract water molecules, contributing to the Grotthuss mechanism, while free water molecules bring the protons [H$^+$] in the form of hydronium ions and move by the vehicular mechanism. Under low humidity, surface sulfonic groups of the Nafion membrane help to maintain proton conductivity during the working of the fuel cell.[66] However, the unexpected change in channel shapes of the Nafion membrane because of the swelling and limited functional groups decreases the chances of high proton conduction and these mechanisms of proton conduction do not work properly which directly affects the overall efficiency of the fuel cell.[67] The nanoparticle-incorporated membrane not only stabilizes the Grotthuss and vehicular mechanisms by increasing the strength of the channel walls and providing hydrophilic functional groups but also increases the water retention capacity which enables high proton conduction and stable fuel cell performance.

3. Properties of the PEM

The membrane's performance depends on the quality of the membrane. A good membrane is able to sustain the performance load for a long period of time without appreciable efficiency or performance loss. There are several properties that need to be present in the PEM to obtain a good DMFC and they are discussed in detail in Table 2.

Different techniques for the application of nanoparticles in the DMFC membrane have been developed that are efficient and reliable for making membranes and Fig. 3 presents the number of articles published on these unique techniques. This research article depicts the importance of nanomaterials in the field of polymer membranes and explains in detail the methods employed in the preparation of nanomaterial-based composite membranes.

Types of inorganic nanomaterials for application in DMFCs:
- Silica
- Titania
- MOFs (*i.e.* UiO-66, ZIF-8, Mil-88, copper-based MOFs)
- Hybrid nanomaterials
- MoS$_2$
- Two-dimensional nanomaterials (*i.e.* layered hydroxides (LDH), graphene oxide, boron nitride, zeolite)
- Clay (*i.e.* sepiolite (SP), montmorillonite (MMT), halloysite nanotubes, bentonite, cloisite)

4. Inorganic nanomaterial coated composite membranes

Nafion based membranes are used in the DMFC due to their high mechanical strength, relatively good IEC and excellent proton conductivity in the hydrated form. However, despite these benefits, they have the drawback of high methanol or fuel crossover from the anode side to cathode side, which has a drastic effect on the efficiency or performance of DMFCs. To prevent the methanol crossover, an appropriate amount of inorganic nanomaterials needs to be incorporated, as they not only support the Nafion membrane during the methanol or fuel crossover but also enhance other properties like proton conductivity, mechanical strength and chemical stability. Moreover, they increase the hydrophilic nature of Nafion and other polymer membranes due to the hydroxyl group on their surface. The following different methods or techniques are usually adopted to apply nanomaterials as coating materials on the surface of the polymer membrane to enhance its physical as well as electrochemical properties. Moreover, these techniques are explained with recent research examples. The details of the inorganic nanomaterial-coated composite membranes are summarized in Table 3.

4.1. Dip coating method

The Nafion membrane's high swelling and fuel crossover as well as its low hydrophilic nature in the case of water holding under load reduce the opportunity to achieve the maximum efficiency of the DMFC. Therefore, the researchers have applied hydrophilic nanomaterials by different methods to the surface of the membrane to sustain the water within the proper membrane as well as minimize the methanol permeability or crossover. Among these methods, the dip coating method has been studied to develop a unique and nanoporous coating with self-attachment ability on the surface of membrane substrates under controllable thickness, which gives a large surface area, high proton conductivity, IEC and good performance in the application of fuel cells in commercial/non-commercial sectors.[85] The general method of making coated membranes is as follows: firstly, the commercial or synthesized nanomaterials are dispersed in an appropriate organic solvent by using sonication or a stirrer under controlled conditions and time. Afterward, a polymer binder is added to this solution and stirred under heat or at room temperature until a homogeneous solution is obtained. Then, the premeasured membrane samples are dipped in this solution for a specific period of time to complete the coating on both sides. Afterward, the modified membrane samples are dried in the air or in an oven at a high temperature in order to evaporate the solvent [Fig. 4].

As an example, Baur *et al.*[86] coated zirconium phosphate on the surface of the commercial Nafion membrane by using the dip coating method. The amount of synthesized zirconium phosphate (ZrP) to be studied in this article was between 0 and 26%. Along with zirconium phosphate, titanium phosphate was also studied in different ratios as a coating material. The researchers found that under hydrothermal treatment, δ-titanium phosphate converted into its alpha phase which increased the crystallinity so it did not support water uptake and conductivity while zirconium phosphate's crystallinity reduced after thermal treatment and it efficiently functioned in absorbing water and conducting protons. Moreover,

Table 2 The important parameters of the membrane of a fuel cell

Characteristics	Equations/measuring test	Details
Water uptake (WU)	$\text{WU}\ (\%) = \dfrac{S_w - S_d}{S_d} \times 100$ S_w: weight of the sample after dipping in water for 24 h S_d: weight of the dry sample	An ideal membrane should capture and hold water in its porous structure for a long period of time at room temperature as well as at high temperatures.[68] The Nafion membrane's water uptake is typically in the range of 20–30%[69]
Swelling ratio (SW)	$\text{SW}_T = \dfrac{\text{TC}_w - \text{TC}_d}{\text{TC}_d} \times 100$ SW_T: swelling ratio according to thickness TC_w: measured thickness of the sample after dipping in water TC_d: measured thickness of the dry sample $\text{SW}_D\ (\%) = \dfrac{D_w - D_d}{D_d} \times 100$ Swelling ratio according to dimension D_d: dimension of the dry sample D_W: dimension of the wet sample after dipping in water	The membrane swelling reduces the strength which causes short circuit. The membrane should avoid swelling of the pores during proton conduction and swelling of the whole structure to increase the protection of the fuel cell. The typical value of SW for different types of Nafion membranes falls in the range of 10–20% in water
Proton conductivity (σ)	$(\sigma) = \dfrac{T}{RA}$ T: thickness value of the dry sample R: impedance value of the sample A: the measured area of the dry sample	The membrane's proton conductivity relies on the quantity of water captured in the channels, the strength of the channels and the swelling ratio. The functional groups of the membrane participate in moving protons while membrane strength eliminates the hurdles during conduction. The membrane with proper structure should possess high proton conduction without resistance. The proton conduction value of the commercial Nafion membrane is in the range of 10^{-2} S cm^{-1} to 10^{-1} S cm^{-1} when temperature increases from room temperature after activation of sulfuric acid/water solution under hydrated conditions.[70] Moreover, when the humidity increases, Nafion conductivity increases[71]
Ion exchange property (IEC)	$\text{IEC} = \dfrac{V_{0.02\text{M NaOH}} \times N}{\text{SW}_d}$ $V_{0.02\,\text{M NaOH}}$: total volume consumed during the titration experiment SW_d: weight of the dry sample N: normality of sodium hydroxide (NaOH)	The exchange of exchangeable ions available on the membrane determines the IEC. It measures the capability of the available membrane to conduct more ions that are necessary to maintain the electrochemical reactions within the fuel cell. An efficient membrane should have a high IEC, which boosts the efficiency of the fuel cell. The IEC of the Nafion membrane is 0.80–1 meq. g^{-1} due to sulfonic groups[72,73]
Methanol permeability (MP)	$P = \dfrac{1}{C_A}\left(\dfrac{\Delta C_{B(t)}}{\Delta t}\right)\left(\dfrac{T.V_B}{A}\right)$ T: thickness of the sample A: area of the sample used in the experiment C_A: concentration of solution in compartment A C_B: concentration of solution in compartment B V_B: volume of compartment B Δt: change in time $\Delta C_{B(t)}$: change of concentration w.r.t. Δt in compartment B	Methanol permeability depends on the hydrophobicity, size of the channels and the tortuous pathway of the membrane. The membrane should have the capability of retaining the fuel crossover at the minimum level without losing the optimum proton conduction[74] which protects the cathode from deterioration and poisoning. The MP value of the Nafion membrane is above 10^{-7} (ref. 75 and 76)
Ruthenium permeability retardation	Dialysis method	When the fuel cell starts working, the flooding of water also drags the electrocatalyst materials through the membrane which is in some cases made of ruthenium. The material crossover turns out to be a disaster for the ORR at the anode. The membrane should be able to restrict the catalyst materials from passing within its circumference which would prevent the power density or efficiency of the fuel cell from declining[77–79]
Thermal stability	DSC/TGA analysis	Thermal stability is also an important parameter that is directly connected to the safety of most of the fuel cells [DMFCs, PEMFCs, etc.]. It also depends on one more factor which is the glass transition temperature of membrane materials. The membrane should be able to sustain its shape without losing its porous structure under heating for continuous protection from short circuit and proton conduction. The Nafion membrane starts melting above 80 °C and it decomposes above 280 °C[80]
Life time	Fuel cell performance test	The lifetime of the membrane depends on stable proton conduction, integrity of the internal structure of the membrane and SR. The membrane should be able to handle water uptake that is necessary to keep the efficiency of the fuel cell at a stable level. The Nafion membrane generally shows stable performance up to 500 h after which its performance starts to decline, while hydrocarbon membranes from PolyFuel show stable performance for 500–5000 h[60]

Table 2 (continued)

| Characteristics	Equations/measuring test	Details
Mechanical stability	Universal tensile strength measuring machine	The pore wall strength and stability of the tortuous pathway within the membrane depend on the mechanical strength of the polymer. The polymer membrane should not be able to breakdown during the assembly or working of the fuel cell. For a commercially available Nafion membrane, the values of tensile strength and Young's modulus are 144.27 MPa and 20.11 MPa, respectively, with a strain value of 80.74%[81]
Electrical conductivity	Current measurement test	The membrane short circuit occurs when the membrane allows electrons as well as protons to pass through it. The safety of the membrane depends on its non-conducive nature. Therefore, the polymer membrane should push electrons towards an external circuit and only allow smooth transmission of ions from its body[82]
Chemical stability	For measuring the chemical stability of the given membrane sample, use Fenton's reagent, which consists of hydrogen peroxide (H_2O_2) [3%] and iron ions (Fe^{3+}) [3 parts per million (ppm)]. Dip the membrane sample in this solution for a specific time. The membrane degradation is measured based on the weight reduction after different time intervals of the test	The polymer membrane should not react with any electrocatalyst material, which keeps its structure stable and free of degradation. The typical weight loss of the Nafion membrane is only 2.5 wt% after testing against Fenton's reagent solution[83]
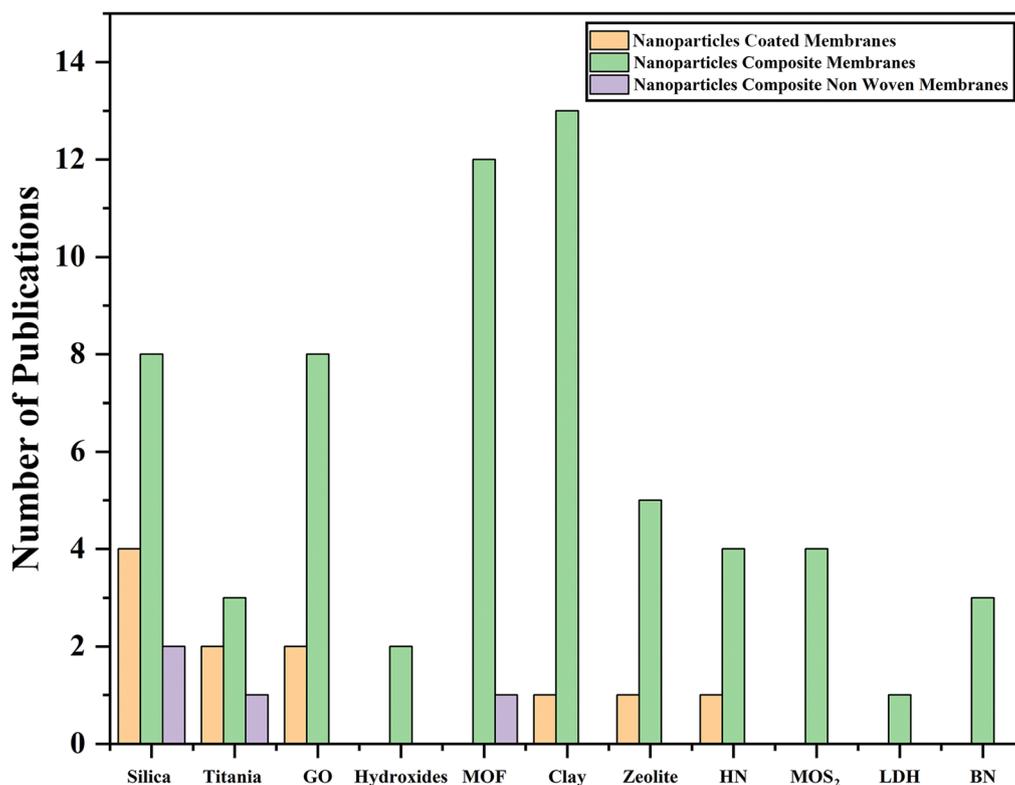
Fig. 3   Total number of published papers on different techniques using several types of nanoparticles.

inorganic materials show high hydrophilicity and their layers on both sides of the Nafion membrane act like a network that interacts with water molecules and bounds them within the ionic channels which promotes proton conductivity through Grotthuss movement. With 8 wt% zirconium phosphate, the composite membrane delivers a maximum proton conductivity value of 13×10^{-3} S cm^{-1} at a relative humidity level of 94%.

The composite membrane also shows a positive response at high temperature and is able to deliver a high conductivity which is higher than that of the commercial Nafion membrane when tested at 80–130 °C and 50–100% humidity level and 21 wt% ZrP. The zirconium phosphate fills the free volume in the polymer, blocks the methanol or fuel crossover through the membrane, and improves the mechanical strength.

Table 3 Details of the inorganic nanomaterial-coated composite membrane

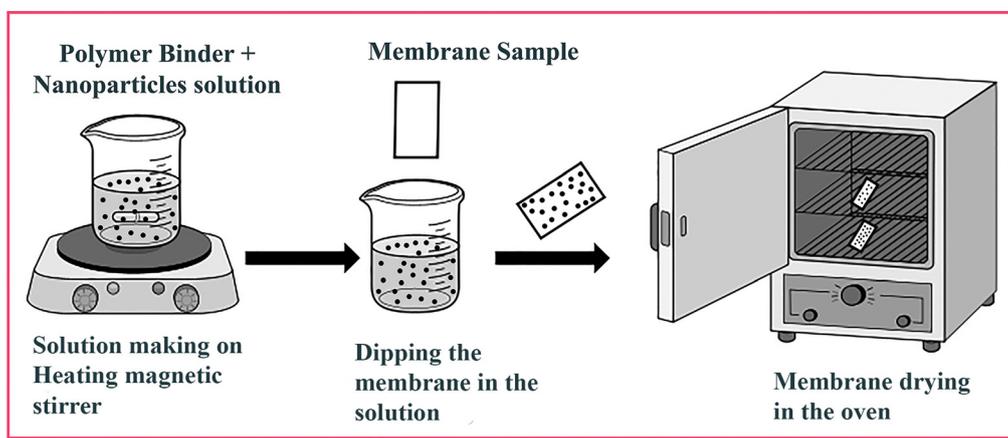| Organic/inorganic nanomaterials	Polymer	Thickness (μm)/ anode supply	Proton conductivity ($\times 10^{-3}$ S cm^{-1})	Methanol permeability ($\times 10^{-7}$ cm^2 s^{-1})	Selectivity ($\times 10^4$ S s cm^{-3})	Power density (mW cm^{-2})	Ref.
SGO-40 °C	Nafion	—/O$_2$	111 (80 °C)	8.4	10.5	30	84
Silica + PEG	Nafion 115	170/—	4.07	0.217	187.3	—	85
ZrP	Nafion	180–190/—	13	7.25	—	—	86
F-Silica-2%	Nafion	180–185/O$_2$	0.1319	8.46	15.6	—	87
Graphene oxide-80 layers	Nafion 117	—/O$_2$	6.7×10^{-5} [30 °C]	9.28 [35 °C]	5.25 (RS)	64.38	88
Silica-5 min	Nafion 117	230/—	48.6 [25 °C]	0.175 [25 °C]	—	—	89
Titania [0.009 mg cm^{-2}]	Nafion	—/O$_2$	0.09	—	—	—	90
Silica/bentonite	Nafion	55/air	66.7	0.2515	—	135.17 [55 °C]	91
Nano silica-10	Nafion 115	10–60/air	91	16.8	5.5	—	92
MOR-zeolite-10 wt%	PTFE/Nafion	17/air	—	14.5	—	81.6 [60 °C]	93
ZrP/PVA	PTFE	—/—	28.1	4.5	—	—	94
ZrSPP-10 wt%	PTFE/SPPESK	180/—	240 [120 °C]	0.011	—	—	95

Fig. 4 Schematic diagram of the dip coating method of the composite membrane.

However, the performance of the DMFC is limited. The performance reduces because under liquid water, zirconium phosphate might work better as compared to the humidity condition.

To further enhance the particle efficiency of the composite membrane, the particle surface is usually functionalized with different groups, which promotes the electrochemical and physical characteristics of the membrane as well as interfacial compatibility between polymers and nanomaterials. As an example, Li et al.[87] prepared a composite based membrane by coating the Nafion substrate with functionalized silica of 45 nanometers (nm), 110 nm and 220 nm in size. The silica particles were synthesized by the solution gel method. They found that the functionalized F-silica nanoparticles of 110 nm size improve the structure of the composite based Nafion membrane because of their compatibility with the pore size of the Nafion substrate. They also found that with the addition of F-silica nanoparticles in the Nafion membrane the crystal size increases which promotes the amorphous region of the membrane and leads to a high proton conductivity value of 200×10^{-3} S cm^{-1} at 80 °C as compared to that of the pristine commercial Nafion membrane, which only shows 160×10^{-3} S cm^{-1}. Moreover, the strong physical interaction [hydrogen bonding] between the oxygen atom of silica and the sulfonic groups of Nafion leads to a lower swelling ratio of 6.70%, improves the methanol permeability resistance

from 9.36×10^{-7} cm^2 s^{-1} to 7.76×10^{-7} cm^2 s^{-1} when particle size increases from 45 to 220 nm and enhances water uptake, while the Nafion membrane delivers 50% low water uptake and 50% high swelling ratio. The interaction between particles and the membrane also increases membrane elongation and mechanical and oxidative stability. With DMFCs, the assembled composite membrane delivers 30% more power output as compared to the pristine Nafion membrane. However, by using these particles, the uniformity of the membrane and mechanical stability are compromised because of their round shapes and low surface area. Graphene oxide is also used as a coating material because of its high surface area due to its two dimensional structure and hydrophilic nature. The researchers found that the compatibility between the Nafion membrane and graphene oxide suppresses the methanol crossover by creating a stable less swollen structure and an ionic cluster, which enhances the proton conductivity and water uptake. Wang et al.[88] prepared graphene oxide coating on the recast Nafion membrane by the LBL method. The GO forms cross-links on the surface of the commercial Nafion membrane using PDHC as the cross-linker. Different graphene layers from 15 to 80 were studied in this case. The hydroxide and carboxylic groups of the graphene oxide sheets not only enhance the water uptake but also contribute to improve the IEC by releasing H$^+$ (IEC = 0.96 meq. g^{-1}). The researchers found that the value of IEC

was slightly higher than that of the recast Nafion 117 (0.89 meq. g^{-1}). The strong crosslinking between GO and Nafion promoted chemical stability by providing resistance against breakage in strong chemicals. According to the researchers, the minimized swelling of the composite based membrane and graphene oxide unipolar and bipolar nature block the methanol from crossing through the ionic channel ultimately reducing methanol permeability. The composite based membrane with 80 layers of GO delivers a methanol permeability value of 0.67×10^{-7} cm^2 s^{-1}, which is 2 times lower than that of the Nafion membrane (18.2×10^{-7} cm^2 s^{-1}) at 30 °C. Moreover, the composite membrane with 50 layers of GO showed an OCV of 0.67 V and a maximum power density value of 64.38 milliwatts (mW) cm^{-2}, which surpass the values of recast Nafion 117 under similar conditions. The functionalization of the graphene oxide surface could provide better adhesion between the surface of the membrane and particles, which further develops a unique pathway for proton flow. So to further enhance the properties of GO, Li et al.[84] synthesized sulfonated graphene oxide (SGO) and coated it on the Nafion membrane by the application of the dip coating process. The dipping time for the SGO coating on the Nafion membrane was set for 3 days at different temperatures from 20 °C to 60 °C. The composite membrane with SGO creates a strong and flexible structure with narrow channels with extra space for hopping water molecules and hydrogen bonding between polymers and hydrophilic functional groups provides a surplus opportunity to pass the protons through Grotthuss as well as vehicular mechanisms [Fig. 5(a)]. Moreover, the strong interaction reduces swelling and provides a comparatively strong structure as compared to the recast Nafion membrane. The researchers found that when the temperature of soaking SGO increases, the water uptake capacity, proton conductivity and reduction in swelling increase because there are more hydrophilic functional groups available in the shape of SGO coating on the surface of Nafion. Although SGO nanosheets create a compact structure, methanol permeability increases because of the loose connection between the polymer and SGO nanosheets at high temperatures [Fig. 5(b and c)]. The scientists discovered that the suitable temperature is 20 °C where water uptake capacity and proton conductivity values are 15.7% and 78.8×10^{-3} S cm^{-1} respectively while the methanol permeability value is 3.6×10^{-7} cm^2 s^{-1}. These values are higher than the results obtained for the original Nafion membrane. The composite membrane retains a conductivity value of 111×10^{-3} S cm^{-1} for a long period of time at 60 °C when tested which evidences the structural stability and connected ionic channels within the polymer matrix. Due to its high selectivity [21.7×10^4 S s cm^3], the composite membrane prepared at 20 °C shows a high power value of 28–30 mW cm^{-2} which is 50% greater than that of the original commercial Nafion membrane.

4.2. Sol–gel method

In composite membranes, sometimes the solution gel of inorganic nanomaterials in the solvent is directly applied to the polymer matrix to produce nanomaterial growth on its surface. This method requires no binding material and strong adhesive layers of nanoparticles stick to the membrane. The inorganic nanomaterials' hydrophilic nature and the strong interaction with polymers like Nafion create several ionic channels, which facilitate proton conduction.[96,97] Lin et al.[89] modified the commercial Nafion membrane surface with silica particles by the sol–gel method. The researchers studied the relationship between dipping time and the number of coating layers. The results show that the second silica coating layer on Nafion after 5 minutes creates a well-defined and porous layer, which improves the dimensional stability and mesoporous silica nanoparticles provide high water holding capacity due to their hydrophilic nature. The improved structure and reduced swelling nature of the composite membrane also improve proton conduction and methanol crossover or permeability resistance. Ultimately, the composite based membrane delivers proton conductivity of 48.6×10^{-3} S cm^{-1} and 68.5×10^{-3} S cm^{-1} and methanol permeability values of 0.175×10^{-7} cm^2 s^{-1} and 0.695×10^{-7} cm^2 s^{-1} at room temperature (25 °C) and 80 °C respectively. These methanol permeability values are 3 times lower than those of the Nafion membrane under a similar condition. The composite membrane provides a great alternative to the commercial Nafion membrane in DMFCs.

However, the membrane coating becomes more uniform when the particle size is small enough, so it does not obstruct the pores and creates a strong wall around the membrane with the help of a polymer binder. Titania has been used as a semiconductor material that comes in small sizes and different shapes,[98] which could further tune the coating. For example, Liu et al.[90] prepared a composite based membrane by dip coating the Nafion/TiO_2 membrane in a solution containing the TTIP precursor by the sol–gel method. The coating of the titania film is found to be crack free and uniform. The composite based membrane exhibits high proton conduction due to the well-developed ionic channel and the hydrophilic nature of the titania nanoparticles. However, with increasing titania, the structure's porous pathway becomes blocked which does not support proton conductivity but supports methanol permeability resistance. The methanol crossover reduces from 32.0×10^{-7} cm^2 s^{-1} to 17×10^{-7} cm^2 s^{-1} at a temperature of 25 °C and from 125×10^{-7} cm^2 s^{-1} to 46.0×10^{-7} cm^2 s^{-1} at a temperature of 85 °C with an increasing amount of titania nanoparticles in the membrane which is 3 times lower than that of the commercial Nafion membrane [36×10^{-7} cm^2 s^{-1} and 130×10^{-7} cm^2 s^{-1} at 25 °C and 85 °C]. The researchers found that the composite membrane delivers a power density of 44 mW cm^{-2} at 0.009 milligrams (mg) cm^{-2} titania contents. The researchers also used different materials along with TEOS to further enhance the coating properties. In one example, Y. Wang and his co-scientists[91] prepared a composite membrane by simply immersing the Nafion 212 membrane in a solution containing TEOS and previously treated bentonite with dodecylamine [modified bentonite]. The scientists set the amount of modified bentonite from 0 wt% to 8.590 wt% in the composite membrane. The Nafion 212 membrane shows a dense structure with patches on its surface [Fig. 6(a and c)]. The silicon and oxygen groups act as a binder in the strong attachment of the modified clay to the surface of the commercial Nafion
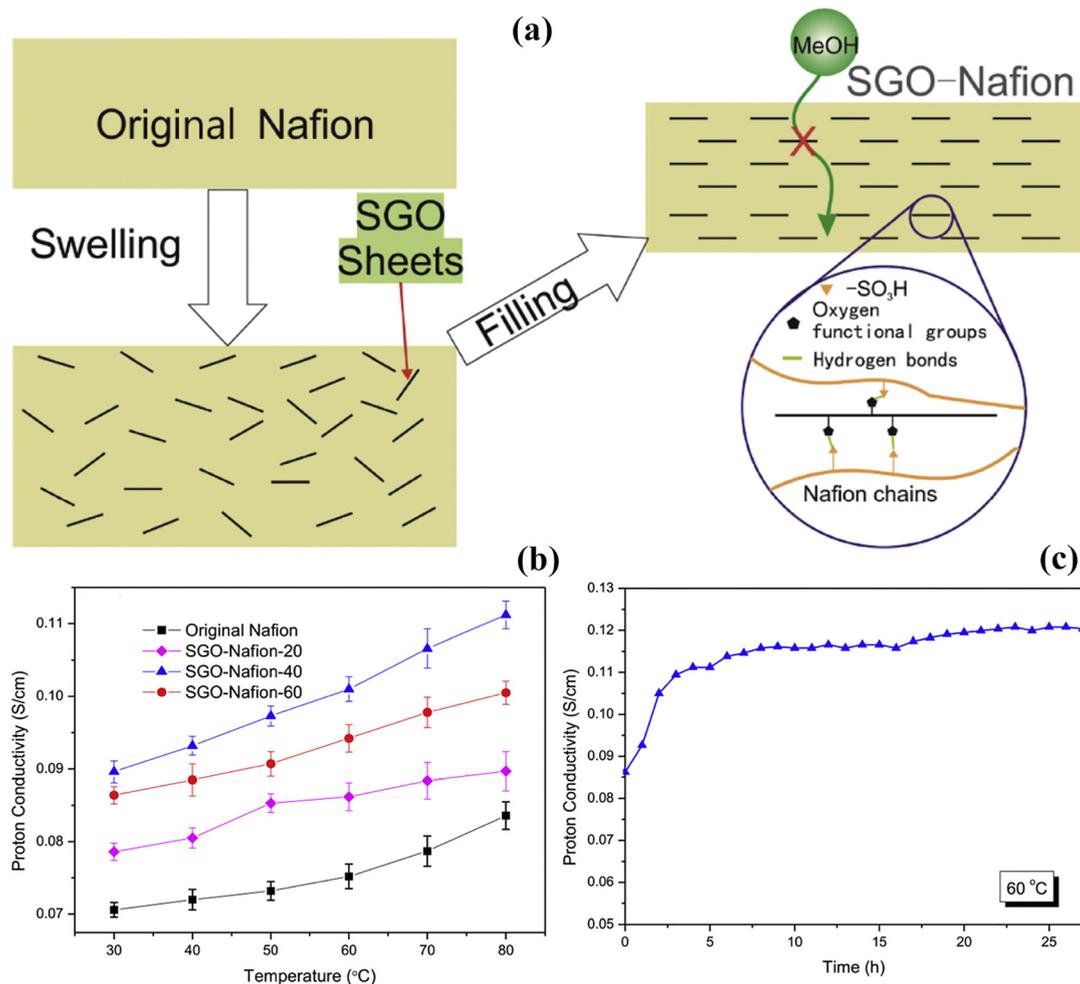
Fig. 5 (a) Schematic diagram of the protection mechanism of methanol through the SGO/Nafion membrane. (b) Temperature *vs.* proton conductivity curve of the SGO based Nafion membranes and the commercial Nafion membrane. (c) Time *vs.* proton conductivity of the SGO based Nafion-20 membrane at 60 °C and 100% RH.[84] With copyright permission, 2018, Elsevier.

membrane, and the thickness of the coating layer was about 5 μm [Fig. 6(b and d)]. The clay structure on the surface of the commercial Nafion membrane minimizes the uptake due to blockage of the Nafion membrane pores and compacts the overall structure which also minimizes the proton conductivity when increasing the modified bentonite clay amount in the composite membrane [Fig. 6(e)]. However, high swelling can be seen at high temperatures but the strong bonding between polymers and clay sustains the rigidity of the composite membrane which does not let it contribute to increasing conductivity. Moreover, the blockage of the pathway due to modified bentonite clay does not contribute to increasing proton conduction but it does produce a positive effect on protecting methanol permeability through the membrane [Fig. 6(f)]. The proton conductivity value of the composite membrane with 6 wt% clay is 66.7×10^{-3} S cm^{-1} which is slightly lower than that of the Nafion 212 membrane which shows a proton conductivity value of 99.1×10^{-3} S cm^{-1}. With the benefits of 20.40% high methanol protection as compared to the commercial Nafion membrane, the composite membrane

delivers a high power density value of 135.17 mW cm^{-2} when assembled in a DMFC single cell at 55 °C. This value is superior to that of the commercial Nafion membrane, which only exhibits a power density value of 118.7 mW cm^{-2} under similar conditions.

The methanol crossover or permeability is still high through the composite membrane which needs to be tuned to further modify the DMFC performance. One of the strategies adopted by the researchers is to develop an additional microporous layer that uses methanol, which tries to pass through the membrane before reaching the cathode.[99,100] In this method, the possibility of the usage of 100% pure methanol increases, which is difficult for most of the researchers to achieve.[101,102] Wu and his research team[103] developed a microporous membrane by sandwiching a thin layer composed of silica, Pt–Ru catalysts and Nafion ionomer between two commercial membranes of Nafion 211. The platinum and rhodium loadings of 0.10 mg cm^{-2} provide a high methanol oxidation reaction with low resistance and silica nanoparticles store the water efficiently due to their hygroscopic nature. The overall performance of the cell with the sandwiched
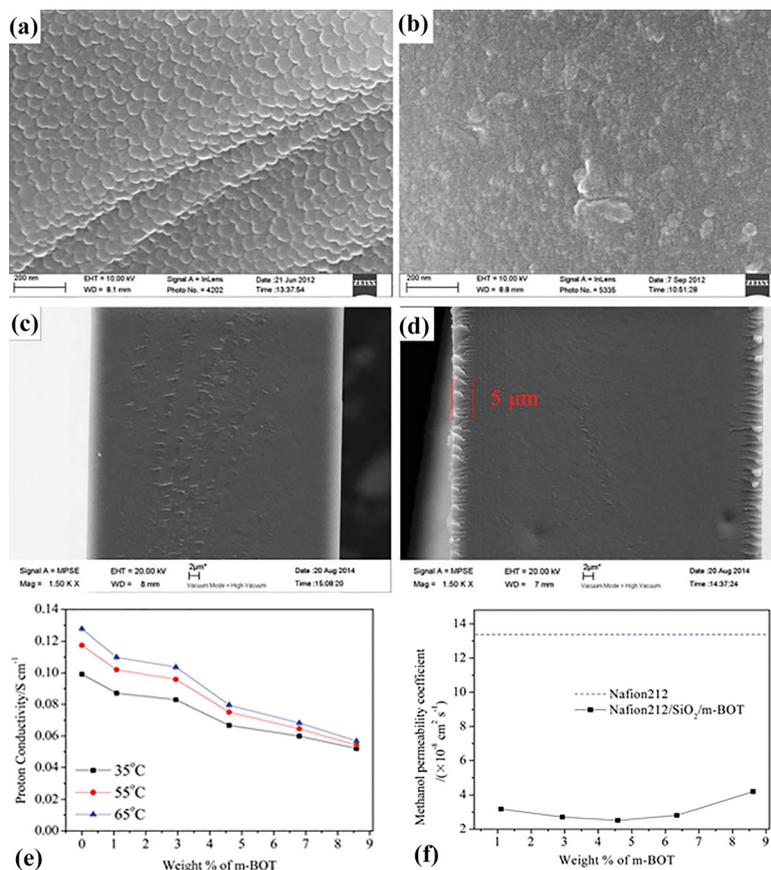
Fig. 6 The SEM images of the top surface (a) and cross section (c) of the Nafion 212 membrane. (b) Top surface and (d) cross section of the Nafion/SiO₂/m-BOT composite membrane. (e) Different amounts of the m-BOT based composite membrane *vs.* proton conductivity at 35 °C, 55 °C and 65 °C. (f) Different amounts of the m-BOT based composite membrane *vs.* methanol permeability values at 25 °C.[91] With copyright permission, 2018, American Chemical Society.

membrane is higher than that of the commercial Nafion 212 membrane.

4.3. Grafting technique

Grafting nanomaterials on the surface of the membrane not only eliminates the expensive and long process of membrane modification but it also makes it feasible to adjust functional groups. Moreover, proton conductivity and methanol or fuel permeability can be controlled by changing the degree of grafting.[104–107] In the previous years, Kim *et al.*[92] created a nano silica layer of about 10–68 nm on the surface of Nafion 115 by using plasma chemical vapor deposition. After examining the SEM results, it is clear that the nano silica develops a smooth surface with a crack free top layer while with an increase in thickness, the surface cracks which indicates that the connection between particles and the surface reduces due to low adhesion between the polymer and nanomaterials. The results show a decreasing trend in proton conductivity while methanol permeability greatly improves when the thickness of the inorganic particle layer increases. The proton conduction and methanol or fuel permeability achieved with a 10 nm thick layer are 20% and 70% greater than those of the pristine commercial Nafion membrane.

4.4. Other substrates used in coating

There are different substrates that can be applied rather than the expensive Nafion membrane such as PTFE substrates, which possess high mechanical strength, high chemical resistance and a thinner structure.[93] For example, Pagidi *et al.*[94] prepared a membrane using chemically treated PTFE film, which was treated with PVA and ZrP solution. The chemical treatment of PTFE breaks down its hydrophobic nature and converts it into a hydrophilic substrate. Moreover, the addition of PVA and ZrP layers to the surface of PTFE further increases its hydrophilicity, which increases proton conduction. The strong interaction between PVA–ZrP and PTFE increases the mechanical strength as well as the thermal stability of the composite membrane. The composite based membrane is able to resist high methanol crossover, and its value limit is 3.8×10^{-7} cm² s⁻¹ at a temperature of 40 °C, which is lower than that of the Nafion 117 membrane [13.6×10^{-7} cm² s⁻¹] [Fig. S1(b), ESI†]. The composite based membrane shows a high mechanical strength value of 44 MPa. Moreover, due to increased water uptake and a tortuous pathway, the composite based membrane is also able to deliver proton conductivity and methanol or fuel crossover values of 28.1×10^{-3} S cm⁻¹ and 14.5×10^{-7} cm² s⁻¹, respectively, at a temperature of 80 °C [Fig. S1(a), ESI†].

The surface attraction between nanomaterials and polymer membranes is lower which leads to the agglomeration of particles and restricts the use of a high amount of nanomaterials. The organic polymer coating on inorganic particles makes them more suitable for membrane coating contributing to mechanical and chemical stability of the membrane as well as an increase in its hydrophilic nature.[107–109] Li et al.[95] prepared a composite membrane in which the PTFE substrate was used as a supporting membrane and a blend of SPPESK and inorganic–organic type ZrSPP with 10–20 wt% was sprayed on it. The membrane was then annealed at a high temperature. The composite membrane shows a well-developed and microporous structure which is caused by the annealing process. The spray-coated membrane showed high mechanical strength and high dimensional stability due to the strong network created by ZrSPP and SPPESK polymers on the PTFE substrate. The nanoparticles tune the ionic channel in the composite membrane and along with sulfonic groups, the composite based membrane holds more water molecules within it. As a result, with 10 wt% ZrSPP, the membrane delivers a proton conduction value of 240×10^{-3} S cm^{-1} at 120 °C which is similar to Nafion proton conductivity at 90 °C [Fig. S1(c), ESI†]. Moreover, the narrow ionic channels and polar nature of the nanoparticles retard the methanol crossover or permeability in the composite membrane and allow more water to be absorbed. A composite membrane with different nanoparticles possesses methanol permeability in the range of 0.127×10^{-7} cm^2 s^{-1} to 0.011×10^{-7} cm^2 s^{-1}, which is comparable with Nafion membrane [Fig. S1(d), ESI†]. All research paper data are collected in Table 3 with related references (Ref.).

5. Inorganic nanomaterial-filled composite membranes

The dip coating method is not a very effective method to bind the nanomaterials to the membrane and also does not efficiently use their potential in the DMFC. Moreover, the chances of the particles detaching from the membrane are always a key issue, which results in the deterioration of the DMFC proton exchange membrane performance and ultimately reduces the overall DMFC power and current density. The composite membrane incorporated with nanomaterials not only prevents the nanomaterials from detaching but also enables their better dispersion, which boosts the conductivity, and the tortuous path permits a low amount of methanol to pass through the membrane. The brief preparation process of an inorganic particle-filled composite membrane is as follows: the polymer and nanomaterials are mixed in the solvent at room temperature or elevated temperature until a uniform dispersion of nanomaterials is achieved. In some cases, ultrasonication is used to get uniform dispersion. After that, the solution is placed on a glass plate or in a Petri dish and dried in a vacuum oven under high pressure.[110] The schematic diagram is shown in Fig. 7.

5.1. Silica (SiO$_2$)

Silica nanoparticles are famous for their high hydrophilic nature and easy preparation method. The silica nanoparticles help to create a narrow ionic channel structure with great stability and less swelling due to hydrogen bonding that exists between oxygen atoms and the sulfonic group of polymers.[111] For example, Yang et al.[112] converted the one dimensional Santa Barbara amorphous (SBA-15) rod shaped particles into 2D hexagonal mesoporous silica by using a surfactant in the solvent extraction process and mixing it with Nafion solution to prepare a composite membrane. The sulfonic groups of Nafion and the silane groups of the mesoporous silica attract more water molecules and the high surface and nanopores of the mesoporous silica hold water due to its high surface area and nanopores, which enhances the uptake. Moreover, hydrogen bonding between polymers and particles creates a mechanically strong and tortuous pathway with surplus ionic channels in which protons could pass through easily. The presence of the pore directing agent (P123) as a copolymer within the mesoporous structure of silica prevents methanol permeability and helps proton transfer through its ether groups. 20% SBA-15 and 15% Nafion deliver a lower methanol crossover value of 27×10^{-7} cm s^{-1} than the recast Nafion [36% high] and pristine Nafion 117 membrane [30% high] but have an adverse effect on the proton conductivity value. The optimum weight percentage of mesoporous silica is found to be 5 wt% in the composite membrane at which the optimal proton conductivity and selectivity values obtained are 39.4×10^{-3} S cm^{-1} and approx. 1.05×10^4 S s cm^{-3} respectively. The composite based membrane with 5 wt% SBA-15 delivers a high power density value of 117 mW cm^{-2} at a temperature of 60 °C which is almost 80% greater than
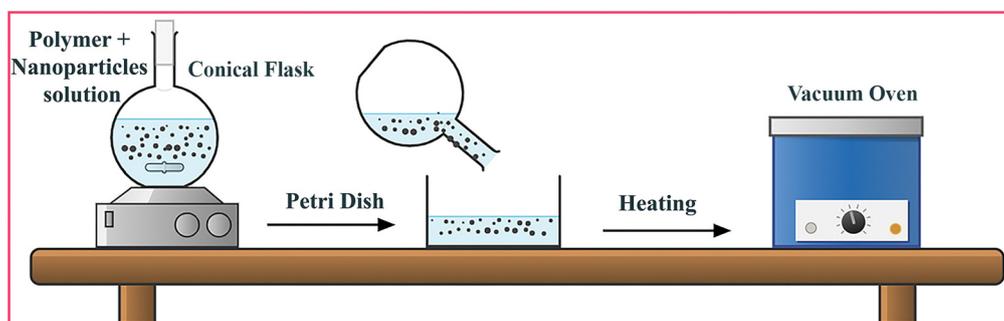

Fig. 7 Schematic illustration of the preparation procedure of an inorganic particle-filled composite membrane.

the performance of the recast Nafion membrane and 23% higher than the values of the commercial Nafion 117 membrane.

As explained in the dip coating section, the sol–gel method is very feasible and unique for getting a uniform dispersion of particles in the polymer with the help of related particle precursors. Therefore, this technique provides better results in making particle incorporated composite membranes. In one of their reports, Yan et al.[113] developed a composite based membrane in which they deposited a silica microporous layer on the surface of the ITO substrate by the Stober-solution method which was then treated with MPTS through the self-assembly method and with H_2O_2/H_2SO_4 to convert it into a mesoporous silica membrane with sulfonic groups. The mechanical strength of the membrane increases by creating a spin coated layer of Nafion on its surface and the overall thickness of the inorganic composite membrane is adjusted to 230 nm. The results are compared with those of the Nafion 212 membrane. The composite double layer membrane possesses vertically aligned channels with a diameter of 0.5 nm that the methanol molecules cannot pass through and a long pathway further restricts their motion through the membrane. The sulfonic groups of the microporous silica layer develop a strong hydrogen bond with water molecules, and as a result, abundant hydration ions are produced which enhance the proton conductivity by the Grotthuss and vehicular mechanisms. The methanol crossover value obtained with the inorganic framework membrane is 0.0164×10^{-7} cm^2 s^{-1}, which is three times lower than the methanol crossover value obtained with the Nafion 212 membrane. This shows the excellent protection ability of the membrane even at low thickness [230 nm]. Moreover, the composite membrane is able to deliver a high areal proton conductivity value of approx. 1800×10^{-3} S cm^{-1} at room temperature and an OCV value of 0.55 V at 8 M methanol concentration.

Particle agglomeration in the membrane is a big problem, which does not allow homogeneous dispersion of particles in the membrane. The researchers functionalized the surface of the nanomaterials and polymers with amino, sulfonic and hydroxyl groups which enhance the attraction between particles and the polymer material.[114,115] Ultimately, the proton conductivity, methanol permeability resistance and hydrophilicity of the composite membrane improved by using this method. Pourzare et al.[116] functionalized the different types of CO_3O_4 (nanospheres, nanooctahedra, and nanorods) with TEOS and amino 3-aminopropyltriethoxysilane (APTES) and added them to the membrane to form a composite membrane [Fig. 8(a)]. They found that the increased interaction between functionalized particles and the polymer in the composite membrane delivers a high proton conductivity value, thermal stability and water uptake. The composite based membrane with 1 wt% fillers provides high proton conductivity which increases with increasing temperature [Fig. 8(b)]. The composite membrane with 5% octahedral nanoparticles delivers a high selectivity value of 15.2×10^4 S s^{-1} cm^{-3} and a methanol permeability value of 5×10^{-7} cm^2 s^{-1}, with the former value being approximately 3.6 times greater than that of the pristine commercial Nafion membrane (selectivity value: 4.2×10^4 S s^{-1} cm^{-3}) [Fig. 8(c)].

In another example, Sharma et al.[117] prepared a silane modified SPEEK polymer composite membrane by treating SPEEK with different concentrations of APTES through the in situ sol–gel method. The results show that hydrogen bonding between amino groups of APTES and sulfonic groups of SPEEK gives strength to the membrane which directly improves the quality of ionic channels. The hydrophilic groups attract a large amount of water and capture it within the channel which not only enhances the proton conductivity but also increases the stability. As a result, the silane functionalized SPEEK membrane with 0.8 wt% APTES shows an improvement in IEC and proton conductivity values of 21% and 70% respectively which are higher than those of the SPEEK membrane. Moreover, due to the tortuous pathway in the modified membrane, the methanol crossover or permeability value reduces to 5.30×10^{-7} cm^2 s^{-1}, while the SPEEK polymer membrane shows a high methanol permeability value of 12.55×10^{-7} cm^2 s^{-1}. With better proton conductivity and limited methanol permeability, the modified membrane is able to attain a high selectivity value of 4.43 S s^{-1} cm^{-3} which is higher than that of the bare SPEEK polymer membrane [0.31 S s cm^{-3}].

Different studies show that the sulfonic groups attached to the nanomaterials positively affect water uptake by overlapping with water through strong interactions between them and create ionic clusters, which ultimately boost the proton conductivity. As an example, Li et al.[118] prepared a composite membrane of the polymer SPEEK with the filling of SSiO$_2$ and S(ZIF-C). The strong interaction between these two inorganic nanoparticles and the polymer led to uniform dispersion and created an ionic channel within the membrane so it could conduct more protons. The sulfonic groups of each component in the composite membrane provide better thermal stability, high water uptake and better methanol retardation. With 1 wt% SSiO$_2$ and 3 wt% S(ZIC-C), the composite based membrane delivers a proton conductivity value of $(164.9 \pm 4.6) \times 10^{-3}$ S cm^{-1} and a methanol crossover value of approx. 3.07×10^{-7} cm^2 s^{-1}, while under similar conditions, the proton conductivity and methanol uptake of Nafion 115 are 139.7×10^{-3} S cm^{-1} and 14.81×10^{-7} cm^2 s^{-1} respectively. When applied in DMFCs, the composite membrane with dual nanoparticles shows an excellent power density value of 128.6 mW cm^{-2}, which is 2 times greater than the value of Nafion 115 under similar conditions. All those research papers that depict the use of silica nanoparticle-based composite membranes are summarized in Table 4.

5.2. Titania (TiO$_2$)

Among these inorganic materials, titanium oxide or tiania (TiO$_2$) is considered a promising candidate for use as a filler due to its hydrophilic nature, inert property and mechanically strong structure that directly improves the physical and electrochemical properties of the membrane in a fuel cell. Due to acid–base interaction, titania creates hydrogen bonds with the polymer which leads to uniform dispersion throughout the polymer matrix without aggregation. Moreover, the inclusion of titania in the polymer matrix greatly reduces the crystallinity of the composite based membrane which creates nano- and
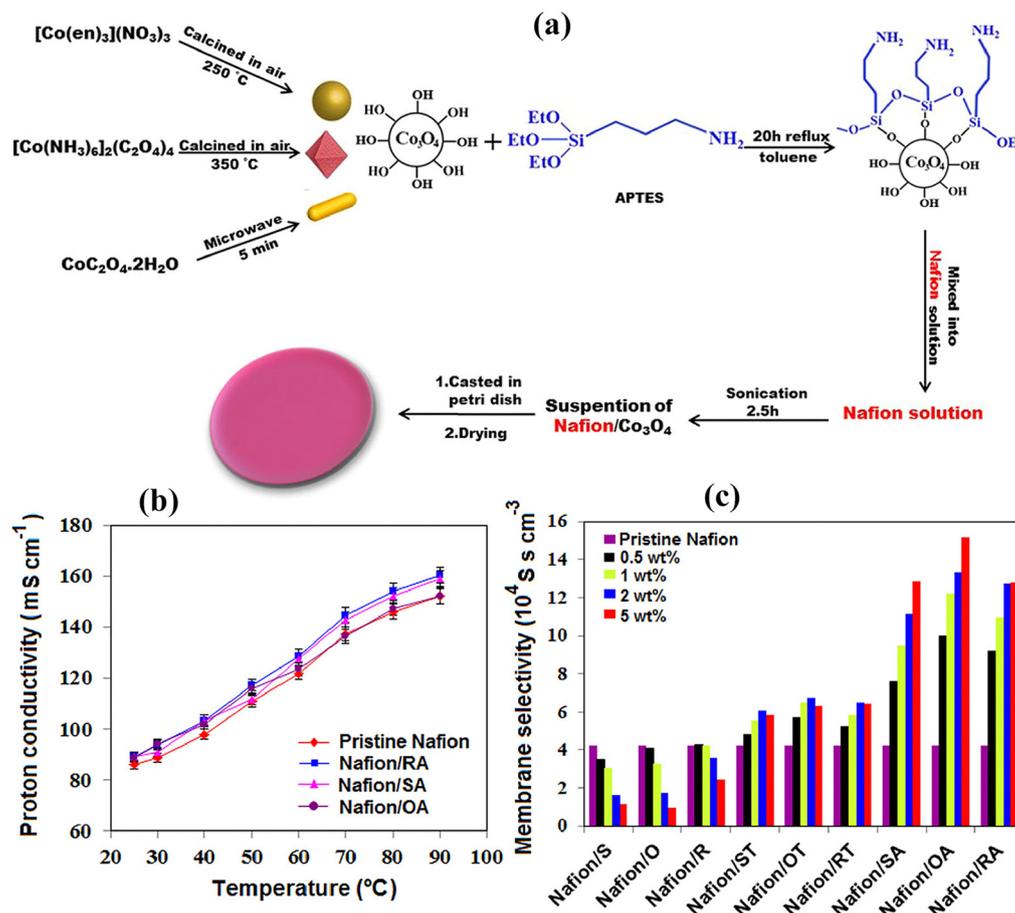
Fig. 8 (a) Schematic illustration of the preparation of different types of Co_3O_4 nanostructures and their functionalization with the silane group as well as the preparation process of the Co_3O_4 nanostructure based Nafion composite membrane. (b) The proton conductivity values of pristine Nafion and Nafion/Co_3O_4 nanocomposite membranes at 95%. (c) Different types of nanostructure based composite membranes *vs.* selectivity values.[116] With copyright permission, 2023, American Chemical Society.

Table 4 Details of the SiO_2 based composite membrane

Organic/inorganic nanomaterials	Polymer	Thickness (µm)/ anode supply	Proton conductivity ($\times 10^{-3}$ S cm^{-1})	Methanol permeability ($\times 10^{-7}$ cm^2 s^{-1})	Selectivity ($\times 10^4$ S s cm^{-3})	Power density (mW cm^{-2})	Ref.
SiO_2–SO_3H-3 wt%	SPEEK/PVA	—/air	62	6.10	10	3.64 [RT]	111
Silica	Nafion	—/O_2	39.4	27.1	—	117 [60 °C]	112
Silica	Nafion	0.230/air	1.8	0.0124	—	—	113
Co_3O_4-5 wt%	Nafion	64 ± 5/—	160	5	5.2	—	116
Silica-0.8 wt%	SPEEK	—/—	23.5 [30 °C]	2.12	11.08	—	117
S(ZIF-C)/SSiO_2-3%	SPEEK	100/O_2	Apporx. 164.9	3.07	—	128.6	118

microspores in the membrane and helps to attain free movement of protons.[119] To test the role of titania in DMFCs, Khalifa *et al.*[120] made a membrane composed of phosphoric functionalized cellulose acetate and different percentages of titania nanoparticles from 0 to 10% using the casting solution method. The nanoparticle addition to the membrane converts it into a smooth and crack free surface. Moreover, surface modification and ultrasonication lead to highly uniform dispersion in polymer solutions. The membrane exhibits high thermal stability and mechanical strength (49.9 MPa) due to the coordination bond between Ti^{4+} and the cellulose acetate group, which

delays the decomposition of the cellulose acetate material. The water uptake value decreases from 0 to 10% because the particles occupy the free volume and reduce the swelling ratio of the composite membrane. The uptake increases with increasing temperature due to the high specific volume, which boosts water absorption. The results show that the IEC of the composite based membrane increases with increasing temperature because of the great attraction between counter ions and the functionalized group of cellulose acetate. The IEC of the prepared composite based membranes achieved a value of 1.13 meq. g^{-1} and 2.010 meq. g^{-1} at temperatures of 25 and

Table 5 Details of the TiO$_2$ based composite membrane

Organic/inorganic nanomaterials	Polymer	Thickness (μm)/ anode supply	Proton conductivity ($\times 10^{-3}$ S cm^{-1})	Methanol permeability ($\times 10^{-7}$ cm^2 s^{-1})	Selectivity ($\times 10^4$ S s cm^{-3})	Power density (mW cm^{-2})	Ref.
TiO$_2$-5 wt%	CA	—/—	—	0.98×10^{-9}		—	120
TIO$_2$	Nafion	—/—	81 [40 °C]	—	—	64 [110 °C]	121

80 °C respectively at 5% titania loading as compared to that of the pristine Ph-Ca membrane which showed a value of 0.6 and 0.81 meq. g^{-1}, respectively, under similar conditions. The composite membrane showed high chemical stability due to high interaction between nanoparticles and cellulose acetate polymer. Titania nanoparticles prevent methanol crossover by minimizing the passage, which protects the cathode from poisoning. The 5% titania composite membrane delivered a methanol crossover or permeability value of $(0.98 \times 10^9) \times 10^{-7}$ cm^2 s^{-1} which is approx. 20% less than that of Nafion 117 $((1.14 \times 10^2) \times 10^{-7}$ cm^2 s$^{-1})$. The performance efficiency factor also increases in the case of the composite membrane with 5% titania nanoparticles due to the high IEC. The conductivity of the titania is still limited due to the hopping of fewer water molecules, which ultimately results in low performance of the proton exchange membrane. Sulfonation of the nanomaterials not only enhances their compatibility with polymers but also increases their hydrophilic properties, which is beneficial for the overall efficiency of the fuel cell by suppressing the methanol crossover and IEC. The researchers sulfonated the titania nanoparticles in order to fulfill the required characteristics of the PEM. Cozzi et al.[121] synthesized the organically modified inorganic nanoparticles named sulfonated titania (TiO$_2$–RSO$_3$H) by grafting a polysulfonic group on the surface of titania nanoparticles [Fig. S2(a), ESI†] and then incorporated them into Nafion solution to convert them into the composite based membrane. The interfacial interaction between the hydrophilic Nafion and the hydrophobic aliphatic chain of titania creates a uniform dispersion of titania nanoparticles throughout the membrane. The interaction between the polymer and nanoparticles creates a rigid structure which promotes thermal stability and protects the composite membrane from excessive swelling. The hydrogen bonding of the titania sulfonic groups with water molecules allows hopping of water molecules inside ionic channels and a high number of dissociate hydration ions are produced which promotes proton transfer through the Grotthuss mechanism. As a result, the composite membrane with 10 wt% functionalized titania is able to deliver a high proton conduction value of 80×10^{-3} S cm^{-1} at a high temperature of 140 °C. The sulfonated titania nanoparticles suppress the ionic channels and convert them into narrow ones which minimize the ability of small molecules like methanol to cross inside the membrane. Their tortuous path further reduces the methanol permeability. High proton conductivity and low methanol crossover result in a better selectivity value of 7.8×10^4 S s cm^{-3} which is greater than that of the recast Nafion membrane which shows 40% lower proton conductivity, selectivity and PD value as well as 40% minimized methanol crossover or permeability value when checking the performance of the DMFC single cell at a high temperature of 110 °C [Fig. S2(b and c), ESI†]. The data related to titania-blend composite membranes are given in Table 5.

5.3. Three dimensional nanomaterial use in composite membranes

The three-dimensional nanomaterials have shapes like cubes, boxes and pyramids. They are recognized by their high surface area, hydrophilic nature and surplus absorption sites. The most common example of three-dimensional nanomaterials is MOFs which are widely used in fuel cells. Due to their remarkable characteristics, such as adjustable structure, high porosity, and huge surface area, metal–organic frameworks (MOFs) which are assembled from metal and ligand components have drawn widespread attention. In a number of applications, such as gas storage,[122–125] medication delivery,[126,127] separation,[128,129] catalysis,[130,131] and others, they have shown excellent potential. The use of MOFs in proton conduction has also recently drawn steadily rising attention. The ability of protons to transfer through hydrogen-bonded networks or functional sites loaded in MOF pores has been established.[132–135]

Different types of MOFs such as ZIF-8, HKUST-1 and UiO-66 have been invented and applied as the PEM for application in different types of fuel cells.[136] The applications of these MOFs in the composite membrane are discussed one by one in detail in the following sections. Moreover, the MOF-related research papers are summarized in Table 6.

5.4. UiO-66

This type of MOF has also been studied along with other MOFs as a filler for PEMs. For example, Wang et al.[137] functionalized a MOF with an amino acid group (UiO-66-NH$_2$) and incorporated it in sulfonated polysulfone (SPSF). The amino acid functionalized MOF using glutamate provides a vehicular mechanism which boosts proton conductivity. Moreover, UiO-66-NH$_2$ accepts protons from glutamate carboxyl groups which accelerates proton dissociation and delivers smooth ionic channels through the Grotthuss mechanism. The UiO-66-NH$_2$-Glu-6 and SPSF based composite membrane delivered a high proton conductivity value of 212×10^{-3} S cm^{-1} at a temperature of 80 °C and a current density value of 70.45 mW cm^{-2} at 60 °C.

MOF aggregation in Nafion still exists due to the low interaction between polymers and nanomaterials. The researchers introduced fluoride in the MOF (UIO-66-NH$_2$) network, which enhances the dispersion and reduces the methanol crossover by creating nano-channels in the metal oxide framework. In one case, Wang et al.[138] prepared anode structures of MOFs modified with F species and mixed them into Nafion solution for making composite based membranes [Fig. 9(a)]. The strong interaction between Zr and F species creates a narrow channel, which promotes proton conductivity and reduces methanol crossover or permeability [Fig. 9(b)]. The researchers also found that the

Table 6 Details of MOF based composite membranes

| Organic/inorganic nanomaterials	Polymer	Thickness (μm)/ anode supply	Proton conductivity (× 10^{-3} S cm^{-1})	Methanol permeability (× 10^{-7} cm^2 s^{-1})	Selectivity (× 10^4 S s cm^{-3})	Power density (mW cm^{-2})	Ref.
BUT-8(Cr)-0.75 wt%	SPEEK	120–130 μm/air	32	1.6	7.2	88.6 (60 °C)	136
UiO-66-NH$_2$ (6 wt%)	SPSF	80 ± 10/O$_2$	212 (80 °C, 100% RH)	5.8	—	70.45 (60 °C)	137
UiO-66 (5 wt%)	Nafion	—/O$_2$	250(80 °C)	7.5	—	26.8	138
UiO-66 (0.6 wt%)	Nafion	—/—	256 (90 °C, 95% RH)	4.41 (40 °C)	—	—	139
GO@UiO-66 (0.6 wt%)	Nafion	—/—	303(90 °C, 95% RH)	0.174 (40 °C)	713 ± 1.305 [40 °C]	—	140
UiO-66/Pd-GO (3 wt%)	SPEEK	—/—	2.11 (25 °C)	3.58	0.6	—	141
MIL-MOFs (1 wt%)	SPAEK	—/O$_2$	184 (80 °C)	7.53	24.4	37.5 (80 °C)	142
MIL-101 (1.5 wt%)	SPAEK	59.4/O$_2$	188(80 °C)	61.8 (80 °C)	30.4	90.8 (80 °C)	143
ZIF-8 (2.5 wt%)	SPEEK	45 ± 5/—	50.24 (120 °C, 30% RH)	2.45 ± 1.9	5.924 ± 0.4680	—	144
ZIF-8 (11 wt%)	SPEEK	—/—	110 [80 °C]	0.0766 (75 °C)	—	113.77 (80 °C)	145
DNA@ZIF-8 (3/25)	PVDF	—/O$_2$	170 (75 °C, RH 97%)	0.125 (75 °C)	1400	9.87 (80 °C)	146
MIL-88B (40 wt%)	PAEK	—/O$_2$	142 (80 °C, RH 100%)	—	—	34.76 (80 °C)	147
MOFs (3 wt%)	SPEEK	170/O$_2$	45 (70 °C, 98% RH)	4.26	11.4	116 (60 °C)	148
Zr–Cr–SO$_3$H (0.5 wt%)	BSP	—/O$_2$	154 (80 °C, RH 100%)	—	—	64.6 (60 °C)	149
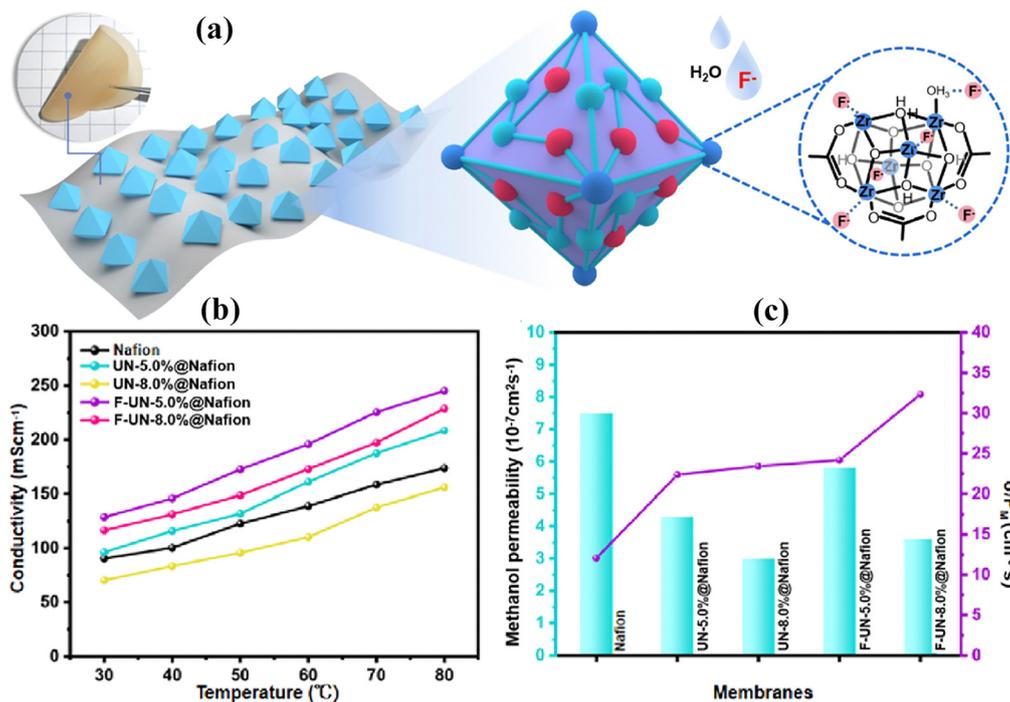
Fig. 9 (a) Graphical representation of the MOF based nanoparticle composite membrane. (b) Temperature *vs.* proton conductivity curves of Nafion and different amounts of UN as well as F-UN filled composite membranes. (c) Different amounts of UN and F-UN filled composite membranes *vs.* methanol permeability and selectivity curves.[138] With copyright permission, 2022, Elsevier.

hydrogen bonding between amino groups and other polar groups suppresses the large volume spaces in the polymer, which increases the thermal stability and reduces the swelling up to 30% which is lower than that of the Nafion membrane. With 8 wt% F-UN particles, the composite membrane delivers a 3.6–5.8 × 10^{-7} cm^2 s^{-1} methanol value which is lower than that of the recast Nafion membrane which shows a methanol crossover or permeability value of 7.5 × 10^{-7} cm^2 s^{-1} [Fig. 9(c)]. In a single cell performance test, the composite membrane with 5.0 wt% F-UN nanoparticles reached a power density value of 26.8 mW cm^{-2} which is nearly 31% greater than that of the recast Nafion membrane (20.4 mW cm^{-2}).

To further enhance the performance of the composite membrane, functionalizing the membrane with sulfonic groups has been developed by researchers. The sulfonic groups provide high water molecule trapping ability making the membrane more suitable for DMFCs. Rao *et al.*[139] prepared a composite based membrane by co-doping functionalized MOFs having both SO$_3$H and SO$_3$–NH$_2$ with Nafion solution. The two functionalized MOF based composite membranes created proper ionic channels and the amino and sulfonic groups bound to more water molecules which promoted proton conduction. Moreover, the 3-dimensional porous structure traps the methanol within the polymer matrix and reduces the

methanol crossover. The proton conductivity of the composite membrane reached a value of 256×10^{-3} S cm^{-1} (90 °C and 95% RH), which is almost 1.17 times greater than that of the recast Nafion membrane (118×10^{-3} S cm^{-1}). The researchers found that even after 3000 minutes of running the fuel cell at 90–95% humidity, there is no change in the proton conductivity value. However, the proton conductivity is still very low and there is a need to improve the structure of the MOFs. For tuning the structure of MOFs, Rao et al.[140] combined graphene oxide nanosheets with UiO-66-NH$_2$ (MOFs) and incorporated them into the Nafion membrane. The graphene oxide's synergistic effect reduces the barrier of vehicular type and Grotthuss type movement of protons. The proton conductivity value reached 303×10^{-3} S cm^{-1} and 3.403×10^{-3} S cm^{-1} under a relative humidity value of 95% and under anhydrous conditions, respectively, at a temperature of 90 °C, which is about 1.57 times and 1.88 times greater than that of the recast Nafion membrane (118×10^{-3} S cm^{-1} and 1.182×10^{-3} S cm^{-1}) respectively under similar conditions. Furthermore, the MOF pores provide a tight control on methanol capture and the GO two-dimensional structure blocks the way of methanol permeability through the composite membrane. To further tune the proton conduction and methanol permeability, Das et al.[141] prepared a composite based membrane consisting of platinum nanoparticles (Pd), graphene oxide nanosheets, UiO-66 and PEEK polymer. The heteroatoms used in the composite membrane trap more and more electrons, which boosts the proton conductivity [2.110×10^{-3} S cm^{-1}]. The strong interaction of platinum nanoparticles with graphene oxide and MOFs creates a uniform ion channel for the passage of protons and reduces the free volume spaces in the polymer, which results in low methanol crossover. The sulfonic groups of SPEEK attract more water molecules. Thus, for the composite consisting of 10 wt% Pd, the selectivity of the composite based membrane reached 0.586×10^4 S s cm^{-3} which is 2 times greater than the selectivity value of Nafion-117.

To enhance the proton conductivity and methanol resistance of MOFs, Ru et al.[142] prepared an ionic liquid filled MOF and mixed it with a SPAEK polymer to make a composite membrane. The sulfonic groups of the ionic liquid and the carboxyl groups of the SPAEK polymer are strongly attached to the amino group of the MOF surface due to electrostatic attraction, which reduces the leakage of the ionic liquid and makes the membrane thermally stable. Moreover, these functional groups create a narrow ionic channel in the membrane to speed up proton conductivity and less tortuosity leads to low methanol uptake. With 1 wt% inorganic fillers, the composite membrane exhibits a proton conduction of 0.184×10^{-3} S cm^{-1} (80 °C), a methanol crossover or permeability value of 7.53×10^{-7} cm^2 s^{-1} and an excellent selectivity of 24.4×10^4 S s cm^{-3}. Moreover, high dimensional stability is provided by the highly compact MEA layer with low resistance which ultimately delivers a high power density value of 37.5 mW cm^{-2} which is greater than that of the SPAEK polymer membrane. However, the ionic liquid leaches out from the MOFs due to weak bonding which depletes the advantage of the

full use of ionic liquids. To tackle the leakage of the ionic liquid, Y. Duan et al.[143] further doped the SPAEK polymer membrane with synthesized alkyl sulfonic group containing MOFs (MNCS). The functional groups of the MOFs create a smooth pathway for proton conduction and the functional groups of the polymer further tune the nano channel created by the MOFs. The acid–base attraction between MOFs and the polymer increases dimensional stability and methanol resistance. With 1.5 wt% MOFs, the composite membrane exhibits a high proton conductivity value of 188×10^{-3} S cm^{-1} and a power density value of 90.80 mW cm^{-2} when assembled in the MEA of DMFCs.

5.5. ZIF-8

ZIF-8 has the ability to coat other surfaces, which not only increases its own performance but is also beneficial for the composite membrane. For example, Sun et al.[144] synthesized the ZIF-8 coated carbon nanotubes (ZCN) and incorporated them into the SPEEK polymer to create a composite membrane. The strong acid–base attraction between the sulfonic groups of the SPEEK polymer and Hmim units of fillers creates a compact structure, which only enhances the thermal stability and structural integrity at room temperature and does not support proton conduction due to the lack of free functional groups. However, the composite membrane containing 2.5 wt% ZCN delivered a high proton conductivity of 50.24×10^{-3} S cm^{-1} when tested at 120 °C and 30% relative humidity which is 11.2 times greater than the values of the pure SPEEK polymer and the composite membrane without ZCN which only deliver 4.50×10^{-3} S cm^{-1} and 24.1×10^{-3} S cm^{-1} respectively. The results show that the ZCN based composite membrane can serve as an efficient PEM for DMFCs.

The tuning of the composite membrane is very important to minimize methanol crossover. It is not possible to just add MOFs to the membrane. MOFs do not provide enough performance for the composite membrane. The researchers doped the MOFs with different materials in order to modify their structure to enhance compatibility with polymers and enhance methanol crossover resistance. Guo et al.[146] created DNA@ZIF-8 by joining the thin film of zinc hydroxide nano strands with single stranded DNA by the solid confinement conversion method at room temperature [Fig. 10(a)]. These modified MOFs are then incorporated into the SPEEK polymer to make the composite membrane. The DNA molecule develops hydrogen bonding with water molecules within the cavities of MOFs (ZIF-8) which promotes a high proton conductivity of 30.4×10^{-3} S cm^{-1} and 170×10^{-3} S cm^{-1} at room temperature (24–25 °C) and 75 °C respectively, under 97% relative humidity [Fig. 10(b and c)]. The compacted nano-channels inside the DNA@ZIF-8 composite based membrane are much smaller than the methanol molecule. So as a result, the methanol crossover was reduced to a value of 12.5×10^{-7} cm^2 S^{-1}. Due to the uniform dispersion of DNA@ZIF-8 and the well-ordered compacted structure, the composite membrane shows zero swelling after a dip in water. The high proton conductivity value and low methanol crossover lead to a high selectivity of
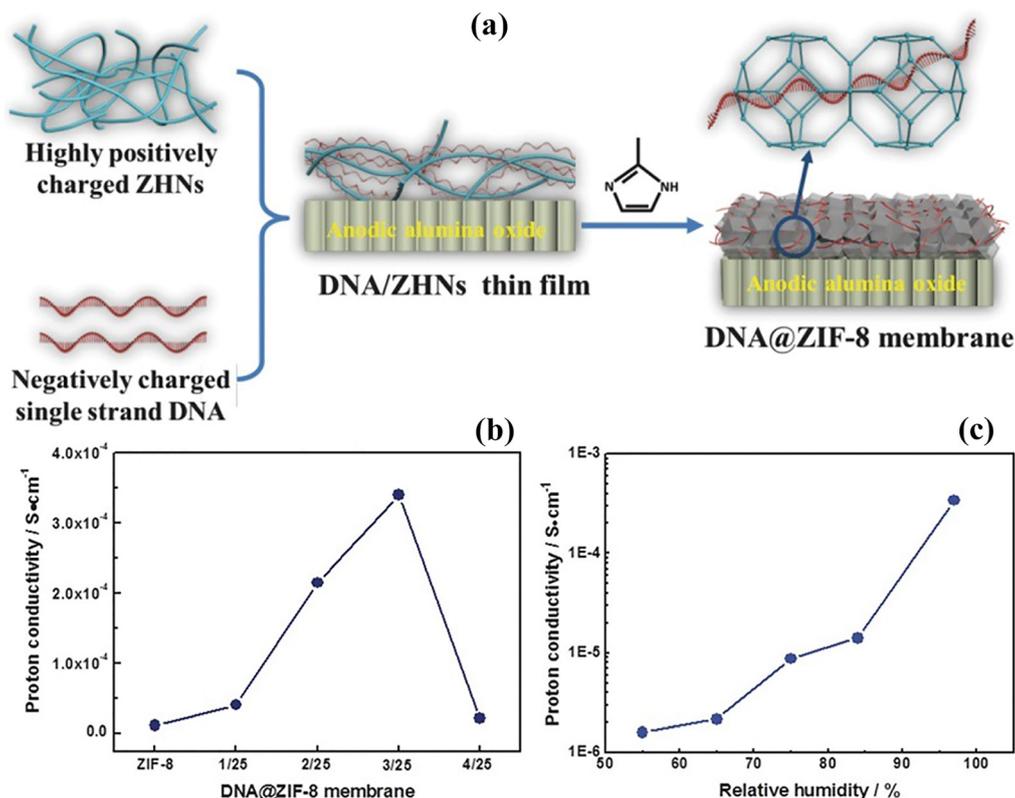
Fig. 10   (a) Schematic diagram of the synthesis procedure of the DNA covered ZIF-8 composite membrane. (b) ZIF-8 based and DNA@ZIF-8 based composite membranes with different amounts of DNA *vs.* proton conduction value curves. (c) Relative humidity (%) *vs.* proton conductivity values of the DNA@ZIF-8 (ratio: 3/25) composite membrane at 25 °C.[146] With copyright permission, 2018, John Wiley and Sons.

the DNA@ZIF-8 membrane. The researchers found that the DNA@ZIF-8 hybrid composite membrane exhibits a power density of 9.87 mW cm^{-2} when assembled in a single cell of DMFC.

MOFs are only used for proton conduction, but hydroxide conduction is also necessary to promote the performance of the DMFC fuel cell. The researchers have studied and found that if MOFs are treated with a material that has the ability to conduct anions and cations at the same time, it could increase the performance of the DMFC. For example, Y. Guo[145] treated ZIF-8 with zwitterion SBMA to create a zwitterion based MOF and incorporated it into the SPEEK polymer to make a composite membrane. The composite membrane has the capability of both cation and anion conductivity. The hydrophilic nature of cationic QA and sulfonate groups of anionic SMBA develop an ionic transport channel in the composite membrane through hydrogen bonding which facilitates hydroxide and proton transfers. The methanol permeability also minimizes due to the nano-size channels (0.34 nm) of the MOF based composite membrane. With 11 wt% SMBA, the PEM possesses a high proton conductivity of 1.030×10^{-3} S cm^{-1} and 36.2×10^{-3} S cm^{-1} and hydroxide conductivity values of 117×10^{-3} S cm^{-1} and 2.520×10^{-3} S cm^{-1} at a temperature of 25 °C and 75 °C respectively under 95% relative humidity. Moreover, due to narrow channels in the composite based membrane, the researchers found that methanol permeability reduces to 0.0766×10^{-7} cm^2 s^{-1} at

75 °C. For the full single cell assembly, the composite based membrane exhibits a better powder density of 113.77 mW cm^{-2} for the DMFC single cell.

5.6.   Mil-88

The MIL-88 family: $[M_3^{III}O(H_2O)_2X(dicarbox)_3]\cdot$guest (M = Fe, Cr; X = F, Cl, acetate) contains an unusual breathing mechanism after absorption of a polar solvent and provides the main framework which acts as an efficient smooth and flexible substrate for application of electrolyte materials.

The scientists also studied the composite membrane containing a Mil-88 based metal organic framework, which shows high physical and electrical performance as compared to the commercial membrane in DMFCs. Z.-H. Li et al.[147] synthesized a sulfonated flexible metal organic framework (FMOF) that is based on chromium metal (sulfonated MIL-88(Cr)-NH$_2$–SO$_3$H or PMNS) and incorporated it into the PAEK polymer to develop a composite membrane [Fig. 11(a)]. The chromium inertness and its bond with a carboxyl group of MOFs make the composite membrane highly thermally as well as chemically stable. Strong physical interaction [hydrogen bonding] between the sulfonic groups of FMOFs and water molecules creates non-swelling ionic channels throughout the membrane which provide an unbreakable proton conducting pathway [Fig. 11(b and c)]. As a result, the proton conductivity of PMNS1 and PMNS2 ultimately reaches values of 66.9×10^{-3} and 22×10^{-3} S cm^{-1} [100% relative humidity and
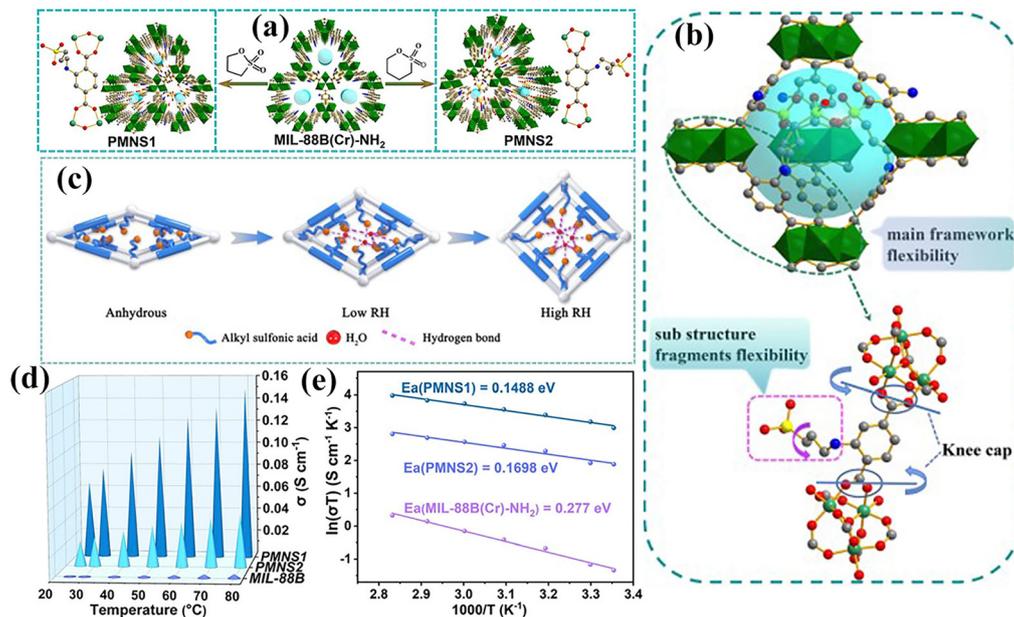
Fig. 11 (a) Illustrations of PMNS1 and PMNS2 synthesis. (b) Schematic explanation of multivariate synergistic self-adaption [PMNS1]. (c) Logical explanation of a model of mechanism containing multivariate synergistic self-adaption of RH. (d) Temperature vs. proton conductivity values of PMNS1-2 and MIL-88B. (e) Arrhenius plots of the proton conductivity of different types of membranes [(PMNS1), (PMNS2) and (MIL-88B (Cr)-NH$_2$)] at a relative humidity value of 100%.[147] With copyright permission, 2021, John Wiley and Sons.

25 °C temperature] respectively which are superior to that of any kind of composite membrane based on MOFs. Moreover, owing to the Grotthuss type proton conduction provided by strong bonding between H$_2$O and –SO$_3$H groups the activation energy is reduced. The composite based membrane is able to deliver a proton conduction value of 152×10^{-3} S cm^{-1} at 100% relative humidity and 80 °C which is 3 times and 38 times greater than that of PMNS2 (46.8×10^{-3} S cm^{-1}) and the pristine MIL-88B (Cr)-NH$_2$ (3.92×10^{-3} S cm^{-1}) under similar conditions [Fig. 11(d and e)]. The long-lasting stability and high proton conduction make the composite membrane a promising candidate for the DMFC fuel cell, which can deliver a power density value of 34.76 mW cm^{-2} when assembled in a single cell.

5.7. Copper based MOFs

HKUST-1 or CU-BTC is a copper-based MOF that is widely used in electrochemical devices because of its high hydrophilic nature, high surface area, chemical stability and easy dispersion in solvents and polymers due to strong interaction.[150] Moreover, the nano-porous structure with pore sizes of 1 Å and 1.4 Å provides efficient blockage of the methanol to further approach the cathode and save it from poisoning. When water molecules interact with HKUST-1 in the composite membrane, it becomes acidic and provides more protons for conduction through an acid–base reaction. Cu-BTC shows a paddle-wheel-like structure. The HKUST with Cu metal corners joined by benzene 1,3,5-tricarboxylate organic linkers. The four oxygen atoms from the BTC connect further with other two copper atoms and ultimately create four linked square metal corners. Other axial coordination sites are classified as open metal sites.[151] N. K. Divya and other scientists[152] synthesized HKUST-1 and incorporated it into a

sulfonated chitosan polymer to make the composite membrane. The physical interaction between the sulfonic groups of the SPEEK polymer and the carboxylic groups of HKUST-1 creates a compact membrane with finger like ionic channels which not only provide mechanical strength and reduce swelling but also stabilize the structure of the composite membrane at high temperatures. The copper sites (Cu^{2+}) in HKUST-1 attract more and more water molecules and increase hydration ions which pass the ionic channels through the Grotthuss and vehicular mechanisms by using hydrogen bonding between the polymer and MOFs. The researchers also found that proton conductivity is directly related to IEC. When proton conductivity goes up, the IEC goes up. The non-swelling nature created by MOFs in the composite membrane restricts the path for the methanol and the tortuous pathway further reduces the methanol permeability throughout the composite membrane. The high methanol permeability and restricted methanol crossover value determine the high selectivity of the composite membrane. Ultimately, the composite membrane with 0.5 wt% MOFs delivers a water uptake of approximately 26% and a proton conductivity value of 5.38×10^{-3} [25 °C] and 6.19×10^{-3} S cm^{-1} [80 °C] compared to the pristine membrane [1.26×10^{-3} S cm^{-1}] [Fig. S3(a and b), ESI†]. Furthermore, it is also able to reduce methanol crossover to a value of 0.301×10^{-7} cm^2 s^{-1} and selectivity to 17.8×10^4 S s cm^{-3}.

The other types of copper based MOFs were also studied for composite membranes which give better results and boost the overall efficiency of the PEM. For example, Niluroutu et al.[153] made a copper based trimesic acid MOF (Cu-TMA) and incorporated it into the SPEEK polymer to make a sheet type composite membrane. The copper ions in the MOF attract a large amount of water molecules and the physical interaction

[hydrogen bond] between the COOH group of the MOF and the sulfonic groups of the polymer creates a bridge to move the proton within the polymer matrix through the Grotthuss mechanism [Fig. S3(c), ESI†]. This hydrogen bonding is also responsible for creating a rigid and less swollen structure with a small diameter of channels that minimize the methanol cross-over while keeping the structure dimensionally stable. Ultimately, thermal stability, mechanical strength, water uptake, proton conductivity and IEC increase. Owing to its low methanol perme-ability and superior ion conductivity, the composite based membrane delivers a high power density value. As shown in Fig. S3(d) (ESI†), due to the strong interactions between the polymer and the MOF, the charge resistance reduces and with 3 wt% MOF content, the proton conductivity reaches 45×10^{-3} S cm^{-1} [98% RH] at a high temperature of 70 °C by minimizing the activation energy [7.26 kJ mol^{-1}]. It also restricts the methanol permeability to a value of 4.26×10^{-7} cm^2 s^{-1} which is lower than the pristine SPEEK membrane methanol permeability value. When applied in the DMFC [single assembled cell], the compo-site membrane with 3 wt% MOF also shows a power density value of 116.0 mW cm^{-2} and a current density value of 570.0 mA cm^{-2}.

5.8. Hybrid nanomaterial use in the composite membrane

The coating of nanomaterials on other particles not only provides structural stability but also enhances their mechanical strength and methanol crossover resistance. For example,

graphene oxide contains a sheet like structure, which enhances the active site area for water absorption in a limited amount because of its amphiphilic nature. Therefore, hybridization with other nanomaterials provides a high synergistic effect, improving mechanical strength and proton conduction through well-ordered and more functionalized channels in the composite membrane.[154] Rath *et al.*[155] synthesized hybrid silica covered graphene oxide by using an economical and efficient *in situ* method followed by the incorporation of nanoparticles in PVDF-HFP material which was converted into a membrane and sulfo-nated. The FESEM results show that the silica semi-spherical particles uniformly cover the graphene. The composite membrane shows a honeycomb like spherical structure. The hybrid nano-particle membrane with sulfonation appears rougher as com-pared to the non-sulfonated composite membrane because of the several groups on the surface (sulfonic, hydroxyl and carboxyl groups). Due to these functional groups, more water molecules are attracted by the composite membrane which ultimately tunes up the proton conductivity [0.13 S cm^{-1}] when tested at room temperature [Fig. 12(b)].

Due to the strong interactions between the polymer and functional nanoparticles, the polymer inner structure does not become damaged due to swelling and gives high conductivity at elevated temperatures [Fig. 12(c)]. Moreover, the functional groups and the covalent bond between graphene oxide and silica bound the methanol which produces less poisoning on
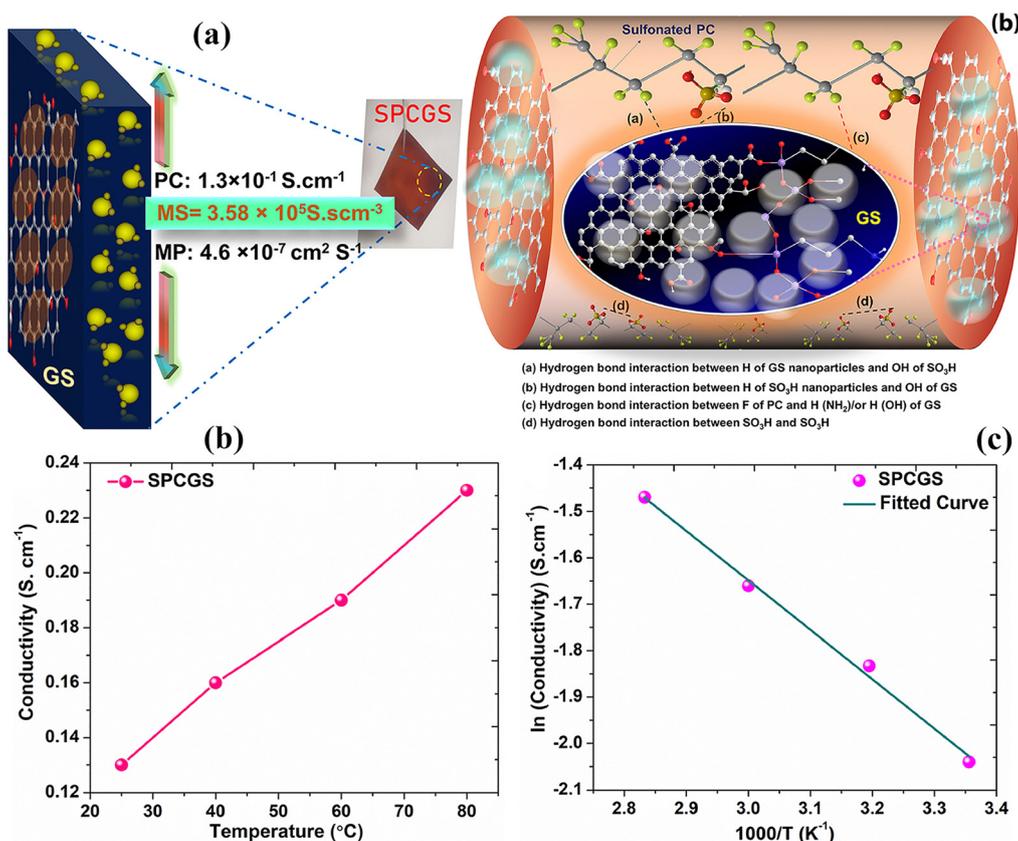

Fig. 12 (a) Graphical representation of the properties of SPCGS and its interactions within the chemical structure. (b) Temperature *vs.* proton conductivity value of the SPCGS membrane. (c) Arrhenius plot of SPCGS.[155] With copyright permission, 2023, Elsevier.

Table 7 Details of hybrid nanomaterial based composite membranes

Organic/inorganic nanomaterials	Polymer	Thickness (µm)/ anode supply	Proton conductivity ($\times 10^{-3}$ S cm^{-1})	Methanol permeability ($\times 10^{-7}$ cm^2 s^{-1})	Selectivity ($\times 10^4$ S s cm^{-3})	Power density (mW cm^{-2})	Ref.
ZnO@Al$_2$O$_3$-7 wt%	SPSF	60 µm/O$_2$	348 [80 °C]	4.21	—	405.7	154
SiO$_2$@GO	SPVDF-HFP	—/—	130 [25 °C]	4.66	35.8	—	155
SiO$_2$–Al$_2$O$_3$ (25/75)	SPEEK	—/—	61	5.00	—	—	157
TiSiO$_4$-2.5 wt%	SPEEK	—/O$_2$	45.37 ± 0.13 [30 °C]	4.27 ± 0.28	12.785 ± 7.16	—	158

the cathode [Fig. 12(a)]. The composite membrane shows a methanol permeability value of 4.66×10^{-7} cm^2 s^{-1}, which is 93.36% less than that of the commercial-Nafion 117 membrane [69.3×10^{-7} cm^2 s^{-1}]. The hydroxyl group of the silane-functionalized graphene forms a covalent bond with silica which enhances the thermal stability as well as the mechanical properties of the composite membrane [606.01 ± 56 MP].

Silica nanoparticles also show low proton conductivity due to their low compatibility with polymers and nonconductive properties. Due to these drawbacks, they easily aggregate in the polymer membrane. Two nanomaterial combinations enhance the deficiencies of each other in the composite membrane.[156] For example, alumina and silica combined nanoparticles were synthesized with the help of SiWA by Ismail *et al.*[157] and added to SPEEK to make a composite membrane. The solid SiWA contents in the composite membrane provide high water uptake due to its three dimensional cage like structure. The nanoparticles and sulfonic groups bound more water molecules, which not only enhances proton conductivity but also plays an important role in membrane stability due to the rigid structure of the nanoparticles. Moreover, the attraction between the sulfonated polymer and inorganic particles creates a dense structure by closing the pores of the membrane, which retards the passage of methanol. The composite based membrane with 66% sulfonation, 70% SiWA, 25% and 75% alumina showed an improved overall factor of 58.95×10^3 which is greater than that of the Nafion membrane which shows 10.65×10^3 under similar conditions.

For example, titania silicon oxide which is usually prepared by the calcination process of titania silica is one of the ceramic hybrid materials that improves the physical and electrochemical properties of the PEM when dispersed in the solution. It has been studied with Nafion[56] and PVDF. As an example, Chikumba *et al.*[158] prepared a composite based membrane by incorporating synthesized titanium silicon oxide (TiSiO$_4$) in a SPEEK polymer by the solution casting method. The hydroscopic nature of the titania silicon oxide boosts the water uptake when its amount increases from 0 to 1.5% in the membrane. The nanoparticles also restrict the polymer chain from expanding and not only hold

more water molecules but also enhance the thermal and mechanical stability of the membrane. The high water uptake due to the sulfonic groups of the polymer and the hydrophilic nature of nanoparticles has a positive impact on the proton conductivity and its value reaches approx. 98.86×10^{-3} S cm^{-1} which is close to the conductivity of the Nafion membrane. With 1.5% and 2.5% nanoparticles, the selectivity of the composite based membrane is 2.5 times greater than that of the commercial Nafion membrane and delivers 23.3% more output power than Nafion. All data related to hybrid nanoparticle-based composite membranes are summarized in Table 7.

5.9. MoS$_2$ use in the composite membrane

MOS$_2$ is one of the inorganic compounds that has a hexagonal two dimensional structure[159] just like graphite and consists of an M atom sandwiched between two S atoms. The hydrophilic nature and high surface area of this material provide a better pathway for proton conduction in the PEM when blended with a polymer.[160] All related research papers on MOS$_2$ use in composite membranes are summarized in Table 8. As an example, Feng *et al.*[161] prepared a composite based membrane consisting of MOS$_2$ flakes and Nafion solution by using the (NH$_4$)$_2$MoS$_4$ precursor. The strong physical interaction between the precursor and the sulfonic group of Nafion helps to form MOS$_2$ flakes around the ionic cluster of the composite based membrane, which promotes proton conduction. The presence of MOS$_2$ in the composite based membrane promoted the retardation of methanol permeability by blocking the channel and boosted the tortuosity of the membrane. The results show that the composite membrane with 0.5% MOS$_2$ proves much better at improving proton conduction and methanol or fuel permeability as compared to 0.1% MOS$_2$ because of the availability of a surplus amount of water molecules in the membrane. Consequently, the composite based membrane selectivity reaches two times that of the Nafion membrane at 50 °C and an 80% volume based methanol.

The exfoliation of the material is the common method by which MOS$_2$ nanoparticles can be converted into nanosheets, which increase the surface area of the material and have a

Table 8 Details of the MOS$_2$ based composite membrane

Organic/inorganic nanomaterials	Polymer	Thickness (µm)/ anode supply	Proton conductivity ($\times 10^{-3}$ S cm^{-1})	Methanol permeability ($\times 10^{-7}$ cm^2 s^{-1})	Selectivity ($\times 10^4$ S s cm^{-3})	Power density (mW cm^{-2})	Ref.
MoS$_2$	PVA		48	17.2	32	—	160
MoS$_2$-0.5 wt%	Nafion	—/—	130 [100% RH]	0.0672 [25 °C]	1700	—	161
E-MOS$_2$	SPES	—/—	3.17 (RT)	0.376	8.43	—	162
MoS$_2$@CNT	SPEEK	—/O$_2$	131 (80 °C)	5.2	3.2	98.5 (70 °C)	163
MoS$_2$	SPEEK	—/O$_2$	123 (80 °C)	21.5 (70 °C)	—	82.7 (70 °C)	164

positive effect on the performance of the DMFC. Divya et al.[162] synthesized the MOS$_2$ nanosheets and incorporated them into SPES polymer solution for making a polymer electrolyte membrane. The physical interaction [hydrogen bond] between the sulfonic groups of SPES and the hydroxyl groups of MOS$_2$ is responsible for maintaining the uniform dispersion of the nanosheets throughout the entire membrane. The MOS$_2$ nanosheets create an ionic channel that enhances the proton conductivity and their hydrophilic nature provides high electrolyte uptake and a lower contact angle when the amount of MOS$_2$ nanosheets increases from 0 to 1% in the composite membrane. The nanosheets also increase the thermal decomposition of the composite membrane by creating a bridge through the hydrogen bonding between MOS$_2$ and SPES and enhance the IEC of their functional groups. The sulfonation of the polymer creates a hydrophilic region as well as a hydrophobic backbone which promotes a narrow ionic channel. Furthermore, after the addition of MOS$_2$ nanosheets from 0.5 wt% to 1 wt%, the size of the channel decreases which reduces the methanol permeability from 0.514×10^{-7} cm^2 s^{-1} to 0.376×10^{-7} cm^2 s^{-1} while Nafion shows a methanol permeability value of 1.77×10^{-7} cm^2 s^{-1} and 55×10^{-7} cm^2 s^{-1}. The superior proton conduction and low methanol crossover or permeability of the composite based membrane deliver a selectivity value of 8.43×10^4 S s cm^{-3} with 1 wt% MOS$_2$ sheets.

MOS$_2$ is also used to convert a conducting surface into a non-conducting material by coating its surface for application in polymer membranes. The coated material with MOS$_2$ easily disperses in the polymer solution because of the physical interaction between them.

Zhong et al.[163] synthesized molybdenum based carbon nanotubes (MOS$_2$@CNT) by the facile in situ method in which molybdenum nanosheets were anchored on the carbon nanotubes with the help of glucose and formed a core–shell structure. These core–shell materials were then added to the SPEEK polymer solution and made into the polymer composite membrane [Fig. S4(a), ESI†]. The one-dimensional structure of CNT and 1 wt% MOS$_2$ nanosheet coating creates an ion channel which provides high water uptake, proton conductivity of about 1.7 times higher than that of the pristine SPEEK polymer membrane and low methanol crossover or permeability. The hydrogen bonding between MOS$_2$@CNT and the SPEEK polymer leads to low crystallinity and thermal decomposition [Fig. S4(b), ESI†]. Moreover, hydrogen bonding also proves effective for improving the mechanical strength of the composite membrane and a composite membrane with 1 wt% MOS$_2$@CNT shows a mechanical strength value of 65.7 MPa as compared to the SPEEK polymer which delivers a tensile strength value of 39.1 MP. The proton conduction value increases with increasing temperature which also proves the stability of the composite membrane under high temperatures [Fig. S4(c), ESI†]. At a temperature of 70 °C, the composite membrane based on SPEEK with 1 wt% MOS$_2$ delivers a power density value of 98.5 mW cm^{-2} which is 73.7% greater than the values of the commercial Nafion-115 membrane and the SPEEK membrane.

To further enhance the surface area of MOS$_2$, Zhang et al.[164] synthesized MOS$_2$ nano-flowers by the eco-friendly hydrothermal

method and included them in the SPEEK polymer solution to make a proton exchange membrane. Due to the high surface area, abundant active sites and physical interaction [hydrogen bonding] between MOS$_2$ and SPEEK polymer, the nano-flower like MOS$_2$ attracts more water molecules and cages them and its three dimensional structure avoids the aggregation of MOS$_2$ nano-sheets in the composite membrane. The strong bonding with water molecules boosts the proton conductivity and with 1 wt% MOS$_2$ the proton conduction of the SPEEK polymer membrane reaches 123×10^{-3} S cm^{-1} when tested at 80 °C. The tortuous path created by MOS$_2$ suppresses the methanol permeation and the value reduces to 21.5×10^{-7} cm^2 s^{-1} at 70 °C. The results show that the composite based membrane containing 1 wt% MOS$_2$ shows a 59.7% increase in proton conductivity and a 79.1% lower methanol crossover or permeability than the pristine SPEEK polymer membrane. With these advantages, when tested in a DMFC single cell at a temperature of 70 °C, the composite membrane is able to deliver a maximum power density value of 82.7 mW cm^{-2} which is 64.7% greater than the value of the bare SPEEK membrane which shows a value of 50.2 mW cm^{-2} under similar conditions. Moreover, the composite based membrane delivers stable performance after 100 h at a temperature of 70 °C.

5.10. Two-dimensional nanomaterial use in composite membranes

The 2D nanomaterials are also employed in composite membranes because of their high surface area, high mechanical strength, and easy blending with polymers without damaging the porous structure.[165] Their micro- to nano-pores deliver cavities to hold more water molecules, and their methanol repulsion property provides methanol crossover protection, which protects the cathode from destruction. These two-dimensional particles have a high surface area, which provides a large active site for water molecules and creates a strong pathway for the transfer of protons through the membrane. The details are summarized in Table 9.

5.10.1. Layered hydroxides (LDH). Layered hydroxides (LDH) are a class of two-dimensional materials, among which magnesium hydroxide also called brucite [octahedral layer] exchanges its divalent magnesium ions with trivalent aluminum ions. As a result, a positive charge is generated which is neutralized by the anion of the interlayer.[179,180] Simari et al.[166] prepared a hydrophilic layered hydroxide and mixed it with Nafion to make a composite membrane. The different methods of making composite membranes, such as the solution casting method by the doctor blade, the solution casting method by a Petri dish and the hydride layer [the doctor blade casting layer + casting solution] method are studied in order to examine the alignment of the 2D material. The results show that the hybrid layer delivers high water uptake, excellent proton conduction and minimum methanol uptake. The hybrid layer composite membrane contained aligned 2D nanomaterials, which act as hydrophilic media to attract more water molecules. Moreover one side [blade casting] retards the methanol and the other side [solution casting] creates an ionic channel for smooth proton crossover. The composite membrane aligned with LDH particles delivers a power density value of 300 mW cm^{-2} at 100 °C.

Table 9 Details of two dimensional nanomaterials used in composite membranes

Organic/inorganic nanomaterials	Polymer	Thickness (μm)/ anode supply	Proton conductivity ($\times 10^{-3}$ S cm^{-1})	Methanol permeability ($\times 10^{-7}$ cm^2 s^{-1})	Selectivity ($\times 10^4$ S s cm^{-3})	Power density (mW cm^{-2})	Ref.
LDH-3 wt%	Nafion	50 ± 5/O$_2$	238.5 ± 0.8 [120 °C]	20	—	300	166
MMT/GO-3%	SA/PVA	—/—	3.695	0.00524	7.053	1.761	167
GO-1.8%	Nafion	—/O$_2$	262 [90 °C]	0.9	177.2	32.5	168
GO-1 wt%	Nafion	—/air	33	—	—	4000	169
GO-0.5%	Nafion	—/O$_2$	20	7.92	5.05	141 [70 °C]	170
GO-0.5 wt%	SPI	—/O$_2$	120 [80 °C]	1.07	290	4	171
GO-SO$_3$H-0.5 wt%	Nafion	—/O$_2$	35% higher than Nafion	36	—	132 [60 °C]	172
Pd-GO	SPEEK	100 ± 10/—	2.5	4.6 ± 0.017	55.7	—	173
F-GO-1.5%/halloysite 3%	SPEEK	50/air	0.47	32.7% lower than Nafion	—	72.2	174
rGO-zeolite-2%	Chitosan	—/—	6.777×10^{-3}	0.20	—	—	175
0.75%	Nafion	—/O$_2$	214 [70 °C]	50% less than Nafion	—	165 [70 °C]	176
Boron nitride-5 wt%	SPEEK	—/—	40.8	1.31	31.12		177
Boron nitride-0.1 wt%	SPEEK	—/—	4.13	3.08	—	11.38	178

5.10.2. GO. Graphene oxide is also a two dimensional material with surplus functional groups (hydroxyl and carboxyl groups) which has a high surface area, a hydrophilic nature and better conductivity.[167,168,181] Due to hydrophilic functional groups, it easily mixes with polymers due to interfacial interaction and converts into sheets for application as the PEM of fuel cells.

Choi et al.[170] synthesized graphene oxide nanosheets and mixed them with Nafion solution to convert them into a composite membrane. They found a strong attraction between the hydrophilic and hydrophobic sulfonic groups of graphene oxide nanosheets which completely changes the microstructure of the Nafion membrane. Due to the well connected structure, more ionic channels develop which have a positive impact on proton conduction and methanol crossover or permeability control. With 0.5 wt% GO, the composite membrane delivers a proton conduction value and methanol crossover or permeability value of 40×10^{-3} S cm^{-1} and 7.92×10^{-7} cm^2 s^{-1} respectively. Due to low methanol permeability, the selectivity value boosts and reaches a value of 5.05×10^4 S s cm^{-3} at room temperature. Moreover, it also delivers a power density value of 141 mW cm^{-2} at 70 °C which is greater than that of the commercial Nafion membrane.

The size of graphene oxide is very important when making it a part of the polymer electrolyte membrane in DMFCs. The particle size affects not only the ionic channel morphology but also the overall efficiency of the fuel cell. He et al.[171] compared the results of different sizes of graphene oxide (60 nm) in the composite membrane. They found that with increasing graphene oxide size in the membrane, the physical and chemical characteristics show regular changes. Moreover, when the particle size decreases, the microstructure of the composite structure becomes well organized and defined which provides a high proton conduction value of $(12 \times 10^2) \times 10^{-3}$ S cm^{-1} at 80 °C and 100% relative humidity. The hydrogen bonding between graphene oxide and the sulfonated polyimide polymer enhances the tortuosity and thermal stability which reduces the methanol crossover to 1.07×10^{-7} cm^2 s^{-1} at room temperature. The overall power density of the composite membrane is 1.4 times greater than that of the pure sulfonated polyimide membrane at room temperature.

Functionalization of graphene oxide with different hydrophilic groups (amino, sulfonic, silane and other groups) makes better connections between the polymer and the nanomaterial which results in high proton conductivity, lower methanol crossover and high performance of the DMFC by depleting swelling and aggregation. For example, the Nafion microporous structure was tuned by adding functional graphene oxide by Choi et al.[172] They found that the sulfonic groups of the nano-fillers bound more water molecules, which promotes proton conductivity, dimensional stability and methanol resistivity through the composite membrane's high barrier ability. Gagliardi et al.[169] prepared a composite based membrane by adding GO to the Nafion solution in the range of 0.5 to 1%. The surplus hydroxyl and carboxyl groups of graphene oxide are responsible for attracting more water molecules and holding them. The graphene oxide also plays an important role in producing an ionic channel, which provides better proton conductivity. With 1% GO, the composite membrane delivers low methanol crossover by increasing membrane tortuosity. With increasing temperature, the composite membrane exhibits good performance and at 60 °C, 1 M methanol concentration and 7 μL min^{-1}, the optimum performance of the membrane is observed.

P. Das et al.[173] made a composite membrane consisting of amino functionalized palladium (Pd) based graphite oxide (GO). The palladium nanoparticles were first introduced on the surface of the graphite oxide nanosheets and then functionalized with L-tyrosine amino acids to convert into L-tyrosine grafted palladium graphite oxide. Then this synthesized material was mixed with a sulfonated PEEK polymer to make the composite membrane. The hydrogen bonding between the sulfonic groups of the SPEEK polymer and the amino functional group of Pd–GO provides better ionic clusters and enhances the stability of the membrane. The ionic channels allow the hopping of more and more water molecules, which promotes proton conductivity by providing surplus hydronium ions for proton transfer through Grotthuss and vehicular mechanisms. However, the proton conductivity of the L-tyrosine amino acid functionalized Pd-GO/SPEEK composite membrane [2.563×10^{-3} S cm^{-1}] is lower than that of the Nafion membrane [6.4×10^{-3} S cm^{-1}] but superior to that of the SPEEK polymer membrane which delivered 1.04×10^{-3} S cm^{-1} under similar conditions. The

narrow ionic channels created by the sulfonic group of polymers and functional groups of the nanomaterials in the composite membrane reduce the methanol crossover or permeability value from 21.8×10^{-7} cm^2 s^{-1} to 4.60×10^{-7} cm^2 s^{-1}. The researchers also found that the methanol reduction is also enhanced by the blocking effects of Pd and GO. Due to the superior proton conductivity and controlled methanol permeability of the SPEEK/Pd-GO-L-Tyr composite membrane, it delivers a high selectivity of 0.557×10^4 S cm^{-3} s which is higher than that of the SPEEK polymer membrane (0.048×10^4 S s cm^{-3}) and Nafion-117 membrane (0.278×10^4 S s cm^{-3}).

GO is also studied by blending with other nanomaterials to enhance the performance of the composite membrane. For example, Gokulakrishnan et al.[174] developed a composite membrane by incorporating silane functionalized graphene oxide (f-GO) and halloysite nanoclay in the SPEEK polymer membrane by the phase inversion method [Fig. 13(a)]. The hydrogen bonding between silane groups of GO as well as halloysite nanotubes and sulfonic groups of the SPEEK polymer compacts the structure with a minimum porous structure to attain maximum strength. The researchers observed that the methanol permeability decreased from 32.7% to 24% when the halloysite nanoclay amount increased from 0 to 5% due to particle agglomeration in the

composite membrane which depletes the free volume present in the polymer matrix. Further methanol permeability reduction occurs when f-GO is added in the composite membrane from 0 to 2 wt%.

The overall methanol crossover or permeability value of the composite membrane with both fillers was 32% lower than that of the pristine SPEEK polymer membrane. Moreover, the functional groups of the composite membrane interact with water molecules and more hydration ions are present for transport through the Grotthuss and vehicular mechanism and ultimately IEC increases from a value of 0.22 to 0.35 meq. g^{-1}. The composite membrane based on 3.0 wt% halloysite nanoclay and 2.0 wt% f-GO delivers proton conductivity and power density values of 0.47×10^{-3} S cm^{-1} and 72.2 mW cm^{-2} respectively, which are almost 2 times higher than that of the pristine SPEEK polymer membrane which shows a proton conduction value of 0.31×10^{-3} S cm^{-1} and a power density of 28 mW cm^{-2} [Fig. 13(b and c)]. The composite membrane with 1.5 wt% f-GO and 3 wt% halloysite nanoclay is a good alternative to the commercial-Nafion membrane in DMFC applications.

Reduced graphene oxide has a similar structure to graphene nanosheets and it is a reduced form of graphene oxide in which the oxygen groups of graphene oxide are reduced to enhance its
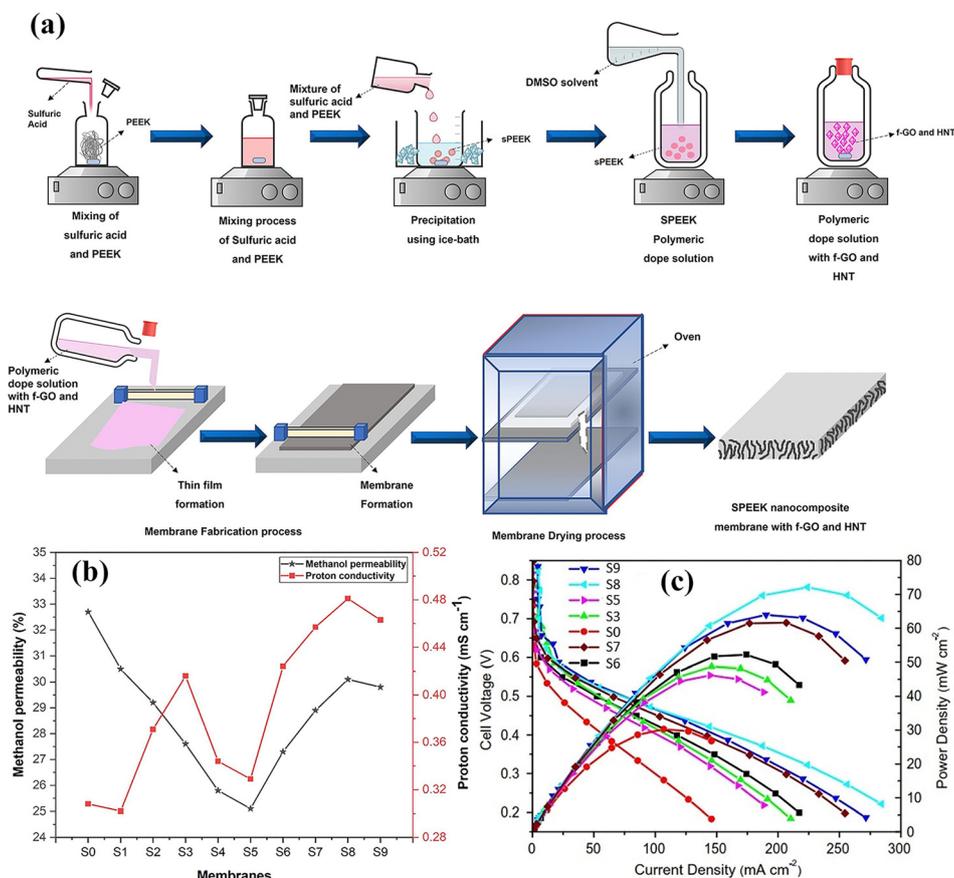

Fig. 13 Schematic diagram of the preparation process of sulfonated SPEEK incorporated with functionalized graphene oxide and HNT. (b) Pristine and SPEEK nanocomposite membranes with f-GO and HNT vs. methanol permeability and proton conduction values. (c) Current density vs. cell voltage and power density curves for different types of membranes with and without F-GO and HNT based membranes in a DMFC single cell.[174] With copyright permission, 2022, Elsevier.

characteristics.[182] Reduced graphene oxide possesses a high surface area along with high thermal and chemical stability. It also exhibits high mechanical strength due to its nanosheet structure. Sihombing et al.[175] checked the effects of rGO on the composite membrane made of chitosan and zeolite [Fig. S5(a), ESI†]. The water uptake capacity increases due to the hydrophilic nature of zeolite, chitosan and reduced graphene oxide and also their sulfonic groups, hydroxyl groups and carboxylic groups attract more and more water molecules due to hydrogen bonding.

However, excess water uptake increases the risk of high swelling when the rGO amount increases from 0 to 2 wt%. The reduced graphene oxide blocks the ionic channel passage, which ultimately reduces the methanol crossover while the functional groups of the nanomaterials and the chitosan polymer dissociate hydration ions which boosts the proton conductivity by eliminating the charge transfer resistance [Fig. S5(b), ESI†] and IEC [0.8121 mmol g^{-1} with 2 wt% rGO based composite membrane]. The 2 wt% reduced graphene in the composite membrane helps to absorb 294.5% water and attains a proton conduction value of 0.0068 × 10^{-3} S cm^{-1} at room temperature [Fig. S5(c), ESI†]. The methanol crossover or permeability of the composite based membrane with 2 wt% rGO reduces to approx. 2000 × 10^{-7} cm^2 s^{-1} which is lower than the value obtained from the composite membrane without rGO (3150 × 10^{-7} cm^2 s^{-1}).

5.10.3. Boron nitride. Boron nitride can be converted into a two-dimensional hexagonal shape called h-BN by arranging the nitrogen and boron atoms in a hexagonal structure. It has also become one of the best choices for researchers as a nano-filler in the composite membrane because of its high thermal stability, mechanical stability and high proton conduction due to the boron and nitrogen groups in the structure.[183,184] In previous years, Parthiban et al.[176] developed a composite based membrane consisting of Nafion and sulfonated h-BN (0–1 wt%). The sulfonation of the hexagonal shaped boron nitride is achieved in two stages. The hydroxyl groups were introduced on h-BN using NaOH by a hydrothermal process followed by treating the nano-fillers with f-MPTES for sulfonation [Fig. 14(a)]. The good compatibility between Nafion and h-BN makes a zigzag path within the composite based membrane which leads to uniform dispersion or distribution of the nanofillers through the membrane. The sulfonic groups of Nafion and hydrophilic h-BN bind more water molecules and draw more hydration ions which facilitate proton conduction through the composite membrane's ionic channels and reduce the charge carrier resistance. With 0.750 wt% h-BN in the composite membrane the proton conductivity reaches 214 × 10^{-3} S cm^{-1} which is 58.0% greater than that of the pristine commercial Nafion membrane [Fig. 14(b and c)]. The effective interaction between the polymer and the nano-filler strongly reduces the methanol crossover and the minimum value achieved with 1.0 wt% h-BN was 84 × 10^{-3} S cm^{-1}, which is 50% less than the value of a pristine
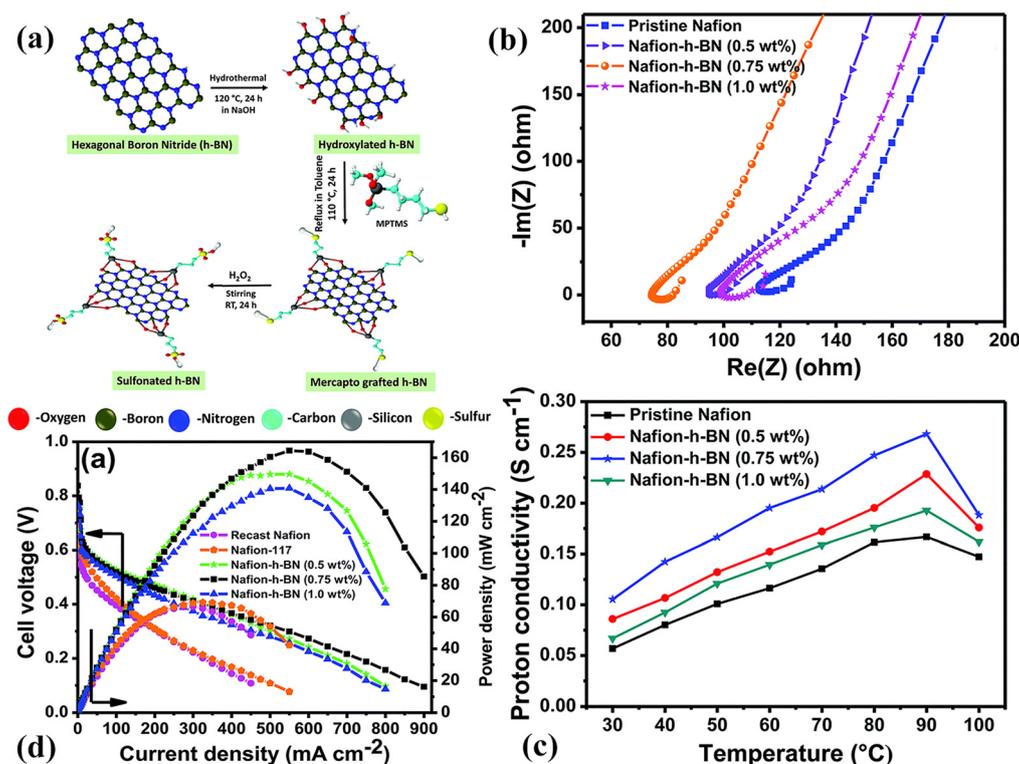

Fig. 14 (a) Synthesis procedure of sulfonic acid based hexagonal boron nitride. (b) AC impedance curves of pristine Nafion and h-BN based Nafion hybrid membranes at the temperature of 70 °C [RH 100%]. (c) Temperature vs. proton conductivity values of pristine Nafion and h-BN based Nafion hybrid membranes at the temperature of 70 °C [RH 100%]. (d) DMFC single cell evaluation tests of pristine Nafion and h-BN based Nafion hybrid membranes at the temperature of 70 °C under ambient temperature.[176] With copyright permission, 2020, Royal Society of Chemistry.

Nafion membrane. Due to high proton conduction and controlled methanol crossover or permeability, the selectivity of the composite membrane improves and reaches a value of 6.63×10^{-2} S mA^{-1}. The results also show that the composite based membrane with 0.75 wt% h-BN can deliver an excellent power density value of 165 mW cm^{-2} which is much higher than the power density value of the commercial Nafion membrane [65 mW cm^{-2}] when assembled in a DMFC [single-cell] under the same conditions.

In the next year, Yadav et al.[177] synthesized SBN using MPTES and hydroxylated modified BN which was then sulfonated by subsequent oxidation of the mercapto group. The amount of sulfonated BN in the composite membrane was in the range of 0–5 wt%. The water molecules hopping in the composite membrane's ionic channels created by sulfonated BN and the SPEEK polymer and their sulfonic groups interact with more and more water molecules and promote proton conduction. The sulfonated BN not only removes the free volume from the composite membrane but also restricts methanol from passing through the membrane. More water uptake increases more number of hydration ions available for ion exchange. As a result, the composite membrane with 5 wt% SBN shows an IEC value of 1.72 meq. g^{-1} which is 28.3% higher than that of the membrane without SBN. Due to surplus groups, it also delivered a superior proton conduction value of 40.80×10^{-3} S cm^{-1} which is 67.9% higher than the value obtained with a pristine SPEEK polymer membrane.

Proton conductivity is still limited even after modifying boron nitride with functional groups due to their low charge carrier ability. The researchers' approach is to graft the polymer instead of the functional group on the surface of boron nitride which not only supports stability but also promotes electrical conductivity by activating more and more charge carrier mobility. In one of the attempts, L. T. Yogarathinam and other scientists[178] prepared a composite membrane containing polyaniline polymer functionalized BN particles and the SPEEK polymer. The first step to form polymer functionalized BN was to add hydroxyl and carboxyl groups to the surface [called activated BN] and then pass these particles through the polymer to attain PANI-BN. The different types of modified and unmodified BN in the composite membrane create a rough surface with a wide area due to hydrogen and heteroatom bonding between them and the polymer matrix. Due to these interfacial interactions, the ionic channels become narrower and allow more resistance towards methanol crossover or permeability while the hydrophilic nature of hierarchical BN and functionalized BN nano-fillers promotes more water towards the composite membrane, which speeds up the proton conduction. With 0.1 wt% functionalized BN the composite membrane can deliver a high water uptake value of 58.420% and an IEC value of 1.760 meq. g^{-1}. Moreover, 0.10 wt% PANI-activated-BN in the composite membrane also reduces the methanol crossover or permeability to a value of 3.08×10^{-7} cm^{-2} s^{-1}. The researchers also tested the performance of the composite based membrane and found that with a small amount of PANI-activated-BN (0.1 wt%), the composite membrane delivers OCV and power density values of 0.1580 V

and 11.380 mW cm^{-2}, respectively [Fig. 14(d)]. Table 9 shows the summary of the data provided by the papers related to two 2-dimensional nanomaterials.

5.11. Zeolite

Zeolite is a uniform microporous structure composed of a framework that consists of oxygen and silicon based aluminosilicates. Its uniform microporous structure allows polar solvents like water to absorb and block methanol permeation. The zeolite provides several ionic channels, which facilitate high proton conduction.

Mordenite is one of the unique types of zeolites which possesses a high surface area and a large pore size, which allow polar solvents such as water to prevail in it without resistance. Moreover, its high chemical stability and thermal stability make the composite membrane dimensionally stable. It has Brønsted and Lewis acid sites which promote the dissociation of hydrogen ions, which increases the proton conductivity within the polymer matrix. Libby et al.[185] prepared a composite based membrane by blending polyvinyl alcohol and mordenite nanoparticles. The results show that the composite membrane delivered twenty times higher selectivity as compared to the commercially fluorinated Nafion polymer membrane. The mordenite and the Nafion membrane have low compatibility due to less attraction between each other which prevents them from contributing fully to the DMFC performance. The researchers functionalized the particles to cater to this problem. For example, Prapainainar et al.[186] modified the surface of the mordenite particles with two silane coupling agents such as GMPTS and MPTES and incorporated these particles into Nafion solution and cast them on the glass plate to make a composite membrane. The researchers not only discussed the functional group effect on the overall performance of the membrane but also evaluated the drying temperature effect on the physical and electrochemical attributes of the composite membrane. The silane groups create bonding with the commercial-Nafion membrane, which provides a compact but dimensionally stable composite membrane. The mordenite nanoparticles establish ionic channels, which allow the hopping of water molecule and the sulfonic group and functional group help in the dissociation of hydration ions, which uplift the proton conductivity and IEC. The more suitable temperature for drying the composite membrane is 100 °C at which IEC achieves a value of 0.10 meq. g^{-1} which is 33.1% greater than that of the membrane cast at 80 °C. However, at 100 °C, the composite membrane shows 0.590% solubility and 1.380% water uptake which are 79.60% and 80.80% lower than those of the membrane cast at 80 °C due to its less porous structure [Fig. S6(a), ESI†]. Moreover, the mordenite treated with MPTES delivers better performance due to better adhesion with the polymer as compared to the GMPT-MOR based composite membrane. The composite membrane with MPTES modified mordenite provides 60% and 5% higher proton conductivity values than the conductivity values of the composite membrane containing GMPTS modified mordenite at temperatures of 30 °C and 70 °C respectively. The less agglomeration of the modified

nanoparticles only allows polar solvents like water and blocks the way of methanol which enhances the methanol permeability resistance. The composite based membrane with MPTES modified mordenite shows excellent methanol crossover reductions of 85% and 25% at temperatures of 30 °C and 70 °C respectively which are lower than those of the GMPT modified mordenite composite membrane. This article is limited to studying casting solutions and does not provide any solvent solution information. In another article, Prapainainar et al.[187] discussed the solvent solution with and without alcohol contents and cost reduction. The mixture of methanol and ethanol (0–5 volume ratio) was used with DMF as a solvent and synthesized GMPT with modified mordenite and Nafion as a material for making the composite membrane. The results show that the composite membrane's solubility decreases with increasing alcohol contents and the 5 vol% alcohol ratio reduces 80% solubility but it is still higher than that of the recast composite membrane without mordenite and the Nafion 117 membrane. The hydrophobic nature of the modified mordenite does not support water uptake because it creates a rigid structure within polymer chains. However, sulfonic presence gives the best IEC [0.1 meq. g^{-1}]. The silane group of the modified mordenite forms a strong covalent bond with sulfonic groups which creates an ionic cluster within the narrow channels and facilitates proton conduction. With a 5 vol% alcohol mixture ratio, the composite membrane delivers 12% and 18% more proton conduction than the recast and commercial Nafion membrane and the narrow channels block the way for non-polar solvents like methanol to pass inside the membrane. Because of its high proton conduction and lower methanol crossover, the composite membrane made of a 5 vol% alcohol ratio could deliver a power density value of 11.5 mW cm^{-2} which is superior to the power density value of the recast mordenite free composite based membrane [7.3 mW cm^{-2}] when tested with a high methanol concentration [2 M] and at a temperature of 343.15 K [Fig. S6(b and c), ESI†].

Even the casting solution on the glass plate protects it from high methanol permeability through the membrane but experiences low proton conductivity because of the blockage of the passage. Researchers like S. Al-Batty and others[188] found a way to add MPTS modified mordenite in the place where it gives more protection from methanol permeability while keeping stable proton conduction [Fig. S6(d), ESI†]. The researcher used an ink jet to add a Nafion/mordenite mixture layer to the catalyst layer of the anode side and checked the results. They observed that only 0.5 wt% well-arranged mordenite in the

composite membrane based barrier layer contributes to methanol crossover control while maintaining the proton conductivity value at 120×10^{-3} S cm^{-1} at a high temperature of 70 °C. Methanol poisoning created by its crossing through the membrane was highly reduced with a thin layer of composite Nafion/mordenite which also reduces the chance of dissembling cathode materials, and ultimately the power density and current density values of the DMFC increase promisingly to high values which are comparable with a pristine Nafion membrane. Table 10 gives the details of these research papers.

5.12. Clay

Clay also called layered silicate is usually used as a flame retardant material with an exceptionally high chemical and mechanical stability; it has a porous structure for ion conduction and easy blending with polymers to act as a PEM for fuel cells especially for application in DMFCs.[189] Different types of clay have been introduced including sepiolite, montmorillonite (MMT), one-dimensional halloysite nanotubes, etc.

5.13. Sepiolite (SP)

Sepiolite (SP), a type of non-swelling, lightweight clay with a needlelike shape, has garnered a lot of interest among inorganic fillers.[190] $Si_{12}Mg_8O_{30}(OH)_4(OH_2)_4 \cdot 8H_2O$ is the formula for its unit cell, and the overall structure is made up of repeating tunnels and blocks. A magnesia layer is placed between two SiO_4 sheets to form each block. The excellent hydrophilicity of this clay is explained by the high density of silanol groups (–SiOH) in SP, while its high surface area (3.0×10^2 m^2 g^{-1}, more than all clay minerals) and porous structure are responsible for its high water absorption capacity.[39] Using the appropriate modifying agents, the reactive silanol groups are also employed for functionalization and surface modification to improve the affinity of polar polymers. Due to these qualities, the researchers are using sepiolite in the composite membrane. For example, Altaf et al.[191] prepared a composite based membrane using synthesized sepiolite and incorporated it into the PVDF-PS grafted polymer followed by sulfonation using chlorosulfonic acid [Fig. S7(a), ESI†]. The hydrophilic nature of the MS and sulfonic groups on the polymer provide strong water holding capacity and boost the proton transport mechanism through the bound water within the polymer matrix. The free water serves as a proton carrier for vehicular proton transport. The addition of MS clay suppresses the ionic channels and increases the diffusion path of the methanol molecule infiltration, which minimizes the methanol crossover [Fig. S7(b), ESI†]. The researchers found that the

Table 10 Details of the zeolite based composite membrane

Organic/inorganic nanomaterials	Polymer	Thickness (µm)/ anode supply	Proton conductivity ($\times 10^{-3}$ S cm^{-1})	Methanol permeability ($\times 10^{-7}$ cm^2 s^{-1})	Selectivity ($\times 10^4$ S s cm^{-3})	Power density (mW cm^{-2})	Ref.
Zeolite-50 vol%	PVA	—/O_2	10	0.1	20 times higher than the Nafion	—	185
Zeolite-MPTES-5 wt%	Nafion	—/—	0.08 [70 °C]	0.01 [30 °C]	—	—	186
Zeolite-GMPTES-3%	Nafion	134.67 ± 6.42/air	80	10 [343.5 K]	—	11.5 [343.5 K]	187
Zeolite-0.5 wt%	Nafion	—/air	90 [40 °C]	45	—	50 [40 °C]	188

composite membrane with 10 wt% MS delivers an ionic conductivity of 144×10^{-3} S cm^{-1} at 100 °C. Moreover, a high power density of 210 mW cm^{-2} is observed at 100 °C when the single DMFC is assembled with the composite membrane. This power density value is higher than the power density value of the commercial Nafion-117 membrane under similar conditions.

5.14. Montmorillonite (MMT)

Montmorillonite clay is a type of aluminum and silica based material composed of repeating units of triple layers of sheets, one octahedral sheet of aluminum sandwiched between two tetrahedral sheets of silica. The thickness of the montmorillonite ranges from 1 to 100 nm. It is one of the most promising candidates as an additive in the composite membrane of DMFCs which shows high thermal stability and a hydrophilic nature at elevated temperatures without losing its structure.[192,193] Due to these attributes, the polymer and MMT clay create a strong interaction, which has a positive influence on the physical and electrochemical characteristics of the proton exchange membrane of DMFCs. Table 11 shows that the researchers are working on this material to enhance the performance of the membrane for DMFCs. Hasani-Sadrabadi et al.[194] prepared a composite membrane composed of sulfonated PPO and MMT. The research shows that there are two factors that affect the proton conductivity. The first is the sulfonation degree, which determines the capability of the diffusion of ions within the polymer matrix. When the sulfonation degree increases, the proton conductivity of sulfonated PPO/MMT increases. The second is the hydrophobic nature of organically treated MMT; when it is incorporated into a polymer membrane, the composite membrane no longer absorbs water in surplus and low protons pass through the membrane. However, these hydrophobic MMT particles suppress the ionic channels and create a tortuous pathway in which the methanol crossover is almost blocked providing safety from the risk of polluting the cathode. The results show that without MMT, the composite based membrane with a 40% degree of sulfonation shows a water uptake of 21%, an IEC value of 2.59 meq. g^{-1} and a proton conduction value of 18.2×10^{-3} S cm^{-1}. When adding MMT particles from 2 to 10 wt% in the composite based membrane, it shows proton conduction and methanol crossover or permeability values in the range of $10.8 - 0.9 \times 10^{-3}$ S cm^{-1} and 1.7×10^{-7} cm^2 s^{-1} – 0.45×10^{-7} cm^2 s^{-1} respectively; when the sulfonation degree reaches 27% for PPO/MMT, the composite based membrane containing 2.0 wt% MMT delivers a selectivity value of nearly 6.35 which is almost 1.6 times higher than that of the pristine Nafion 117 membrane [40 500]. Moreover, with the same percentage of MMT, the composite based membrane can deliver a power density

value of 125 mW cm^{-2} which is superior to the power density value of the commercial-Nafion 117 membrane [108 mW cm^{-2}] when tested in a DMFC single cell with a methanol concentration of 5 M [Fig. S8(a), ESI†].

Along with the polymer, the sulfonation of the MMT clay also enhances its hydrophilicity and water holding capacity, which directly affects the performance of the DMFC. Researchers like T. K. Kim and his colleague[195] prepared a composite membrane that consisted of the Nafion polymer and sulfonated MMT and used PET film as a substrate instead of a glass plate. They also discussed the effects of different ratios of NMP and DMAc solvents on membrane morphology and properties. The 10 wt% solvent ratio provides the best value of reduced methanol crossover and proton conductivity [14.6×10^{-7} cm^2 s^{-1}] as NMP solvent with a small amount creates an ionic channel because it evaporates in the last after DMAc due to its high boiling point while a large amount of NMP provides a coarse membrane because of the sufficient amount left in the membrane without drying. After increasing the amount of S-MMT in the composite based membrane from 0 to 10 wt%, the membrane proton conductivity graph comes down from 96.0×10^{-3} S cm^{-1} to 77×10^{-3} S cm^{-1} S cm^{-1} because of the interfacial interaction between S-MMT and the SPEEK polymer which reduces the free volume and depletes the ionic channels in the composite membrane. For comparison purposes, a 7 wt% S-MMT composite membrane was chosen which shows a proton conductivity value of 0.081×10^{-3} S cm^{-1}. The researchers also found that the methanol crossover value decreases from 19.5×10^{-7} cm^2 s^{-1} to a value of 12.6×10^{-7} cm^2 s^{-1} when the amount of S-MMT in the composite membrane increases from 0 to 5 wt% and increases when the amount of S-MMT exceeds 5 wt%. This trend shows that 5 wt% S-MMT is enough to restrain the methanol from passing through the ionic channels. The researchers also studied the different concentrations of polymers and materials in the solvent mixture. The maximum concentration with suitable viscosity is found in the range of 30–32% for making the composite membrane. After being assembled in a DMFC single cell, the composite based membrane delivers a power density value of 30 mW cm^{-2}, which is slightly greater than that of the pristine Nafion 115 membrane (25 mW cm^{-1}) when a voltage value of 0.35 V is set.

To further enhance the structure of the MMT for less swelling and high hydrophilicity in the composite membrane, R. Gosalawit and his colleagues[196] functionalized the MMT with a silane group which was further modified with 4-sulfophthalic acid, and then incorporated into a sulfonated PEEK polymer to

Table 11 Details of sepiolite and MMT clay based composite membranes

Organic/inorganic nanomaterials	Polymer	Thickness (μm)/ anode supply	Proton conductivity ($\times 10^{-3}$ S cm^{-1})	Methanol permeability ($\times 10^{-7}$ cm^2 s^{-1})	Selectivity ($\times 10^4$ S s cm^{-3})	Power density (mW cm^{-2})	Ref.
Sepiolite-10 wt%	PPMS	—/O$_2$	144 [100 °C]	30	—	210 [100 °C]	191
Montmorillonite-10 wt%	SPPO	100–140/O$_2$	18.2	Approx. 2	6.35	125	194
S-MMT-7 wt%	Nafion	—/air	93	11.4	8.2	—	195
SMMT-3 wt%	SPEEK	100/air	71.3 [60 °C]	72 [60 °C]	—	19	196
BTA-MMT-3%	Nafion	—/air	90	0.6	11	144	197

make a composite based membrane. The clay insertion in the composite based membrane makes the membrane rigid and rough and a large amount of clay blocks the ionic channels by aggregating the clay, which loosens the interaction between water and functional groups of SMMT. As a result, the composite based membrane with 0–5 wt% SMMT shows a drop in water uptake from a value of 28 to 10%. However, a high amount of SMMT in the composite membrane has a positive effect on the thermal stability and mechanical strength [38.6 to 51.2 MPa, 0–3 wt%]. The narrow channels and compacted structure restrict the methanol from entering the composite membrane and the composite membrane with SMMT clay delivers high methanol protection and reduces the methanol crossover value to 72×10^{-7} cm^2 s^{-1} [60 °C], which is higher than that of the Nafion and pristine SPEEK polymer. The 3 wt% SMMT based composite membrane still performs better and delivers a high proton conduction value of 71.3×10^{-3} S cm^{-1} at a high temperature of 60 °C because of more water molecules bonding with the hydroxyl (OH) and sulfonic (SO$_3$H) groups of the SMMT clay. Due to good methanol protection and high proton conductivity, the composite based membrane is able to deliver a power density value of 19 mW cm^{-2}.

Additional amino groups on the nanomaterials also provide strong attraction to polymers of PEMs which helps the protons to jump through the membrane and their hydrophilic nature also hold water to improve good wettability. As an example, M. M. Hasani-Sadrabadi and his co-scientists[197] modified the MMT clay with amino functionalized groups using amino benzotriazole (BTA) as a source and through ion exchange reactions [Fig. S8(c), ESI†]. The acid–base interaction between the triazine group of modified MMT and the sulfonic groups of Nafion creates ionic channels and BTA groups hold water molecules by making hydrogen bonds. The increasing amount of functionalized modified MMT in the composite based membrane minimizes the methanol permeability and especially shows high proton conductivity with increasing temperature [Fig. S8(b), ESI†]. The methanol crossover value and proton conductivity attained with 3 wt% modified MMT are higher than the values of the unmodified MMT and cloisite 30A based composite membrane [Fig. S8(d), ESI†]. Moreover, with the same amount, the overall efficiency of the DMFC single cell is 21% which is higher than that of the Nafion 117 membrane [13.72%]. With a 5 M methanol concentration, the composite based membrane delivers a high power density of 144 mW cm^{-2} while the commercial-Nafion membrane only delivers a power density value of 39 mW cm^{-2} under similar conditions. The details of sepiolite and MMT clay based membranes are summarized in Table 11.

5.15. Halloysite nanotubes

Halloysite nanotubes are one type of clay nanomaterial which have a high surface area and a micro and mesoporous structure that allows more protons to pass and hopping of water molecules efficiently. Their compatibility with polymers make them an efficient candidate as a PEM material for application in DMFCs. All related research articles are summarized in Table 12. Researchers like H. Bai and colleagues[198] modified halloysite nanotubes (SHNT) with sulfonate polyelectrolyte brushes through the distillation and precipitation methods and incorporated them into chitosan (CS) solution to convert them into a composite based membrane [Fig. S9(a), ESI†]. The surface morphology shows a rigid structure with the rough surface of the composite membrane due to the strong physical interaction [hydrogen bond] between halloysite sulfonic groups and chitosan, which makes the membrane mechanically strong and thermally stable by releasing volume from the polymer. With 9% modified halloysite nanotubes, the composite membrane exhibits tensile strength and Young's modulus values of 52.8 and 942.8 MPa respectively, which are higher than the simple pristine chitosan membrane. Even though HNT fills the mechanical strength deficiency and has a good effect on controlling swelling, it reduces the water uptake due to the depletion of cavities in the composite membrane [9% modified HNT] and as a result the water uptake value is approximately 49.7% which is lower than that of the pristine CS membrane which delivers a water uptake value of 58.1% at room temperature. The sulfonic groups of modified halloysite and the amide groups of chitosan dissociate more and more hydration ions and their incorporation in the composite creates a hydrogen bonded network, which passes the ions through the vehicular and Grotthuss mechanisms. As a result, the IEC and proton conductivity values reach a range of 0.214 mmol g^{-1} to 0.267 mmol g^{-1} and approx. 11×10^{-3} to 18×10^{-3} S cm^{-1} respectively when 3–15% modified HNT is added to the composite membrane. Even with increasing amount of modified HNT in the membrane, the proton conductivity increases due to the less stretching of the polymer chain [Fig. S9(b), ESI†]. The composite membrane shows a low methanol crossover or permeability value of 10.8×10^{-7} cm^2 s^{-1} to 7.0 10^{-7} cm^2 s^{-1} when the modified HNT amount increases from 3 to 12% in the composite membrane due to the reduced free volume and the tortuous path. These results are superior to those of the composite membrane with unmodified HNT and the CS membrane. The results show that the sulfonation is not effective enough to produce good proton conductivity and water uptake. The HNT needs further modification by blending with other materials or material coatings which help it even when

Table 12 Details of the HNT based composite membrane

Organic/inorganic nanomaterials	Polymer	Thickness (μm)/ anode supply	Proton conductivity ($\times 10^{-3}$ S cm^{-1})	Methanol permeability ($\times 10^{-7}$ cm^2 s^{-1})	Selectivity ($\times 10^4$ S s cm^{-3})	Power density (mW cm^{-2})	Ref.
SHNT-12%	CS	—/—	44	7.0	2.51	—	198
UiO-66-SO$_3$H@HNT-10 wt%	SPEEK	—/O$_2$	15 [20 °C]	5 [20 °C]	2.92	98.5 [70 °C]	199

the rigidity of the composite membrane dominates. To tackle this problem, S. Zhao and colleagues[199] synthesized sulfonated UiO-66 and coated it on one dimensional halloysite nanotubes. Afterward, these modified nanotubes were incorporated into chitosan to convert them into a composite based membrane using the solution casting method. The hybrid nanoparticle amount set in this paper is 5–15 wt% in the composite membrane. The results show that the composite membrane has a dense and rough surface which points out the unique dispersibility of the modified hallyosite nanotube in the membrane. However, the modified nanotubes create aggregation if the amount extends beyond 10 wt% in the membrane. Also the strong interfacial interaction [hydrogen bond] between the sulfonic groups of the modified nanotubes and chitosan compacts the structure, provides high mechanical strength and thermal stability and reduces the swelling ratio [Fig. S9(c), ESI†]. The sulfonic groups of the MOF modified halloysite nanotubes and hydroxyl groups provide better water holding capacity and increase the water uptake from 61.1% to 69.3% and 76.2% to 88.0% at 20 °C and 80 °C temperature respectively when the amount of modified nanotubes increases from 5 to 15 wt%. These values reported are higher than that of the chitosan membrane [58.2% at 20 °C and 72.5% at 80 °C]. With more available functional groups on the MOF-modified halloysite, the composite membrane shows high IEC and the value increases from 0.2130 mmol g^{-1} to 0.2470 mmol g^{-1} when the filler amount increases from 5 to 10%. Through benefits from de-protonation and protonation, the 10.0 wt% MOF modified composite based membrane is able to deliver proton conductivity and power density values of 46.2×10^{-3} S cm^{-1} and 84.5 mW cm^{-2} respectively at temperatures of 80 °C and 70 °C respectively, which are 57.6% and 77.1% higher than the values of the chitosan membrane.

5.16. Bentonite

Bentonite clay is very similar to MMT clay and contains a high surface area and high IEC.[200] Due to its ease of blending with polymers, it is applied in various fields, including water management,[201] agriculture, and civil engineering.[202] The researchers have also applied it as an additive to polymer membranes in DMFCs due to its hydrophilic nature and water loving properties. Kumar et al.[203] prepared a composite membrane by incorporating bentonite and cloisite clay into the SPEEK polymer. The physical interaction [hydrogen bond] between polymers and clay compacts the overall structure, which makes the surface rough and reduces the free volume in the composite membrane. However, the thermal stability as well as methanol permeability reduces in the cavity free membrane but it has a bad effect on water uptake and proton conductivity, which become lower than that of the pristine SPEEK polymer membrane at room temperature. However, the composite based membrane shows high proton conduction when the amount of cloisite and bentonite clay rises to 0.5 wt%. Ultimately, the composite based membrane delivers water uptake and proton conduction values of 19.80% and 30.5×10^{-6} S cm^{-1} [80 °C] respectively [Fig. S10(a), ESI†]. The sulfonic groups of the SPEEK polymer and hydroxyl (OH) groups of

clay promote the diffusion of hydration ions, which increase the IEC and ultimately increase the overall selectivity of the membrane.

However, despite the good protection from methanol permeability or crossover in the composite membrane, the clay still faces water absorption due to its high hydrophilicity which reduces the strength of the composite based membrane and increases swelling. The modification of the bentonite clay further improves overswelling of the clay and enhances compatibility within the polymer structure. Different surface modified groups like sulfonic groups, amino groups and alkyl groups are created using different techniques and surfactants. According to the researcher, the sulfonic groups can be attached by treating the clay with the 3-MTPS surfactant after treating the material with H_2O_2 and H_2SO_4. One of the efforts made by Sasikala et al.[204] was that K^+-bentonite was converted into organo-sulfonic group (HSO_3) functionalized bentonite by silane condensation and added to a sulfonated PEEK polymer in order to make a composite based membrane. The composite based membrane is also made with hydrogen group functionalized bentonite (H^+-B), K^+-bentonite and SPEEK. The presence of sulfonic groups of the SPEEK polymer and organo-sulfonic groups of the modified bentonite clay creates a compact structure with less free volume that enhances the mechanical strength and thermal stability, and protects it from methanol absorption and swelling. However, the physical interaction [hydrogen bond] between the polymer and modified bentonite increases the IEC and proton conductivity by dissociating more water molecules but the composite membrane does not support more water absorption due to its dense and fully packed structure while the hydrogen and potassium based bentonite composite membrane shows high water uptake capacity and less swelling. The composite based membrane shows IEC and proton conductivity values of 0.45 meq. g^{-1} and 113×10^{-3} S cm^{-1} which are higher than the IEC and proton conductivity values of the pristine SPEEK polymer membrane at 30 °C. Due to high methanol protection and high proton conduction, the composite membrane is able to deliver an excellent power density value of 140 mW cm^{-2}, which is almost 2 times greater than the power density value of the pristine SPEEK polymer membrane [71 mW cm^{-2}] at 70 °C [Fig. S10(b), ESI†].

For the alkyl group's attachment, the hexadecyltrimethylammonium chloride (HDTA) surfactant is being used due to its easy availability. For example, S. Sasikala and her team[205] treated the clay with HDTA to convert it into alkyl group based clay and incorporate it into the SPEEK polymer membrane. HDTA intercalation with bentonite was confirmed through various characterization techniques. The physical interaction [hydrogen bond] between sulfonic groups of the SPEEK polymer and alkyl groups of modified bentonite clay creates a compact structure with a high mechanical strength value of 25 MP as well as high elongation due to the softness created by EDTA intercalation. The modified clay based composite membrane has tortuous and narrow channels within the polymer matrix that hold water molecules and functional groups conduct the proton through vehicular and Grotthuss mechanisms. However, the

Table 13 Details of the bentonite based composite membrane

Organic/inorganic nanomaterials	Polymer	Thickness (μm)/ anode supply	Proton conductivity ($\times 10^{-3}$ S cm^{-1})	Methanol permeability ($\times 10^{-7}$ cm^2 s^{-1})	Selectivity ($\times 10^4$ S s cm^{-3})	Power density (mW cm^{-2})	Ref.
Bentonite and cloisite	SPEEK	100/—	3.05×10^{-2} (80 °C)	3.82	58.5	—	203
HSO$_3$–bentonite	SPEEK	160/O$_2$	113	1.93		140	204
Bentonite–HDTA-20%	SPEEK	—/O$_2$	78	1.64	—	153	205

clay incorporation in the polymer depletes the free volume, which makes the composite membrane have low water uptake while swelling is greatly reduced. The composite membrane with 20% modified clay and 80% SPEEK polymer shows high performance and when the clay amount increases, the overall performance efficiency of the composite membrane reduces. The proton conductivity and methanol permeability values achieved by this ratio are 119×10^{-3} S cm^{-1} and 1.64×10^{-7} cm^2 s^{-1} which are superior to the values of the pristine composite membrane [proton conductivity: 63×10^{-3} S cm^{-1}, methanol permeability: 2.73×10^{-7} cm^2 s^{-1}] at 70 °C [Fig. S10(c), ESI†]. When assembled in the DMFC single cell, the composite based membrane is also able to achieve a power density value of 153 mW cm^{-2}, which is 2.1 times greater than that of the pristine SPEEK membrane (73 mW cm^{-2}) [Fig. S10(d), ESI†]. All research data on bentonite clay use in composite membranes are described and summarized in Table 13.

5.17. Cloisite

Cloisite or organoclay cloisite is a material composed of montmorillonite (MMT) and the cation di-tallow. Tallow is a mixture of hexadecyl, tetradecyl and octadecyl. Octadecyl is the major component whose amount is more than 60%. Due to being modified with MMT, the cloisite provides good compatibility with polymers when added in the membrane and this property makes it one of the most promising candidates for application in the membrane of fuel cells. The cloisite addition in the membrane tunes the internal structure of the channels which further smooths the pathway for proton conduction and its hydrophilic nature provides better grip to hold water molecules. There are generally several types of cloisite including cloisite®15A, cloisite®30B and cloisite-H$^+$ which are usually used in DMFCs. When sodium based motmorillonite (Na$^+$-MMT) is treated with bis-(2-hydroxyethyl)methyl tallow alkyl ammonium cations, it converts into cloisite®30B (30B). For obtaining cloisite®15A (15A), MMT-Na$^+$ is modified with dimethyl, dehydrogenated tallow and quaternary ammonium cations.[206] Cloisite-H$^+$ is prepared by treating sodium based MMT with HCl which is then washed with water and dried. According to the literature, these types of cloisite when are blended with polymers produce good effects in protecting methanol crossover rather than

supporting ion conduction.[207,208] The details of cloisite based membranes are summarized in Table 14.

Cloisite 30B is being applied in PEM fabrication for DMFCs because of its high quality and compatibility with the polymer membrane. Prasad *et al.*[209] prepared a composite membrane by blending SPEEK and PVDF-HFP and then incorporated cloisite 30A. The study shows that the hydrophobic nature of PVDF-HFP in the composite membrane promotes the membrane's mechanical and dimension stability as well as chemical stability by reducing the free volume of the polymer matrix while sacrificing water uptake. The hydrophilic cloisite 30A provides high water uptake by creating hydrogen bonding between the sulfonic groups of the SPEEK polymer and binding the water within the ionic channels created by polymers. With more water molecules within the composite membrane, more ions pass through it, which increases the proton conductivity. The compacted structure attained with hydrophobic PVDF-HFP and cloisite 30A contains a tortuous pathway that is suitable for protonic ions, and prevents the methanol molecules from further passing through the membrane which prevents the poisoning of the cathode. With 5 wt% Cloisite and 25% PVDF-HFP, the composite based membrane exhibited a proton conduction value of 0.1×10^{-3} S cm^{-1}, and methanol permeability and selectivity values of 1.350×10^{-7} cm^2 s^{-1} and 9.630×10^4 S s cm^{-3} respectively [Fig. S11(a), ESI†]. When tested with a full DMFC single cell, a power density value of 55 mW cm^{-2} and an OCV value of 0.79 V are achieved using the prepared membrane.

The researchers found that some polymers' compatibility with clay is not high which results in high methanol crossover and ultimately reduces overall performance. To further enhance the protection from ethanol crossover, the compatibilizer has been used to promote the interaction between polymers and inorganic materials. In one of the efforts, Jaafar *et al.*[210] prepared a composite membrane using inorganic clay cloisite 15A and TAP compatibilizer in the sulfonated PEEK polymer. The hydrogen bonding between the polymer, Cloisite and TAP creates a compact structure by reducing the free volume within the polymer chain and inorganic clay prolongs the ionic channels, which reduces the methanol crossover or permeability, while sacrificing the proton conductivity [Fig. S11(b), ESI†]. Despite the lower proton conductivity of

Table 14 Details of the cloisite based composite membrane

Organic/inorganic nanomaterials	Polymer	Thickness (μm)/ anode supply	Proton conductivity ($\times 10^{-3}$ S cm^{-1})	Methanol permeability ($\times 10^{-7}$ cm^2 s^{-1})	Selectivity ($\times 10^4$ S s cm^{-3})	Power density (mW cm^{-2})	Ref.
Cloisite-30B-5 wt%	SPEEK/PVDF-HFP	—/air	81.0 [70 °C]	5.00	8.40		209
Cloisite-15A	SPEEK	—/—	3.87	1.29	3	—	210

the commercial Nafion 112 membrane [12×10^{-3} S cm^{-1}], the composite membrane shows a high proton conductivity value of 3.87×10^{-3} S cm^{-1} which is still superior to that of the pristine SPEEK polymer membrane [1.91×10^{-3} S cm^{-1}]. Moreover, due to the tortuous pathway, the composite based membrane is able to minimize methanol permeability to a value of 1.29×10^{-7}, which is lower than that of the Nafion 112 [15.72×10^{-7} cm^2 s^{-1}] and pristine SPEEK [3.06×10^{-7} cm^2 s^{-1}] polymer membrane. Due to low methanol crossover or permeability and superior proton conductivity, the selectivity of the composite based membrane with clay and compatibilizer increases and reaches a value of 3×10^4 S s cm^{-3} [Fig. S11(c), ESI†]. Table 14 gives the details of the research papers related to cloisite clay.

6. Inorganic nanomaterial-filled non-woven mats

The simple electrospun non-woven membrane or mats have large pores which easily lose water when compressed under load or during conductivity tests in the fuel cells. This causes low performance and an instant decline in voltage during the running of the fuel cells.[7]

Non-woven mats are prepared with an efficient and high accuracy electrospinning method [Fig. 15], which provides the membrane with high strength and porosity due to its mesh type structure and high hydrophilic nature due to phase change. Moreover, an ultra-high area–volume ratio and controllable thickness can be achieved with it which makes it very suitable

for making PEMs.[211–214] The details of nonwoven based membranes are summarized in Table 15.

However, high seepage of methanol and limited hydrophilicity of the electro-spun nanofiber's one-dimensional continuous structure hinder its direct application in alcohol fuel cells especially in DMFCs. The inclusion of inorganic nanomaterials in the polymer nanofiber membrane not only enhances its hydrophilicity but also enhances its thermal stability.[221] Moreover, inorganic nanomaterials minimize the methanol crossover. The preparation of inorganic nanomaterial filled nonwoven mats is as follows: first, the polymer is mixed with nanomaterials in an organic/inorganic solvent and then this solution is electro-spun to make a non-woven mat. Table 15 shows that the composite nano-fibrous membrane has a good effect and is comparable with the commercial membrane when applied in DMFCs. Dong et al.[215] prepared the composite nanofiber membrane by incorporating titania nanofibers into the SPEEK polymer. The synthesized titania nanofiber shows a smooth cylindrical surface without any headed surface. It completely blends with the polymer to make a uniform nanofibrous polymer electrolyte membrane. The results show that the thermal stability increases with the addition of titania nanofibers because of their thermal resistance property and ability to fill the unoccupied spaces in the SPEEK polymer chain. The hydrophilic nature of the titania nanofibers also increases the water uptake to 25.7% with a 1.5% titania amount and the swelling ratio reduces to 9.7%. Moreover, titania water uptake capability and high aspect ratio make a proton passage which promotes proton conductivity [Fig. S12(b), ESI†]. The proton conductivity value at 70 °C is 102.6×10^{-3} S cm^{-1} with
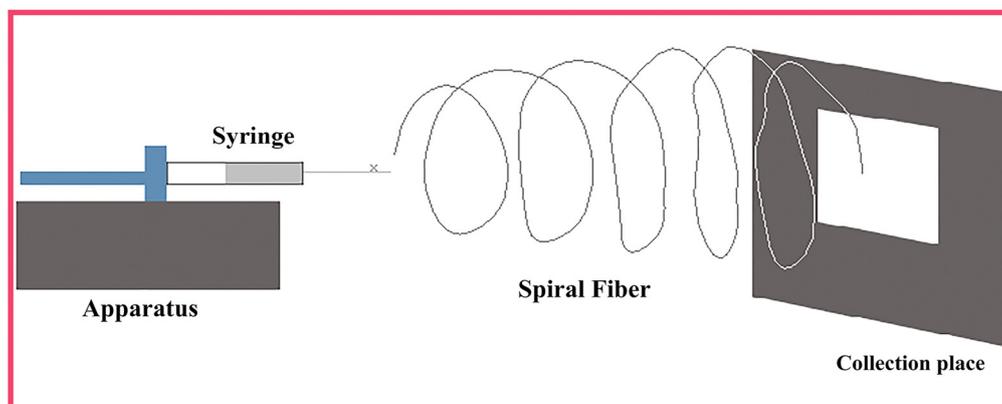

Fig. 15 Schematic representation of non-woven mat preparation by the electrospinning method.

Table 15 Composite non-woven polymer electrolyte membrane

Organic/inorganic nanomaterials	Polymer	Thickness (μm)/ anode supply	Proton conductivity ($\times 10^{-3}$ S cm^{-1})	Methanol permeability ($\times 10^{-7}$ cm^2 s^{-1})	Selectivity ($\times 10^4$ S s cm^{-3})	Power density (mW cm^{-2})	Ref.
TiFNs-1 wt%	SPEEK	—/O$_2$	100	2	15	57.1	215
S-SiO$_2$	CS-PVDF	—/O$_2$	21.2	4.2	4.80	86.3 [80 °C]	216
SiO$_2$	Nafion-Cys	—/—	242.4 (80 °C)	6 [Nafion-Gly]	—	—	217
SiO$_2$-3%	SPES	—/O$_2$	230 (80 °C)	7.22 (80 °C)	—	77.22	218
SO$_4^{2-}$/FSnO$_2$-7.5 wt%	SPPESK	80–100/O$_2$	226.7 (80 °C)	3.7	—	147.3	219
UiO-66-NH$_2$-8%	SPES	—/—	260 (80 °C)	7.54	15.25	95.490	220

1.0% titania nanofibers. The titania nanofibers also minimize the methanol passage by creating a connected structure [Fig. S12(a), ESI†].

Inorganic particle agglomeration is one of the big problems in electrospinning that makes the fiber rough and edgy. The researchers found that the inorganic particle precursor establishes better compatibility between nanomaterials and the polymer which helps to develop a better structure as compared to direct application of nanomaterials in the membrane. For example, Liu et al.[216] composed a silane (–si–) group containing silica coated PVDF nano-fiber mat by the electrospinning method using the TEOS precursor and polydopamine [Fig. S12(c), ESI†]. The nano-fibrous mat was then treated with a silane coupling agent named TPS. Afterward, this nanofibrous mat was treated with a chitosan (CS) solution. There are two types of interactions that exist in the composite membrane. The first is between the oxygen groups of silica and the hydroxyl groups of polydopamine which strengthens $SiO_2@PVDF$ and the second is between the SO_3H of functionalized silica and the NH_3 of CS which further promotes the structural stability of the membrane with less swelling. Therefore, the chitosan membrane's mechanical strength increases with the incorporation of the functionalized $SiO_2@PVDF$ nano-fibrous mat within its structure. As a result, the composite membrane containing functionalized $SiO_2@PVDF$ nanofibers shows a tensile and elongation value of 25.2 MP and 83.5%, which is 3 times and 1.60 times greater than that of the pristine CS membrane. The hydrophobic nature of the PVDF resists the methanol crossover and the hydrophilic nature of the amino groups and sulfonic groups favors the water uptake. Moreover, the physical interactions between sulfonic groups and silane groups created narrow ionic channels, which promote the hydration ions through vehicular and Grotthuss mechanisms. Ultimately, the proton conduction of the composite based membrane reaches a value of 21.20×10^{-3} S cm^{-1}, which is about 2.8 times greater than that of the pristine CS membrane. Moreover, the methanol permeability or crossover value for the composite membrane is limited to a value of 4.20×10^{-7} cm^2 s^{-1} [26% lower than that of the commercial Nafion 115 membrane]. When tested in DMFC [single assembled cell], the composite membrane exhibits an excellent power density value of 86.3 mW cm^{-2} at 80 °C with a 5.4% loss when tested for 100 h at a current density value of 0.35 A cm^{-2}.

The functionalization of nanomaterials further enhances their hydrophilicity and compatibility with polymers. Moreover, the hydroxyl group, amino group and carboxyl group based nanomaterials attract more water molecules and dissociate into hydration ions through ionic channels which boosts the proton conductivity. Their hydrogen bonding with the polymer creates narrow ionic channels which reduce the risk of overflow of methanol within the composite membrane. As an example, Wang et al.[217] prepared a composite based membrane by incorporating Nafion and biofunctional silica nanofibers. The SiO_2 nanofibers prepared by the electrospinning method were functionalized with groups (the sulfonic (SO_3H) groups, the hydroxyl (OH) groups and the amine groups) using different types of amino acids and further mixed with Nafion based solution for preparing the PEM for DMFCs. The amino acid groups act as proton carriers by creating an efficient pathway. Moreover, these groups are involved in improving thermal strength, mechanical strength, water uptake capacity, proton conductivity and methanol permeability or crossover resistance. The amino acid cysteine treated silica composite membrane shows the highest proton conductivity of 242.4×10^{-3} S cm^{-1} at 80 °C while the glycine treated silica composite membrane shows low water uptake and proton conduction due to the lower amount of hydrophilic groups on the surface [Fig. S12(d), ESI†].

In another example, Wang et al.[218] prepared a membrane by incorporating amino functionalized silica in sulfonated poly-(ether sulfone) (SPES) by the electrospinning method followed by impregnating with Nafion solution. In this research, hydrophilic functional groups of modified silica create hydrogen bonds with sulfonic groups of SPES and develop internal channels while the rest of the functional groups make bonds with the Nafion membrane and make it mechanically strong. Nafion coating attracts more water molecules and amino functionalized silica entraps the water inside the composite based membrane, which enhances water uptake capacity, proton conduction and protection from methanol uptake. With 3% amino functionalized silica, the SPES/Nafion membrane possesses the highest proton conductivity of 230×10^{-3} S cm^{-1} at 80 °C and a methanol crossover value of 7.22×10^{-7} cm^2 s^{-1} at room temperature [Fig. S12(e), ESI†]. The DMFC [single assembled cell] assembled with a composite nanofiber membrane exhibits a high power output of 42.34% which is superior to that of the Nafion membrane at a temperature of 60 °C and a relative humidity value of 100%.

According to researchers, the nanomaterials in small amounts prevent the creation of ionic channels within the polymer matrix, which does not increase the proton conductivity and water uptake up to the desired level. One-dimensional nanofibers are one of the choices, because they have a high surface area due to their high length, or thickness, which facilitates surplus ionic clusters through the membrane. Moreover, hydrogen bonding between their functional groups and polymers makes the membrane dimensionally and thermally stable for high temperature work in fuel cells. For example, Chen et al.[219] proposed a composite membrane that was made of synthesized one dimensional nanofibers and the SPPESK polymer. The nanofibers were synthesized using sulfated tin oxide and their arrangement in the nanofiber was set by electrospinning and annealing techniques [Fig. 16(a and c)]. The nanofibers possessed a high surface area of around 28.0 m^2 g^{-1} with a large aspect ratio. The functional groups on the surface of the hollow nanofibers such as SO_4^{2-}, Sn^{4+} and Sn–OH provide high attraction towards water molecule hopping which ultimately boosts high proton conductivity through the provision of abundant hydration ions [Fig. 16(b)]. The physical interaction [hydrogen bond] between sulfonic groups of the SPPESK polymer and functional groups of one-dimensional hollow nanofibers develops long narrow channels through the membrane, which

enhances the mechanical strength to a value of 31 MPa in the hydrated form and the proton conductivity to a value of 226.7 × 10^{-3} S cm^{-1} [80 °C]. Due to high water uptake and high proton conductivity, the SO$_4^{2-}$/FSnO$_2$ composite membrane exhibits a power density value of 147.3 mW cm^{-2}, which is superior to the power density values of the zero-dimensional nanoparticle-incorporated composite membrane and Nafion 115.

Along with one-dimensional inorganic nanomaterials, three-dimensional nanomaterials are also applied in DMFCs because of their nano and microporous structures with a high surface area and water holding capacity. The metal organic framework is one of the 3D structures with good physical and electrochemical properties. The primary amine group (NH$_2$–) of MOFs has a strong interaction with the sulfonic group of the polymer based membrane, which controls the morphology of the

composite membrane and methanol crossover. As an example, Wang et al.[220] used UiO-66-NH$_2$ and combined it with the SPES polymer to obtain nanofibers. Afterward, these nanofibers were mixed with Nafion based solution and made into the composite based membrane by the solution spreading or casting method. The study shows that strong physical interaction [hydrogen bond] exists between the sulfonic groups of the SPES polymer and the amine groups of UiO-66-NH$_2$, which creates a compact, strong and thermally stable structure with less swelling that occupies the free volume of the polymer [Fig. 16(d)]. The hydrophilic sulfonic groups as well as the amine groups also show high hydrophilicity and anchor more water molecules which promotes water uptake. The polar nature of the MOFs repels the absorption of the methanol and narrow ionic channels lengthen the pathway for methanol permeability while
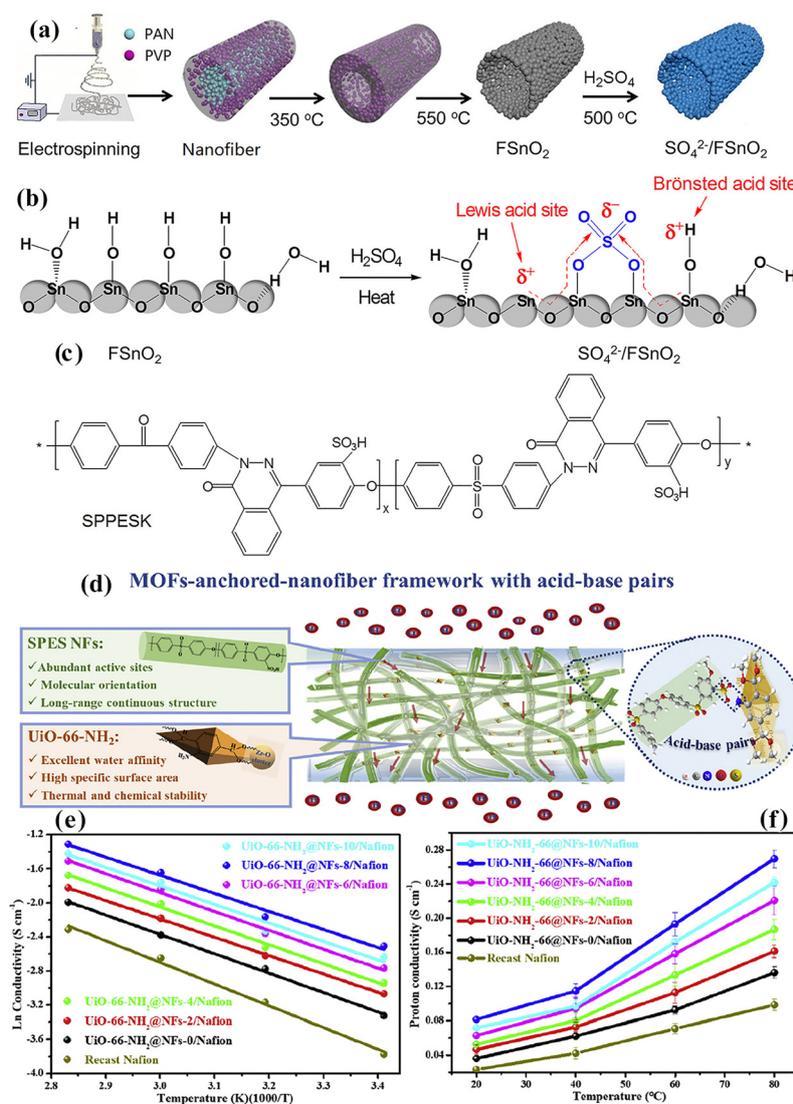

Fig. 16 (a) Preparation procedure of the hollow nanofiber composed of SO$_{42}$/FSnO$_2$, (b) sulfonation reaction of SnO$_2$ and (c) sulfonated PPESK polymer matrix [chemical structure]. (d) Schematic diagram of a UiO-66-NH$_2$-based nanofiber hybrid membrane. (e) Nyquist plots and (f) temperature vs. proton conductivity value curves of different amounts of MOF-based nanofiber/Nafion composite membrane and recast Nafion membrane.[219,220] With copyright permission, 2019 and 2020, Elsevier and American Chemical Society.

surplus hydration ions which are created by high water uptake promote proton conductivity by Grotthuss and vehicular mechanisms [Fig. 16(e and f)]. The Nafion composite based membrane with 8 wt% MOFs (UiO-66-NH$_2$@NFs) delivers a methanol crossover value of 7.54×10^{-7} cm^2 s^{-1} and an excellent proton conduction value of 270×10^{-3} S cm^{-1} at a temperature of 80 °C and a relative humidity of 100%. After the addition of 8 wt% MOFs to the composite membrane, the proton conduction value decreases due to severe agglomeration and blockage of ionic channels within the polymer matrix. However, the proton conduction value of the composite membrane is superior to that of the recast Nafion membrane.

7. Summary and future prospects

The high proton conduction and minimum methanol crossover or permeability through the polymeric membrane in the DMFC are essential for its better performance and high efficiency. The commercially available Nafion membrane, with its dense and porous structure, somehow fulfils the requirements due to its interfacial interaction between sulfonic groups and water molecules. However, due to its high cost and limited physical and electrochemical characteristics, the non-fluorinated polymer membrane with high ability to attract more water molecules, high hydrophilic nature, chemical stability, impressive proton dissociation ability, and proton conduction with low methanol permeability replaces the Nafion membrane. The polymeric membrane alone or with different polymers and nano-fillers fulfils these requirements. The composite type membrane in which polymers and inorganic nano-fillers blend is among the top choices of the PEM for DMFCs. The inorganic nanomaterial's hygroscopic nature and strong interaction with polymers create uniform and small diameter channels in the composite membrane, which allow easy hopping of water molecules and more dissociation of the hydration ions boosting the conductivity through the membrane. The polar nature of the nanomaterials prevents the methanol molecules from entering the PEM, which prevents poisoning and deterioration of the cathode material. Inorganic nanomaterials with solid, hollow, and multilayered structures have been developed and applied in PEM for DMFCs. Different techniques have been developed to make inorganic nanomaterials part of the polymeric membrane, such as coating, blending and non-woven mats. The coating method is a very environmentally friendly, quick, and efficient method in which a polymer binder and nanoparticle layer are developed on the surface of the polymer base substrate. In some cases, the precursor's solution creates a coating of the inorganic nanomaterials on the substrate with a more uniform and connected porous structure through the solution gel method. The obtained composite membrane possesses a thin layer of particles with better water absorption and methanol permeability resistance. On the other side, the composite membrane requires the blending of polymers with inorganic nanomaterials using polar solvents at room temperature or high temperature, and after that, the solution passes

through the stirring process. The prepared solution is generally cast on a glass plate or Petri dish and converted into a membrane. This kind of composite membrane possesses strongly bound particles within the polymer matrix, several ionic channels, and a free volume to accommodate water molecules and proton transfer. In a composite non-woven matrix, the polymer solution containing inorganic nanomaterials or precursors passes through the electrospinning process, which converts it into a nanofiber membrane with a high specific area and a mechanically strong structure. Sometimes, the nanomaterials are directly applied to the nanofiber matrix or after surface modifications to enhance the attributes of the proton exchange membrane. Inorganic nanoparticle surface modifications, such as functionalization with amino acid groups, hydroxyl groups, carboxylic groups, catalytic material, and sulfonic groups, are adopted to further tune them to make them more compatible with polymer membranes.

Despite these advantages, the composite membrane still suffers from low performance in the form of limited proton conduction and high methanol or fuel permeability or crossover. It is due to the low interaction between polymers and inorganic nanomaterials, which creates agglomeration and prevents the application of large amounts of nanomaterials in proton exchange membranes. Moreover, the blockage of the ionic channel due to agglomeration limits the hopping of water molecules and ultimately produces low proton conductivity. The surface modification has a bad impact on the membrane's mechanical strength, and the loss of connection in the polymer chain creates pores that lose water molecule absorption. The following drawbacks still exist in the application of different techniques for membrane modification that need to be overcome.

• In the coating method, the adhesion between nanomaterials and substrates is not sufficient and needs more focus on designing the thin layer and better adhesion between the two of them.

• The grafting method for nanoparticle coating also needs to be considered because of its high accuracy in particle coating and quick process.

• In the solution casting method, humidity and temperature of drying need to be improved for an efficient and uniform porous structure.

• On the other hand, in nanofiber membranes, particle size and shape are the main concerns. The surface of the composite membrane becomes rough and irregular with the use of sharp edges in the nanomaterials. The small particles need to be considered for making nano-fibrous and solution casting membranes because of their easy wall formation without damaging the ionic channels.

• The stability of the MOFs needs to be improved so they do not dissolve in acidic ionomers like SPEEK or Nafion.

• The particle agglomeration and lack of adhesion between fiber and nanomaterials need to be concentrated more. In the case of the solution casting method, the particle's distribution in the polymer solution, heating time, and temperature need to be studied deeply for a better mechanical structure.

Author contributions

Muhammad Rehman Asghar: writing draft, concept. Weiqi Zhang: formal analysis. Huaneng Su: resources, investigation. Junliang Zhang: software, formal analysis, supervision. Huiyuan Liu: grammar check. Lei Xing: formal analysis, software. Xiaohui Yan: technical check, format setting. Qian Xu: supervision, funding, resources.

Data availability

The data supporting this article have been included as part of the Supplementary Information.

Conflicts of interest

The authors declare that they have no known competing financial interests or personal relationships that could have appeared to influence the work reported in this paper.

Acknowledgements

References

1 K. Jiao, J. Xuan, Q. Du, Z. Bao, B. Xie, B. Wang, Y. Zhao, L. Fan, H. Wang, Z. Hou, S. Huo, N. P. Brandon, Y. Yin and M. D. Guiver, *Nature*, 2021, **595**, 361–369.

2 R. Haider, Y. Wen, Z. F. Ma, D. P. Wilkinson, L. Zhang, X. Yuan, S. Song and J. Zhang, *Chem. Soc. Rev.*, 2021, **50**, 1138–1187.

3 H. Zhang and P. K. Shen, *Chem. Soc. Rev.*, 2012, **41**, 2382–2394.

4 M. R. Asghar, M. T. Anwar, T. Rasheed, A. Naveed, X. Yan and J. Zhang, *IOP Conf. Ser. Mater. Sci. Eng.*, 2019, **654**, 012017.

5 L. Guan, W. Yu, M. Rehman Asghar, W. Zhang, H. Su, C. Li, L. Xing and Q. Xu, *Fuel*, 2024, **360**, 130503.

6 M. T. Anwar, X. Yan, M. R. Asghar, N. Husnain, S. Shen, L. Luo, X. Cheng, G. Wei and J. Zhang, *Chin. J. Catal.*, 2019, **40**, 1160–1167.

7 M. R. Asghar, M. T. Anwar, A. Naveed and J. Zhang, *Membranes*, 2019, **9**, 78.

8 M. R. Asghar, M. T. Anwar, G. Xia and J. Zhang, *Mater. Chem. Phys.*, 2020, **252**, 123122.

9 M. T. Anwar, X. Yan, M. R. Asghar, N. Husnain, S. Shen, L. Luo and J. Zhang, *Int. J. Energy Res.*, 2019, **43**, 2694–2721.

10 M. R. Asghar, Y. Zhang, A. Wu, X. Yan, S. Shen, C. Ke and J. Zhang, *J. Power Sources*, 2018, **379**, 197–205.

11 K. Divya, M. R. Asghar, N. Bhuvanendran, H. Liu, W. Zhang, Q. Xu, S. Y. Lee and H. Su, *React. Funct. Polym.*, 2024, **199**, 105903.

12 M. Rehman Asghar, K. Divya, H. Su and Q. Xu, *Eur. Polym. J.*, 2024, **213**, 113110.

13 H. Liu, C. Song, L. Zhang, J. Zhang, H. Wang and D. P. Wilkinson, *J. Power Sources*, 2006, **155**, 95–110.

14 S. Wasmus and A. Küver, *J. Electroanal. Chem.*, 1999, **461**, 14–31.

15 N. Shaari, S. K. Kamarudin, R. Bahru, S. H. Osman and N. A. I. Md Ishak, *Int. J. Energy Res.*, 2021, **45**, 6644–6688.

16 X. Fu, Z. Xia, R. Sun, H. An, F. Qi, S. Wang, Q. Liu and G. Sun, *ACS Energy Lett.*, 2018, **3**, 2425–2432.

17 Y. Zhang, Y. Song, D. Chen, Q. Jin, J. Chen and Y. Cao, *Polymer*, 2023, **265**, 125589.

18 T. Zhang, P. Wang, H. Chen and P. Pei, *Appl. Energy*, 2018, **223**, 249–262.

19 C. Y. Wong, W. Y. Wong, K. Ramya, M. Khalid, K. S. Loh, W. R. W. Daud, K. L. Lim, R. Walvekar and A. A. H. Kadhum, *Int. J. Hydrogen Energy*, 2019, **44**, 6116–6135.

20 R. E. Rosli, A. B. Sulong, W. R. W. Daud, M. A. Zulkifley, T. Husaini, M. I. Rosli, E. H. Majlan and M. A. Haque, *Int. J. Hydrogen Energy*, 2017, **42**, 9293–9314.

21 J. Park, H. Oh, T. Ha, Y. Il Lee and K. Min, *Appl. Energy*, 2015, **155**, 866–880.

22 W. E. Mustain, M. Chatenet, M. Page and Y. S. Kim, *Energy Environ. Sci.*, 2020, **13**, 2805–2838.

23 H. Zhang and P. K. Shen, *Chem. Rev.*, 2012, **112**, 2780–2832.

24 J. Lin, R. Wycisk and P. N. Pintauro, in *Polymer Membranes for Fuel Cells*, Springer US, Boston, MA, 2008, vol. 80, pp. 1–19.

25 M. R. Asghar and Q. Xu, *J. Polym. Res.*, 2024, **31**, 125.

26 A. Mahmoud, A. Fahmy, A. Naser and M. A. Saied, *Sci. Rep.*, 2022, **12**, 22017.

27 J. Aburabie, B. Lalia and R. Hashaikeh, *Membranes*, 2021, **11**, 539.

28 G. P. Jiang, J. Zhang, J. L. Qiao, Y. M. Jiang, H. Zarrin, Z. Chen and F. Hong, *J. Power Sources*, 2015, **273**, 697–706.

29 M. Hosseinpour, M. Sahoo, M. Perez-Page, S. R. Baylis, F. Patel and S. M. Holmes, *Int. J. Hydrogen Energy*, 2019, **44**, 30409–30419.

30 J. Zhang, H. Liu, Y. Ma, H. Wang, C. Chen, G. Yan, M. Tian, Y. Long, X. Ning and B. Cheng, *J. Power Sources*, 2022, **548**, 231981.

31 M. Zhiani, S. Majidi, H. Rostami and M. M. Taghiabadi, *Int. J. Hydrogen Energy*, 2015, **40**, 568–576.

32 L.-Y. Li, B.-C. Yu, C.-M. Shih and S. J. Lue, *J. Power Sources*, 2015, **287**, 386–395.

33 S. Mondal, S. Soam and P. P. Kundu, *J. Membr. Sci.*, 2015, **474**, 140–147.

34 S. S. Araya, F. Zhou, V. Liso, S. L. Sahlin, J. R. Vang, S. Thomas, X. Gao, C. Jeppesen and S. K. Kær, *Int. J. Hydrogen Energy*, 2016, **41**, 21310–21344.

35 W. N. E. Wan Mohd Noral Azman, J. Jaafar, W. N. W. Salleh, A. F. Ismail, M. H. D. Othman, M. A. Rahman and F. R. M. Rasdi, *Mater. Today Energy*, 2020, **17**, 100427.

36 X. Liu, Y. Zhang, Y. Chen, C. Li, J. Dong, Q. Zhang, J. Wang, Z. Yang and H. Cheng, *J. Membr. Sci.*, 2017, **544**, 58–67.

37 G. Rambabu and S. D. Bhat, *Electrochim. Acta*, 2015, **176**, 657–669.

38 S. Mollá and V. Compañ, *Int. J. Hydrogen Energy*, 2014, **39**, 5121–5136.

39 F. Lufrano, V. Baglio, P. Staiti, A. S. Arico and V. Antonucci, *J. Power Sources*, 2008, **179**, 34–41.

40 N. Horimatsu, T. Takahashi, D. Kobayashi, A. Shono and K. Otake, *Desalin. Water Treat.*, 2013, **51**, 5254–5259.

41 S. Das, K. Dutta, S. Hazra and P. P. Kundu, *Fuel Cells*, 2015, **15**, 505–515.

42 H. Farrokhzad, T. Kikhavani, F. Monnaie, S. N. Ashrafizadeh, G. Koeckelberghs, T. Van Gerven and B. Van der Bruggen, *J. Membr. Sci.*, 2015, **474**, 167–174.

43 R. Rath, S. Mohanty, S. K. Nayak and L. Unnikrishnan, *Polymer*, 2021, **234**, 124248.

44 K. Dutta, S. Das and P. P. Kundu, *J. Membr. Sci.*, 2014, **468**, 42–51.

45 C. Manea and M. Mulder, *J. Membr. Sci.*, 2002, **206**, 443–453.

46 C. Simari, E. Lufrano, G. A. Corrente and I. Nicotera, *Solid State Ionics*, 2021, **362**, 115581.

47 A. R. Kim, C. J. Park, M. Vinothkannan and D. J. Yoo, *Composites, Part B*, 2018, **155**, 272–281.

48 F. Mack, V. Gogel, L. Jörissen and J. Kerres, *J. Power Sources*, 2013, **239**, 651–658.

49 H. A. Elwan, M. Mamlouk and K. Scott, *J. Power Sources*, 2021, **484**, 229197.

50 F. Liu, S. Wang, D. Wang, G. Liu, Y. Cui, D. Liang, X. Wang, Z. Yong and Z. Wang, *J. Power Sources*, 2021, **494**, 229732.

51 H. Chen, S. Wang, J. Li, F. Liu, X. Tian, X. Wang, T. Mao, J. Xu and Z. Wang, *J. Taiwan Inst. Chem. Eng.*, 2019, **95**, 185–194.

52 M. Han, G. Zhang, M. Li, S. Wang, Z. Liu, H. Li, Y. Zhang, D. Xu, J. Wang, J. Ni and H. Na, *J. Power Sources*, 2011, **196**, 9916–9923.

53 G. Alberti and M. Casciola, *Annu. Rev. Mater. Res.*, 2003, **33**, 129–154.

54 R. M. Nauman Javed, A. Al-Othman, M. Tawalbeh and A. G. Olabi, *Renewable Sustainable Energy Rev.*, 2022, **168**, 112836.

55 N. F. Raduwan, N. Shaari, S. K. Kamarudin, M. S. Masdar and R. M. Yunus, *Int. J. Hydrogen Energy*, 2022, **47**, 18468–18495.

56 Y. Devrim, S. Erkan, N. Baç and I. Eroglu, *Int. J. Hydrogen Energy*, 2012, **37**, 16748–16758.

57 X. Liang, W. Yu, Y. Xu, X. Shen, L. Wu and T. Xu, *Handbook of Energy Materials*, Springer Nature Singapore, Singapore, 2022, pp. 1–42.

58 C. M. Branco, S. Sharma, M. M. de Camargo Forte and R. Steinberger-Wilckens, *J. Power Sources*, 2016, **316**, 139–159.

59 J. Zhou, J. Cao, Y. Zhang, J. Liu, J. Chen, M. Li, W. Wang and X. Liu, *Renewable Sustainable Energy Rev.*, 2021, **138**, 110660.

60 V. Neburchilov, J. Martin, H. Wang and J. Zhang, *J. Power Sources*, 2007, **169**, 221–238.

61 S. S. Munjewar, S. B. Thombre and R. K. Mallick, *Ionics*, 2017, **23**, 1–18.

62 M. Vinothkannan, A. R. Kim and D. J. Yoo, *RSC Adv.*, 2021, **11**, 18351–18370.

63 S. Mo, L. Du, Z. Huang, J. Chen, Y. Zhou, P. Wu, L. Meng, N. Wang, L. Xing, M. Zhao, Y. Yang, J. Tang, Y. Zou and S. Ye, *Electrochem. Energy Rev.*, 2023, **6**, 28.

64 R. Kuwertz, C. Kirstein, T. Turek and U. Kunz, *J. Membr. Sci.*, 2016, **500**, 225–235.

65 C. Y. Wong, W. Y. Wong, K. Ramya, M. Khalid, K. S. Loh, W. R. W. Daud, K. L. Lim, R. Walvekar and A. A. H. Kadhum, *Int. J. Hydrogen Energy*, 2019, **44**, 6116–6135.

66 X. Ling, M. Bonn, K. F. Domke and S. H. Parekh, *Proc. Natl. Acad. Sci. U. S. A.*, 2019, **116**, 8715–8720.

67 M. B. Karimi, F. Mohammadi and K. Hooshyari, *Int. J. Hydrogen Energy*, 2019, **44**, 28919–28938.

68 K. D. Kreuer, *J. Membr. Sci.*, 2001, **185**, 29–39.

69 M. R. Berber and I. H. Hafez, *Int. J. Hydrogen Energy*, 2024, **57**, 1126–1138.

70 L.-Y. Zhu, Y.-C. Li, J. Liu, J. He, L.-Y. Wang and J.-D. Lei, *Pet. Sci.*, 2022, **19**, 1371–1381.

71 M. A. Barique, E. Tsuchida, A. Ohira and K. Tashiro, *ACS Omega*, 2018, **3**, 349–360.

72 F. Xu, Y. Chen, J. Li, Y. Han, B. Lin and J. Ding, *J. Membr. Sci.*, 2022, **664**, 121045.

73 H.-Y. Li and Y.-L. Liu, *J. Mater. Chem. A*, 2014, **2**, 3783–3793.

74 A. S. Aricò, S. Srinivasan and V. Antonucci, *Fuel Cells*, 2001, **1**, 133–161.

75 D. Liu, Y. Xie, Z. Zhao, J. Li, J. Pang and Z. Jiang, *J. Energy Chem.*, 2023, **85**, 67–75.

76 P. Joghee, J. N. Malik, S. Pylypenko and R. O'Hayre, *MRS Energy Sustain.*, 2015, **2**, 3.

77 N. Wan, *J. Power Sources*, 2023, **556**, 232470.

78 A. Mehmood, M.-G. An and H. Y. Ha, *Appl. Energy*, 2014, **129**, 346–353.

79 A. M. Zainoodin, S. K. Kamarudin, M. S. Masdar, W. R. W. Daud, A. B. Mohamad and J. Sahari, *Appl. Energy*, 2014, **135**, 364–372.

80 S. R. Samms, S. Wasmus and R. F. Savinell, *J. Electrochem. Soc.*, 1996, **143**, 1498–1504.

81 O. S. J. Elham, S. K. Kamarudin, N. Shaari, A. M. Zainoodin, Z. Zakaria and M. R. Yusof, *J. Environ. Chem. Eng.*, 2024, **12**, 111514.

82 S. J. Peighambardoust, S. Rowshanzamir and M. Amjadi, *Int. J. Hydrogen Energy*, 2010, **35**, 9349–9384.

83 W. Wang, B. Shan, L. Zhu, C. Xie, C. Liu and F. Cui, *Carbohydr. Polym.*, 2018, **187**, 35–42.

84 J. Li, G. Xu, W. Cai, J. Xiong, L. Ma, Z. Yang, Y. Huang and H. Cheng, *Electrochim. Acta*, 2018, **282**, 362–368.

85 C. W. Lin, K. C. Fan and R. Thangamuthu, *J. Membr. Sci.*, 2006, **278**, 437–446.

86 F. Bauer and M. Willert-Porada, *J. Power Sources*, 2005, **145**, 101–107.

87 J. Li, G. Xu, X. Luo, J. Xiong, Z. Liu and W. Cai, *Appl. Energy*, 2018, **213**, 408–414.

88 L. Sha Wang, A. Nan Lai, C. Xiao Lin, Q. Gen Zhang, A. Mei Zhu and Q. Lin Liu, *J. Membr. Sci.*, 2015, **492**, 58–66.

89 Y. Lin, H. Li, C. Liu, W. Xing and X. Ji, *J. Power Sources*, 2008, **185**, 904–908.

90 Z. Liu, B. Guo, J. Huang, L. Hong, M. Han and L. M. Gan, *J. Power Sources*, 2006, **157**, 207–211.

91 Y. Wang, G. Han, Z. Tian, M. Wang, J. Li and X. Wang, *RSC Adv.*, 2014, **4**, 47129–47135.

92 D. Kim, M. A. Scibioh, S. Kwak, I.-H. Oh and H. Y. Ha, *Electrochem. Commun.*, 2004, **6**, 1069–1074.

93 G.-N. Bae, H.-W. Kim, E.-M. Jung, S. Kang, Y.-G. Shul and D.-H. Peck, *Int. J. Hydrogen Energy*, 2023, **48**, 18879–18889.

94 A. Pagidi, G. Arthanareeswaran and M. M. Seepana, *Int. J. Hydrogen Energy*, 2020, **45**, 7829–7837.

95 F. Dong, Z. Li, S. Wang, L. Xu and X. Yu, *Int. J. Hydrogen Energy*, 2011, **36**, 3681–3687.

96 J. A. Dura, V. S. Murthi, M. Hartman, S. K. Satija and C. F. Majkrzak, *Macromolecules*, 2009, **42**, 4769–4774.

97 S. Kim, J. A. Dura, K. A. Page, B. W. Rowe, K. G. Yager, H. J. Lee and C. L. Soles, *Macromolecules*, 2013, **46**, 5630–5637.

98 C. Jiang and J. Zhang, *J. Mater. Sci. Technol.*, 2013, **29**, 97–122.

99 N. Nakagawa, M. A. Abdelkareem and K. Sekimoto, *J. Power Sources*, 2006, **160**, 105–115.

100 G. Q. Lu, C. Y. Wang, T. J. Yen and X. Zhang, *Electrochim. Acta*, 2004, **49**, 821–828.

101 L. Feng, J. Zhang, W. Cai, L. Liang, W. Xing and C. Liu, *J. Power Sources*, 2011, **196**, 2750–2753.

102 S. Eccarius, F. Krause, K. Beard and C. Agert, *J. Power Sources*, 2008, **182**, 565–579.

103 Q. X. Wu, T. S. Zhao, R. Chen and L. An, *Appl. Energy*, 2013, **106**, 301–306.

104 K. Scott, W. M. Taama and P. Argyropoulos, *J. Membr. Sci.*, 2000, **171**, 119–130.

105 T. Kallio, K. Jokela, H. Ericson, R. Serimaa, G. Sundholm, P. Jacobsson and F. Sundholm, *J. Appl. Electrochem.*, 2003, **33**, 505–514.

106 T. Hatanaka, N. Hasegawa, A. Kamiya, M. Kawasumi, Y. Morimoto and K. Kawahara, *Fuel*, 2002, **81**, 2173–2176.

107 M. Cao, J. Chu, X. Fan, F. Wang, J. Wang, F. Cheng, Z. Xu, F. Hu, H. Liu and C. Gong, *J. Membr. Sci.*, 2023, **675**, 121558.

108 A. S. Aricò, V. Baglio, P. Cretì, A. Di Blasi, V. Antonucci, J. Brunea, A. Chapotot, A. Bozzi and J. Schoemans, *J. Power Sources*, 2003, **123**, 107–115.

109 Z. Gaowen and Z. Zhentao, *J. Membr. Sci.*, 2005, **261**, 107–113.

110 P. Dimitrova, *Solid State Ionics*, 2002, **150**, 115–122.

111 H. S. Thiam, S. F. Tee, Y. S. Lim, L. H. Saw and S. O. Lai, *Int. J. Hydrogen Energy*, 2024, DOI: 10.1016/j.ijhydene.2024.05.077.

112 C.-W. Yang, C.-C. Chen, K.-H. Chen and S. Cheng, *J. Membr. Sci.*, 2017, **526**, 106–117.

113 X. Yan, H. Li, C. Lin, J. Chen, A. Han, S. Shen and J. Zhang, *Sustain. Energy Fuels*, 2020, **4**, 772–778.

114 L. Wang, N. Deng, G. Wang, J. Ju, M. Wang, B. Cheng and W. Kang, *ACS Sustain. Chem. Eng.*, 2020, **8**, 12976–12989.

115 S. Mohanapriya, G. Rambabu, S. Suganthi, S. D. Bhat, V. Vasanthkumar, V. Anbarasu and V. Raj, *RSC Adv.*, 2016, **6**, 57709–57721.

116 K. Pourzare, M. Zargar, S. Farhadi, M. M. Hassani Sadrabadi and Y. Mansourpanah, *ACS Appl. Nano Mater.*, 2023, **6**, 296–304.

117 V. Sharma, P. Upadhyay, N. H. Rathod, J. Sharma, S. Mishra, S. K. Raj, V. Kishore and V. Kulshrestha, *Int. J. Hydrogen Energy*, 2023, **48**, 37784–37795.

118 J. Li, W. Wang, Z. Jiang, B. Deng and Z. Jie Jiang, *J. Power Sources*, 2022, **543**, 231853.

119 V. Baglio, A. Di Blasi, A. S. Arico, V. Antonucci, P. L. Antonucci, C. Trakanprapai, V. Esposito, S. Licoccia and E. Traversa, *J. Electrochem. Soc.*, 2005, **152**, A1373.

120 R. E. Khalifa, A. M. Omer, M. H. Abd Elmageed and M. S. Mohy Eldin, *ACS Omega*, 2021, **6**, 17194–17202.

121 D. Cozzi, C. de Bonis, A. D'Epifanio, B. Mecheri, A. C. Tavares and S. Licoccia, *J. Power Sources*, 2014, **248**, 1127–1132.

122 O. Yaghi, *Acta Crystallogr., Sect. A: Found. Crystallogr.*, 2005, **61**, c69.

123 M. Dinca, A. Dailly, Y. Liu, C. M. Brown, D. A. Neumann and J. R. Long, *J. Am. Chem. Soc.*, 2006, **128**, 16876–16883.

124 R. Zou, A. I. Abdel-Fattah, H. Xu, Y. Zhao and D. D. Hickmott, *CrystEngComm*, 2010, **12**, 1337–1353.

125 P. Canepa, N. Nijem, Y. J. Chabal and T. Thonhauser, *Phys. Rev. Lett.*, 2012, **110**, 026102.

126 M. O. Rodrigues, M. V. de Paula, K. A. Wanderley, I. B. Vasconcelos, S. Alves and T. A. Soares, *Int. J. Quantum Chem.*, 2012, **112**, 3346–3355.

127 S. Nagata, K. Kokado and K. Sada, *Chem. Commun.*, 2015, **51**, 8614–8617.

128 J.-R. Li, J. Sculley and H.-C. Zhou, *Chem. Rev.*, 2012, **112**, 869–932.

129 J. R. Li, R. J. Kuppler and H. C. Zhou, *Chem. Soc. Rev.*, 2009, **38**, 1477–1504.

130 J. Lee, O. K. Farha, J. Roberts, K. A. Scheidt, S. T. Nguyen and J. T. Hupp, *Chem. Soc. Rev.*, 2009, **38**, 1450.

131 T. Zhang and W. Lin, *Chem. Soc. Rev.*, 2014, **43**, 5982–5993.

132 J. M. Taylor, K. W. Dawson and G. K. H. Shimizu, *J. Am. Chem. Soc.*, 2013, **135**, 1193–1196.

133 J. M. Taylor, R. Vaidhyanathan, S. S. Iremonger and G. K. H. Shimizu, *J. Am. Chem. Soc.*, 2012, **134**, 14338–14340.

134 J. A. Hurd, R. Vaidhyanathan, V. Thangadurai, C. I. Ratcliffe, I. L. Moudrakovski and G. K. H. Shimizu, *Nat. Chem.*, 2009, **1**, 705–710.

135 V. G. Ponomareva, K. A. Kovalenko, A. P. Chupakhin, D. N. Dybtsev, E. S. Shutova and V. P. Fedin, *J. Am. Chem. Soc.*, 2012, **134**, 15640–15643.

136 K. Divya, H. Liu, W. Zhang, Q. Xu and H. Su, *J. Appl. Polym. Sci.*, 2024, **141**, e55749.

137 S. Wang, H. Luo, X. Li, L. Shi, B. Cheng, X. Zhuang and Z. Li, *Int. J. Hydrogen Energy*, 2021, **46**, 1163–1173.

138 Z. Wang, J. Ren, Y. Sun, L. Wang, Y. Fan, J. Zheng, H. Qian, S. Li, J. Xu and S. Zhang, *J. Membr. Sci.*, 2022, **645**, 120193.

139 Z. Rao, B. Tang and P. Wu, *ACS Appl. Mater. Interfaces*, 2017, **9**, 22597–22603.

140 Z. Rao, K. Feng, B. Tang and P. Wu, *J. Membr. Sci.*, 2017, **533**, 160–170.

141 P. Das, D. Mukherjee, B. Mandal and S. Gumma, *ACS Appl. Mater. Interfaces*, 2021, **13**, 29619–29630.

142 C. Ru, Y. Gu, H. Na, H. Li and C. Zhao, *ACS Appl. Mater. Interfaces*, 2019, **11**, 31899–31908.

143 Y. Duan, C. Ru, J. Li, Y. Sun, X. Pu, B. Liu, B. Pang and C. Zhao, *J. Membr. Sci.*, 2022, **641**, 119906.

144 H. Sun, B. Tang and P. Wu, *ACS Appl. Mater. Interfaces*, 2017, **9**, 35075–35085.

145 Y. Guo, Z. Jiang, X. Wang, W. Ying, D. Chen, S. Liu, S. Chen, Z. Jiang and X. Peng, *J. Mater. Chem. A*, 2018, **6**, 19547–19554.

146 Y. Guo, Z. Jiang, W. Ying, L. Chen, Y. Liu, X. Wang, Z.-J. Jiang, B. Chen and X. Peng, *Adv. Mater.*, 2018, **30**, 1705155.

147 Z.-H. Li, H. Zeng, G. Zeng, C. Ru, G. Li, W. Yan, Z. Shi and S. Feng, *Angew. Chem., Int. Ed.*, 2021, **60**, 26577–26581.

148 N. Niluroutu, K. Pichaimuthu, S. Sarmah, P. Dhanasekaran, A. Shukla, S. M. Unni and S. D. Bhat, *New J. Chem.*, 2018, **42**, 16758–16765.

149 S. Neelakandan, R. Ramachandran, M. Fang and L. Wang, *Int. J. Energy Res.*, 2020, **44**, 1673–1684.

150 H. J. Kim, K. Talukdar and S.-J. Choi, *J. Nanoparticle Res.*, 2016, **18**, 47.

151 C. Prestipino, L. Regli, J. G. Vitillo, F. Bonino, A. Damin, C. Lamberti, A. Zecchina, P. L. Solari, K. O. Kongshaug and S. Bordiga, *Chem. Mater.*, 2006, **18**, 1337–1346.

152 K. Divya, M. S. Sri Abirami Saraswathi, A. Nagendran and D. Rana, *J. Appl. Polym. Sci.*, 2022, **139**, 1–15.

153 N. Niluroutu, K. Pichaimuthu, S. Sarmah, P. Dhanasekaran, A. Shukla, S. M. Unni and S. D. Bhat, *New J. Chem.*, 2018, **42**, 16758–16765.

154 L. Li, G. Wei, H. Liu, Y. Guo and Y. Ma, *J. Membr. Sci.*, 2024, **697**, 122525.

155 R. Rath, S. Mohanty, P. Kumar, S. K. Nayak and L. Unnikrishnan, *Surf. Interfaces*, 2023, **38**, 102761.

156 Y. Cui, Y. Liu, J. Wu, F. Zhang, A. P. Baker, M. Lavorgna, Q. Wu, Q. Tang, J. Lu, Z. Xiao and X. Liu, *J. Power Sources*, 2018, **403**, 118–126.

157 A. F. Ismail, N. H. Othman and A. Mustafa, *J. Membr. Sci.*, 2009, **329**, 18–29.

158 F. T. Chikumba, M. Tamer, L. Akyalçın and S. Kaytakoğlu, *Int. J. Hydrogen Energy*, 2023, **48**, 14038–14052.

159 P. Afanasiev, G.-F. Xia, G. Berhault, B. Jouguet and M. Lacroix, *Chem. Mater.*, 1999, **11**, 3216–3219.

160 P. Kumar and P. Das, *ACS Appl. Polym. Mater.*, 2023, **5**, 8459–8473.

161 K. Feng, B. Tang and P. Wu, *ACS Appl. Mater. Interfaces*, 2013, **5**, 13042–13049.

162 K. Divya, M. S. Sri Abirami Saraswathi, D. Rana, S. Alwarappan and A. Nagendran, *Polymer*, 2018, **147**, 48–55.

163 F. Zhong, Z. Zeng, Y. Liu, R. Hou, X. Nie, Y. Jia, J. Xi, H. Liu, W. Niu and F. Zhang, *Polymer*, 2022, **249**, 124839.

164 F. Zhong, P. Xie, R. Hou, W. Niu, J. Huang, F. Hu, G. Zheng, H. Liu, T. Qu and Y. Zhu, *J. Mater. Sci.*, 2021, **56**, 6531–6548.

165 N. Baig, *Composites, Part A*, 2023, **165**, 107362.

166 C. Simari, A. Enotiadis, C. Lo Vecchio, V. Baglio, L. Coppola and I. Nicotera, *J. Membr. Sci.*, 2020, **599**, 117858.

167 M. T. Musa, N. Shaari, S. K. Kamarudin and W. W. Yin, *J. Appl. Polym. Sci.*, 2023, **140**, e54560.

168 Z. Rao, A. Zhang, X. Liu, D. Zhu, G. Wang, M. Lan, Z. Wang, L. Jiang, B. Tang and H. Liu, *ACS Appl. Polym. Mater.*, 2023, **5**, 7539–7547.

169 G. G. Gagliardi, A. El-Kharouf and D. Borello, *Fuel*, 2023, **345**, 128252.

170 B. G. Choi, Y. S. Huh, Y. C. Park, D. H. Jung, W. H. Hong and H. Park, *Carbon*, 2012, **50**, 5395–5402.

171 Y. He, C. Tong, L. Geng, L. Liu and C. Lü, *J. Membr. Sci.*, 2014, **458**, 36–46.

172 B. G. Choi, J. Hong, Y. C. Park, D. H. Jung, W. H. Hong, P. T. Hammond and H. Park, *ACS Nano*, 2011, **5**, 5167–5174.

173 P. Das, B. Mandal and S. Gumma, *Chem. Eng. J.*, 2021, **423**, 130235.

174 S. A. Gokulakrishnan, V. Kumar, G. Arthanareeswaran, A. F. Ismail and J. Jaafar, *Fuel*, 2022, **329**, 125407.

175 Y. A. Sihombing, Susilawati, S. U. Rahayu and M. D. Situmeang, *Mater. Sci. Energy Technol.*, 2023, **6**, 252–259.

176 V. Parthiban and A. K. Sahu, *New J. Chem.*, 2020, **44**, 7338–7349.

177 V. Yadav, A. Rajput, N. H. Rathod and V. Kulshrestha, *Int. J. Hydrogen Energy*, 2020, **45**, 17017–17028.

178 L. T. Yogarathinam, J. Jaafar, A. F. Ismail, P. S. Goh, A. Gangasalam, M. F. R. Hanifah, K. C. Wong, M. N. Subramaniam and J. Peter, *J. Environ. Chem. Eng.*, 2021, **9**, 105876.

179 S. K. Yun and T. J. Pinnavaia, *Chem. Mater.*, 1995, **7**, 348–354.

180 B.-K. Kim, G.-H. Gwak, T. Okada and J.-M. Oh, *J. Solid State Chem.*, 2018, **263**, 60–64.

181 P. Pattanayak, N. Pramanik, P. Kumar and P. P. Kundu, *Int. J. Hydrogen Energy*, 2018, **43**, 11505–11519.

182 M. Tahriri, M. Del Monico, A. Moghanian, M. Tavakkoli Yaraki, R. Torres, A. Yadegari and L. Tayebi, *Mater. Sci. Eng., C*, 2019, **102**, 171–185.

183 S. Hu, M. Lozada-Hidalgo, F. C. Wang, A. Mishchenko, F. Schedin, R. R. Nair, E. W. Hill, D. W. Boukhvalov, M. I. Katsnelson, R. A. W. Dryfe, I. V. Grigorieva, H. A. Wu and A. K. Geim, *Nature*, 2014, **516**, 227–230.

184 Q. Weng, X. Wang, X. Wang, Y. Bando and D. Golberg, *Chem. Soc. Rev.*, 2016, **45**, 3989–4012.

185 B. Libby, W. H. Smyrl and E. L. Cussler, *Electrochem. Solid-State Lett.*, 2001, **4**, A197.

186 P. Prapainainar, A. Theampetch, P. Kongkachuichay, N. Laosiripojana, S. M. Holmes and C. Prapainainar, *Surf. Coat. Technol.*, 2015, **271**, 63–73.

187 P. Prapainainar, Z. Du, A. Theampetch, C. Prapainainar, P. Kongkachuichay and S. M. Holmes, *Energy*, 2020, **190**, 116451.

188 S. Al-Batty, C. Dawson, S. P. Shanmukham, E. P. L. Roberts and S. M. Holmes, *J. Mater. Chem. A*, 2016, **4**, 10850–10857.

189 J. Kim, J.-D. Jeon and S.-Y. Kwak, *Microporous Mesoporous Mater.*, 2013, **168**, 148–154.

190 C. Beauger, G. Lainé, A. Burr, A. Taguet and B. Otazaghine, *J. Membr. Sci.*, 2015, **495**, 392–403.

191 F. Altaf, S. Ahmed, D. Dastan, R. Batool, Z. U. Rehman, Z. Shi, M. U. Hameed, P. Bocchetta and K. Jacob, *Mater. Today Chem.*, 2022, **24**, 100843.

192 R. Claire Greaves, S. P. Bond and W. R. McWhinnie, *Polyhedron*, 1995, **14**, 3635–3639.

193 P. C. Lebaron, Z. Wang and T. J. Pinnavaia, *Appl. Clay Sci.*, 1999, **15**, 11–29.

194 M. M. Hasani-Sadrabadi, S. H. Emami and H. Moaddel, *J. Power Sources*, 2008, **183**, 551–556.

195 T. K. Kim, M. Kang, Y. S. Choi, H. K. Kim, W. Lee, H. Chang and D. Seung, *J. Power Sources*, 2007, **165**, 1–8.

196 R. Gosalawit, S. Chirachanchai, S. Shishatskiy and S. P. Nunes, *J. Membr. Sci.*, 2008, **323**, 337–346.

197 M. M. Hasani-Sadrabadi, S. R. Ghaffarian and P. Renaud, *RSC Adv.*, 2013, **3**, 19357.

198 H. Bai, H. Zhang, Y. He, J. Liu, B. Zhang and J. Wang, *J. Membr. Sci.*, 2014, **454**, 220–232.

199 S. Zhao, Y. Yang, F. Zhong, W. Niu, Y. Liu, G. Zheng, H. Liu, J. Wang and Z. Xiao, *Polymer*, 2021, **226**, 123800.

200 L. Wu, T. Wei, Z. Tong, Y. Zou, Z. Lin and J. Sun, *Fuel Process. Technol.*, 2016, **144**, 334–340.

201 K. Sanavada, M. Shah, D. Gandhi, A. Unnarkat and P. Vaghasiya, *Environ. Nanotechnol., Monit. Manage.*, 2023, **20**, 100784.

202 N. Worasith and B. A. Goodman, *Appl. Clay Sci.*, 2023, **242**, 106980.

203 V. Kumar, S. A. GokulaKrishnan, G. Arthanareeswaran, A. F. Ismail, J. Jaafar, D. B. Das and L. T. Yogarathinam, *Polym. Bull.*, 2023, **80**, 13005–13023.

204 S. Sasikala, S. Meenakshi, S. D. Bhat and A. K. Sahu, *Electrochim. Acta*, 2014, **135**, 232–241.

205 S. Sasikala, G. Rambabu, A. Shukla, N. Nagaraju and S. D. Bhat, *J. Electrochem. Soc.*, 2018, **165**, F1358–F1368.

206 L. As'habi, S. H. Jafari, H. A. Khonakdar, R. Boldt, U. Wagenknecht and G. Heinrich, *Exp. Polym. Lett.*, 2013, **7**, 21–39.

207 J.-M. Thomassin, C. Pagnoulle, G. Caldarella, A. Germain and R. Jérôme, *J. Membr. Sci.*, 2006, **270**, 50–56.

208 J.-M. Thomassin, C. Pagnoulle, D. Bizzari, G. Caldarella, A. Germain and R. Jérôme, *e-Polymers*, 2004, **4**, 1–13.

209 M. Prasad, S. Mohanty and S. K. Nayak, *RSC Adv.*, 2014, **4**, 61178–61186.

210 J. Jaafar, A. F. Ismail and T. Matsuura, *J. Membr. Sci.*, 2009, **345**, 119–127.

211 J. B. Ballengee and P. N. Pintauro, *Macromolecules*, 2011, **44**, 7307–7314.

212 J. B. Ballengee and P. N. Pintauro, *J. Membr. Sci.*, 2013, **442**, 187–195.

213 C. Boaretti, L. Pasquini, R. Sood, S. Giancola, A. Donnadio, M. Roso, M. Modesti and S. Cavaliere, *J. Membr. Sci.*, 2018, **545**, 66–74.

214 N. Awang, M. A. M. Yajid and J. Jaafar, *J. Environ. Chem. Eng.*, 2021, **9**, 105319.

215 C. Dong, Z. Hao, Q. Wang, B. Zhu, C. Cong, X. Meng and Q. Zhou, *Int. J. Hydrogen Energy*, 2017, **42**, 25388–25400.

216 G. Liu, W.-C. Tsen and S. Wen, *Mater. Des.*, 2020, **193**, 108806.

217 H. Wang, X. Li, X. Zhuang, B. Cheng, W. Wang, W. Kang, L. Shi and H. Li, *J. Power Sources*, 2017, **340**, 201–209.

218 H. Wang, X. Wang, T. Fan, R. Zhou, J. Li, Y. Long, X. Zhuang and B. Cheng, *Solid State Ionics*, 2020, **349**, 115300.

219 W. Chen, M. Chen, D. Zhen, T. Li, X. Wu, S. Tang, L. Wan, S. Zhang and G. He, *ACS Appl. Mater. Interfaces*, 2020, **12**, 40740–40748.

220 L. Wang, N. Deng, Y. Liang, J. Ju, B. Cheng and W. Kang, *J. Power Sources*, 2020, **450**, 227592.

221 S. A. Haddadi, A. Ramazani, S. Talebi, S. Fattahpour and M. Hasany, *Ind. Eng. Chem. Res.*, 2017, **56**, 12596–12607.